UNIVERSITÄT DER BUNDESWEHR MÜNCHEN
FAKULTÄT FÜR BAUINGENIEUR- UND VERMESSUNGSWESEN

E. Dutescu

Digital 3D Documentation of Cultural Heritage Sites Based on Terrestrial Laser Scanning

der Bundeswehr Universität München

UNIVERSITÄT DER BUNDESWEHR MÜNCHEN
FAKULTÄT FÜR BAUINGENIEUR- UND VERMESSUNGSWESEN

Digital 3D Documentation of Cultural Heritage Sites Based on Terrestrial Laser Scanning

Eugen Dutescu

Vollständiger Abdruck der von der Fakultät für Bauingenieur- und Vermessungswesen der Universität der Bundeswehr München zur Erlangung des akademischen Grades eines Doktor- Ingenieurwissenschaften (Dr.–Ing.) genehmigten Dissertation.

Vorsitzender: Univ.-Prof. Dr.-Ing. K.-H. Thiemann
1.Berichterstatter: Univ.-Prof. Dr.-Ing. O. Heunecke
2.Berichterstatter: Univ.-Prof. Dr.-Ing. habil W. Niemeier
3.Berichterstatter: Univ.-Prof. Dr.-Ing. habil L. Gründig

Diese Dissertation wurde am 8. Februar 2006 bei der Universität der Bundeswehr München eingereicht.

Tag der mündlichen Prüfung: 29. Mai 2006

Contents

Chapter 1
Introduction 9

Chapter 2
Cultural Heritage Documentation 10
2.1 General Explanation 10
2.2 Digital 3D Documentation 14
2.3 Case Scenarios 14

Chapter 3
Data Acquisition 17
3.1 Geodetic Measurements 17
3.1.1 Traditional Surveying 17
3.1.2 Image Processing and Close-Range Photogrammetry 19
3.1.3 Terrestrial Laser Scanning 22
3.2 Non-Geodetic Measurements 23
3.3 Combining Laser Scanning Data with Surveying and Close Range Photogrammetry Data 25
3.4 Thermography Data Processing 26

Chapter 4
From Point Cloud to 3D Model 28
4.1 Point Clouds Registration 28
4.1.1 Point Clouds Registration Using Targets 29
4.1.2 3D Similarity Registration 30
4.1.3 Feature Registration 31
4.2 Point Cloud Treatment 32
4.2.1 Remove Unwanted Points 32
4.2.2 Detect and Remove Outliers 33
4.2.3 Detect and Remove Disconnected Components 34
4.2.4 Noise Reduction 34
4.2.5 Redundancy Reduction, Point Clouds Sampling and Decimation 36
4.2.6 Adding Points 37
4.3 Create 3D Geometry from Point Clouds 39
4.4 Create and Fit Basic Geometric Primitives 39
4.4.1 Fitting a Planar Patch to 3D Point Sets 41
4.4.2 Fit a Sphere to a 3D Point Sets 45
4.5 Create and Fit Basic Shapes 49
4.6 Create 3D Objects 53
4.7 Create Triangular Meshes 58
4.8 Clean and Edit Triangular (Polygonal) Meshes 59
4.9 NURBS (Non-Uniform Rational B-Spline) Curves and Surfaces 68

Chapter 5
Virtual Reconstruction 70
5.1 Introduction 70
5.2 The Virtual Reconstruction Process 73
5.2.1 Data Collection 73
5.2.2 Process Design 74
5.2.3 Virtual Reconstruction Aspects 75

Chapter 6
Visualization 82

Chapter 7
Case scenarios 87
7.1 Project Maximilian Straße 87
7.2 Schönberg (Dealu Frumos) 90
7.3 St. Michael church 93
7.4 Test objects 98
7.5 Hohenburg ruins 101
7.6 Aspects of a 3D Cultural Heritage Documentation System 106

Chapter 8
Conclusions 110

Acknoledgments 112
Biography 113

Annex I Basic 3D Object Creation 114
Annex II Software 115
Annex III Video Format Test 116
Annex IV Data flow – case scenarios 117
Annex V Project Schönberg (Dealu Frumos), Romania – Virtual Reconstruction at different building stages 119
Annex VI Core Data Index to Historical Buildings and Monuments of the Architectural Heritage 121
V.I Maximilian Straße 121
V.II Schönberg (Dealu Frumos) 124
V.III Hohenburg 127
Annex VII Collection of Common Shaders and Standard Mapping Techniques Used by Common CG Software (3ds Max , Alias Maya, etc.) 130
Annex VIII Case Scenarios – Enclosed Multimedia CD Content 131

References 132

List of figures

Fig. 2.1 Schematic representation of a record structure for a building or monument [Thomas and Bold, 1998] 12
Fig. 2.2 Screenshot of digital documentation in myColex open source software [www20] 13
Fig. 2.3 Screenshot from Tiris cultural cadastre system [www19] 13

Fig. 3.1 Histogram equalization using Gimp 2.2 (see project St. Michael, Chap. 7.3) 19
Fig. 3.2 Rectified image using MatLab (see project "*Maximilian Str*.", Chap. 7.1) 21
Fig. 3.3 Hohenburg ruins, geo-electrical resistivity (see Chap. 7.5) 23
Fig. 3.4 Texture mapping (e.g. stained-glass window, see Chap. 7.4) 26
Fig. 3.5 Thermogram displayed in a black and white color palette (see Chap. 7.4) 26
Fig. 3.6 Building 3D model mapped with thermographic and digital images (see Chap. 7.4) 27

Fig. 4.1 Point clouds registration using targets (project "Test objects", see Chap. 7.4) 29
Fig. 4.2 Unwanted points removal 32
Fig. 4.3 Outlier detection and removal 33
Fig. 4.4 Detection and removal of the disconnected components 34
Fig. 4.5 "Phantom points" (project "Test objects", see Chap. 7.4) 35
Fig. 4.6 "Jumping" and "in-depth" points (project "Test objects", see Chap. 7.4) 35
Fig. 4.7 Point clouds sampling: uniform sampling (performed with Cyclone 5.1), grid sampling (performed with Geomagic Studio 6), curvature sampling (performed with RapidForm 2004), (project "Test objects", see Chap. 7.4) 37
Fig. 4.8 Hole filling process performed with Geomagic Studio 6 38
Fig. 4.9 Refining point cloud(performed with Geomagic Studio 6) 38
Fig. 4.10 Create complex 3D objects from point clouds – generic scheme 39
Fig. 4.11 Reconstructed model with geometric primitives (project "Test objects", see Chap. 7.4) 40
Fig. 4.12 Fitting a basic object to a point cloud 41
Fig. 4.13 Fitting a planar patch to a 3D set of points 42
Fig. 4.14 Tolerances in planar patch region grow algorithm 43
Fig. 4.15 Region grow-sphere (example performed in Cyclone 5.3) 49
Fig. 4.16 Automatic edge detection (examples performed with Geomagic Studio 6) 50
Fig. 4.17 Generic edge detection algorithm 50
Fig. 4.18 Semi-automatic edge detection (performed with Cyclone 5.3) 51
Fig. 4.19 Data tracing performed with CloudWorx 3.1 (project "Test objects", see Chap. 7.4) 51
Fig. 4.20 The union operator 53

Fig. 4.21 The combine operator 54
Fig. 4.22 Intersection operator 54
Fig. 4.23 Subtraction operator 54
Fig. 4.24 Fragment operator 55
Fig. 4.25 Voxel representation vs. Octree decomposition [Manner, 2004] 56
Fig. 4.26 Delaunay triangulation vs. Voronoi diagram (2D case) [www8] 58
Fig. 4.27 Acquired point cloud data (see project "Test objects", Chap. 7.4) 59
Fig. 4.28 Samples of topological and geometrical errors. 59
Fig. 4.29 Detect and correct self-intersecting triangles 60
Fig. 4.30 Detect and remove crossing faces 60
Fig. 4.31 Redundant face within a mesh 61
Fig. 4.32 Redundant faces of two overlapping meshes 61
Fig. 4.33 Detect and clean non-manifold faces 62
Fig. 4.34 Detect and repair bad normal faces 62
Fig. 4.35 Detect open edges 62
Fig. 4.36 Detect and remove spikes (see project "*Hohenburg*", Chap. 7.5) 63
Fig. 4.37 Samples of basic topological and geometrical errors correction and mesh editing procedures; for initial mesh, see Fig. 4.28 (see project "Test objects", Chap. 7.4) 63
Fig. 4.38 Final mesh features 64
Fig. 4.39 Add new triangles 64
Fig. 4.40 Edit a current triangle 65
Fig. 4.41 Filling holes 65
Fig. 4.42 Mesh zippering 66
Fig. 4.43 Mesh stitching 66
Fig. 4.44 Refine mesh (generated using 3ds max 6) 66
Fig. 4.45 Mesh decimation 67
Fig. 4.46 Vertex clustering algorithm 67
Fig. 4.47 Vertex decimation algorithm 67
Fig. 4.48 Iterative contraction algorithm 68
Fig. 4.49 NURBS surface with control points (green dots) and control network (yellow grid) (section wall element, project "St. Michael", see Chap. 7.3) 69

Fig. 5.1 Virtual reconstruction data sources 70
Fig. 5.2 Virtual reconstruction process related to the project "Hohenburg" (see Chap. 7.5) 71
Fig. 5.3 Computer representation of an altar (project "St. Michael", see Chap. 7.3) 72
Fig. 5.4 Reconstructed model with uncertainty level representation 73
Fig. 5.5 Data collection output information 74
Fig. 5.6 Input data for reconstructed model 74
Fig. 5.7 The manual geometry reconstruction of buildings 75
Fig. 5.8 The automatic geometry reconstruction of buildings 76
Fig. 5.9 3D Model generated automatically from a 2D hand sketch using PlanTracer [www59] 76
Fig. 5.10 Generic materials in a VR scene using 3ds Max 6 (project "Hohenburg", see Chap. 7.5); for a description of the used terms see Annex VII 77
Fig. 5.11 Local illumination (left view) vs. global illumination (right view) 79
Fig. 5.12 Simulated day light (Munich, 10:00 left view, 13:00 right view) 81

Fig. 6.1 Definition of visualization [Scott, 1999] 82
Fig. 6.2 Generic description of the visualization processes 83
Fig. 6.3 Visualization data flow 86

Fig. 7.1 Maximilian Straße 6, Munich 87
Fig. 7.2 3D wire-frame representation and point cloud comparison (AutoCAD with CloudWorx) 88
Fig. 7.3 Geometry generation in 3ds Max 6 (west façade) 89
Fig. 7.4 Photorealistic representation (view from north-west; for further views see multimedia CD) 89
Fig. 7.5 Fortified church Schönberg, Romania 90
Fig. 7.6 Create 3D ruled surface from sections 91
Fig. 7.7 Modeling decision stage - with arrows areas are identified which have to suffer modifications or improvements (main entrance view) 92
Fig. 7.8 Schönberg, 3D representation 92
Fig. 7.9 Wooden truss: generalized model (left), detailed junction (right) 93
Fig. 7.10 St. Michael Church, Perlach (Munich) 93
Fig. 7.11 Create basic geometry (cylinders and patches) in Cyclone 5.3 94
Fig. 7.12 Create a loft surface identifying a detail of altar (see highlighted arrows nr. 2 in Fig. 7.17) using 3ds Max 6 94
Fig. 7.13 Create textured triangular meshes 95
Fig. 7.14 Types of maps for object representation 95
Fig. 7.15 Create a complete object (candlestick) 95
Fig. 7.16 Create an object from digital images 96
Fig. 7.17 Main altar – St. Michael church (default 3ds Max 6 Scanline renderer) 96
Fig. 7.18 Representation of the St. Michael church. The image is rendered in approx. 12 minutes with default 3ds Max 6 Scanline renderer. 97
Fig. 7.19 Small statue of the goddess Athena (object size 25 x 25 x 70 cm) 98
Fig. 7.20 Statue representing the goddess Athena –screenshot in Cult3D. 98
Fig. 7.21 Side view of the church from the campus of University Bundeswehr 99
Fig. 7.22 Point cloud to polygons deviation in Geomagic Studio 6 (trial version) 100
Fig. 7.23 Detailed views over the exterior and interior of the church from the campus of the University of Bundeswehr Munich. 100
Fig. 7.24 Hohenburg ruins, view at the main tower ruins 101
Fig. 7.25 Laser scanner HDS 3000 in one of the scanning positions (it can be observed the large vegetation coverage) 101
Fig. 7.26 Contour lines (red color - 5 m equidistance, black color – 0.5 m equidistance) 102
Fig. 7.27 DTM and break-lines. In order to be viewable the break-lines – magenta color -are displayed here with an offset in vertical direction. 103
Fig. 7.28 Hohenburg seen from south, copperplate by M.Wenig 103
Fig. 7.29 Virtual reconstruction versus source data 104
Fig. 7.30 Virtual reconstruction versus source data 106
Fig. 7.31 Technical representation of the old Hohenburg castel – south view 105
Fig. 7.32 Schematic view of a possible 3D cultural heritage system 107
Fig. 7.33 3D environment – the church from the campus of University of Bundeswehr Munich 108
Fig. 7.34 Measurements performed with ModelPress Reader – St. Michael church main altar 109

List of tables

Table 2.1 Case scenarios evaluation 16

Table 4.1 Point clouds registration types 28
Table 4.2 Best-fit plane using singular value decomposition – Matlab code 45
Table 4.3 Best-fit plane using polygonal regression – Matlab code 45
Table 4.4 Best-fit sphere using iteration algorithm – Matlab code 47
Table 4.5 Best-fit sphere using polygonal regression – Matlab code 48
Table 4.6 Best-fit line – Matlab code 52

Table 5.1 Ray tracing vs. Radiosity 80

Table III. 1 Video format test 116

Chapter 1

Introduction

Until recently, regardless if is referring to architecture, construction, industry, surveying or cultural heritage, the technical documentation was mainly realized in two dimensions. Nowadays, this standing is threatened by the introduction and the development of new tools and methods able to generate high quality three dimensional digital models.

The migration from 2D to 3D seems to be more accepted or even expected in the relationship between the contractor or the service provider and the customer and less used in the current activity between different service providers. This is due to the fact that a non-technical viewer is more comfortable with a 3D visualization, and a 2D representation is more natural for a technical user, however.

Mainly, two methods could be involved when creating 3D models. The first method is referring to a conversion from the current 2D plans to 3D objects using specific CAD and modeling software. The second method implies the usage of systems capable to record and represent directly 3D data.

Nowadays, starting with these pre-requisites and considering also that, generally, the cultural heritage area suffers from implementation of databases restricted to descriptive data and limited digitalized spatial information, it seems more natural that the next step in documenting cultural heritage (Chap. 2) to be realized directly in 3D.

From a series of methods involved in acquiring spatial data needed to generate 3D models (Chap. 3), the laser scanning techniques seems to be, at this moment, one of the suitable choices to be inquired when documenting cultural heritage. Its biggest advantage is the ability to record large sets of 3D data that can be used "as it is" in the cultural heritage documentation. Due to the compatibility and access reasons, generally, a conversion to a 3D solid model is needed in order to unify the data acquired with different techniques and to create more familiar representations for large categories of users. Having as main filters the level of detail and the quality of the represented object, the 3D model's geometry creation varies from simple geometrical primitives to more complex surfaces represented as polygonal networks or NURBS (Non-Uniform Rational B-Spline) entities (Chap. 4 and Chap. 5).

Even though a reverse conversion from 3D to 2D is possible, it is more expected that the final model to be presented and explored in three dimensions. This is realized by tools developed to visualize large sets of 3D data in an acceptable, viewable form having as platform the internet or a local computer (Chap. 6).

The aim of this thesis is to identify and describe a generic data flow for cultural heritage documentation, from the acquiring of 3D data to the model visualization as it is described above (Chap. 7, including Annex IV). The data flow concept is exemplified in various case scenarios that refer to a large spectrum of situations when dealing mainly with building's cultural heritage documentation.

Chapter 2

Cultural Heritage Documentation

A correct understanding of the term "cultural heritage" is essential before one can refer to cultural heritage documentation and the feasible methods of its realization. About 21 millions[1] results with more than a general use of the term "cultural heritage" are revealed to the inquirer using one of the common internet search engines.

2.1 General Explanation

The Encyclopedia Britannica Online [www15] defines culture as "*integrated pattern of human knowledge, belief, and behaviour that is both a result of and integral to the human capacity for learning and transmitting knowledge to succeeding generations* and Webster Dictionary [www16] defines "heritage" as *that which is inherited, or passes from heir to heir*.

Following these two definitions a distinction between cultural heritage and culture, for a non familiarized person, is difficult to be made since culture is by definition inherited. Still, one can say that cultural heritage defines the means or objects through which cultural information is transmitted.

A general approved definition for cultural heritage was given by UNESCO in its Convention Concerning the Protection of the World Cultural and Natural Heritage [UNESCO, 1972]. The following is to be considered as cultural heritage:

- *monuments: architectural works, works of monumental sculpture and painting, elements or structures of an archaeological nature, inscriptions, cave dwellings and combinations of features, which are of outstanding universal value from the point of view of history, art or science*;
- *groups of buildings: groups of separate or connected buildings which, because of their architecture, their homogeneity or their place in the landscape, are of outstanding universal value from the point of view of history, art or science*;
- *sites: works of man or the combined works of nature and of man, and areas including archaeological sites which are of outstanding universal value from the historical, aesthetic, ethnological or anthropological points of view*.

While the first attempt for coherent and logically defensible cultural heritage preservation was referring only to the building conservation – Society for the protection of Ancient Building's Manifesto of 1877 [www17] - nowadays, also due to the globalization tendency, the above mentioned traditional definition of cultural heritage is enhanced by including also non-physical aspects like traditions, folklores, religions and cultural identity.

[1] http://www.google.de, accessed at 28.09.2005

Documentation and inventories of cultural heritage are vital for their identification, interpretation, protection, preservation, restoration and conservation. Cultural heritage documentation is used as a tool to:

- acquire, systematization and management of knowledge referring to cultural heritage;
- share the cultural heritage information between organizations, institutions, sciences which are contributing to the study and the protection of the cultural heritage;
- identify suitable methods for cultural heritage study and to minimize the physical damage, authenticity versus acceptable changes, widening access versus conservation, preservation versus reconstruction, etc.;
- transmit and propagate the cultural heritage knowledge as cultural tourism or education;
- link cultural heritage to social life and define the role of cultural heritage in spatial development;
- identify social and environmental threats to cultural heritage, etc.

Until recently, the cultural heritage documentation is carried out on a local or a national level. Nowadays, internationally agreed standards for cultural heritage documentation are essential due to the globalization trends in economic activity, cultural awareness, the need to share and use of cultural heritage knowledge at a global scale and never the less the crime activity.

Some of the approved standards are identified by [Thomas and Bold, 1998], [COE, 2001] having the core information required for common access, contact and information sharing in documenting the architectural, archeological and movable heritage:

- The core data index to historic buildings and monuments of the architectural heritage (1995) [www18] (see Annex VI for an enhanced format);
- International core data standard for archaeological sites and monuments (1995) [Thomas and Bold, 1998];
- Object ID (1997), international standard for the information needed to identify cultural objects [Thomas and Bold, 1998].

These standards contain a minimum and harmonized set of data elements and technical specifications necessary to record and inventory cultural heritage objects which take advantage of the computer systems capabilities as well. The standards are organized in sections referring to:

- the name and the reference that identify the cultural heritage object or site;
- the precise dating or periods in terms of cultural and time criteria and historical summary;
- the spatial location of the monument or sites in terms of political, postal, geographical, administrative and geodetic criteria;
- the functional type and category;

- the physical condition to define the integrity and the state of the monument or site;
- the structural and construction condition of the monument or site in terms of building and covering materials and techniques;
- the dimensions of the cultural heritage objects;
- the protection, conservation and restoration status.

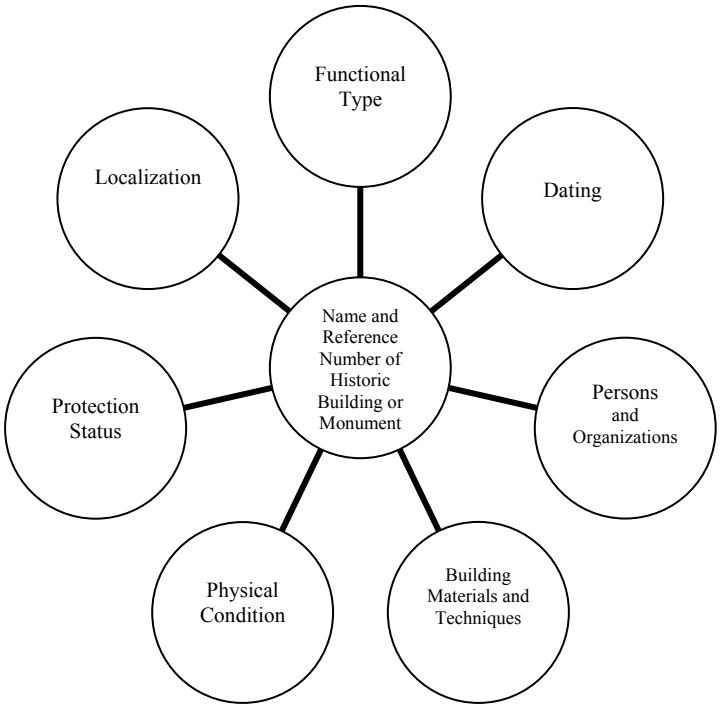

Fig. 2.1 Schematic representation of a record structure for a building or monument [Thomas and Bold, 1998]

Digital documentation was introduced once with the development of the computer systems as a response to the request of widening the access to the cultural knowledge to a larger and diverse category of users. The custom digital documentation has generally the shape of a database containing the same written and graphical information as the traditional documentation.

The myColex© system (Fig. 2.2) is an example of a open source software that addresses mainly cultural heritage collection inventories in a simple and inexpensive manner but maintains the level of information required by the expert user [www20]. A similar SQL database is currently in use also by the Bayerische Landesamt für Denkmalpflege [H. Dietrich, 2005]. Tiris© for instance is a multiple information system of the region Tirol, Austria. One of its sections regards the cultural cadastre. It is available via internet [www19] and is a good example of a user friendly system that addresses a larger public. The level of information required by an expert user is not satisfied or maybe just restricted to the common user (Fig. 2.3), however.

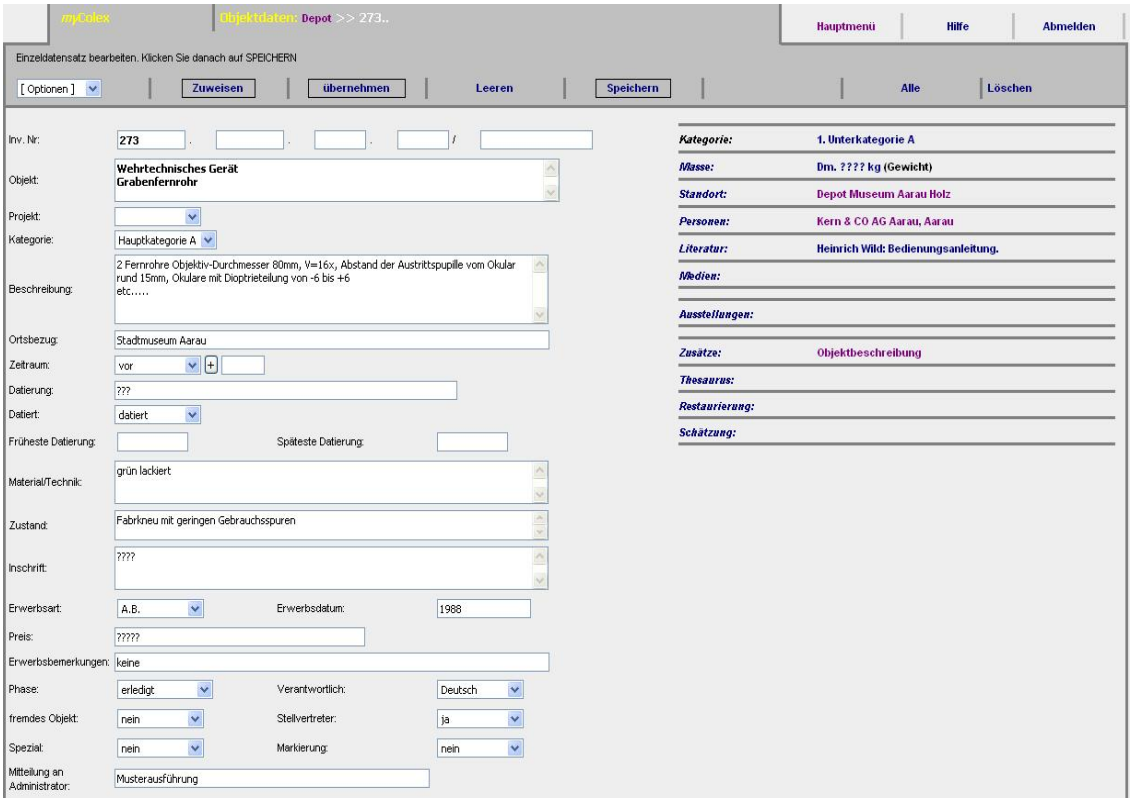

Fig. 2.2 Screenshot of digital documentation in myColex open source software [www20]

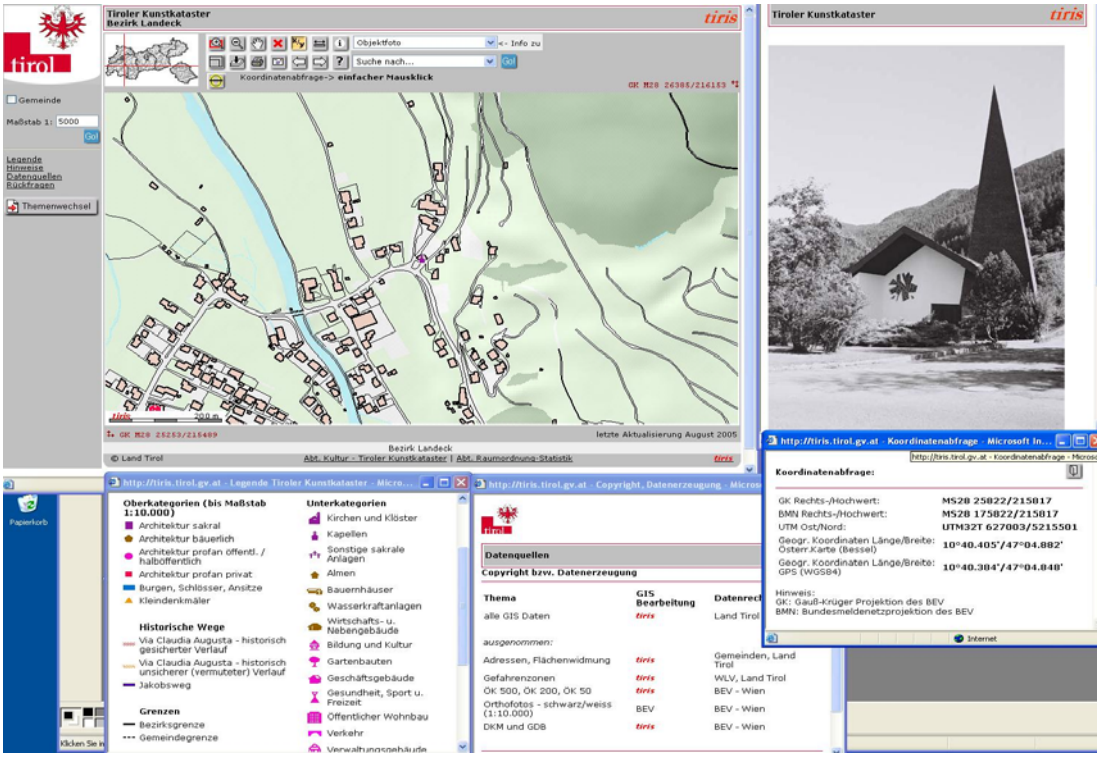

Fig. 2.3 Screenshot from Tiris cultural cadastre system [www19]

Nowadays, new methods are under research and development that allow to experience the cultural knowledge at global securized access on its higher level, personalized interaction, using the technologies such as human-computer interaction, virtual and augmented reality.

2.2 Digital 3D Documentation

A new level of digital documentation rose with the new technologies which produced rich new ways of recording, inventorying, conserving, restoring and presenting cultural heritage. Recording techniques allow the specialized or non-specialized user to increase the detail level of acquired data and to perform simple or complex analysis direct on site on large scale 3D data. Inventorying methods allow widened real time access to the recorded data and the analysis results. Restoration involves the completion of the recorded 3D data with virtual and even physical data that permit a better guide for the restaurateurs and conservators in order to find the most accurate, realistic and secure restoration solution. New multimedia techniques allow large and complex cultural heritage items to be visualized to the highest detail by the expert users as well as by the broader public.

Examples of how the new technologies are used to enhance the user's perception of the cultural heritage objects are projects like:

- 3D Murale (3D measurement and virtual reconstruction of ancient lost worlds of Europe); a multinational project that uses photogrammetry techniques as main data recording method and suitable software to obtain 3D data. Computer vision techniques are used to combine the excavated archaeological fragments and for virtual reconstruction of the complete model [www21];
- ArchaeoPackPro is a software package that supports the specialized user during archaeological campaign and enables the interactive data analysis after campaign ends [www22] ;
- Archeoguide (Augmented Reality-based Cultural Heritage On-site Guide); a system that provides enhanced information access at cultural heritage sites combining the on-site real data with virtually reconstructed models [www23].

In the traditional standards and charters for cultural heritage documentation (see Chap. 2.1) the shape and dimensions of the monument or site are restricted to alphanumerical descriptions or 2D graphical annexes. A digital documentation has to remove this limitation and a main aspect of documentation has to be focused on the visualization and 3D analysis of the object. Other standard information are not omitted, they are just being enhanced by the detailed 3D model.

2.3 Case Scenarios

The main aspect of this thesis concentrates on terrestrial laser scanning technology as main 3D spatial data acquisition method and the usage of the computer vision methods to create highly detailed cultural heritage models. The thesis concentrates on buildings as cultural heritage sites. In the case scenarios the followings items are distinguished in particular:

- object geometry complexity versus model complexity;
- physical status of the building;

- functional type of the cultural heritage object;
- virtual reconstruction level;
- combining different recording techniques with laser scanning acquisition method;
- deliverables and visualization characters.

With respect to the above stated factors the following case scenarios are chosen:

- a modern building dated around middle 20th century. The construction is a part of an architectural ensemble situated on Maximilian Street, one of the most famous luxurious shopping streets in Munich, Germany. The project entitled as "*Maximilian Str."* was realized in a two weeks time period in spring 2004;
- the fortified church Schönberg – Dealu Frumos, Romania. The Romanesque basilica (about 13th century) enters in 2003 under the patronage of the University of Architecture and Urbanism "Ion Mincu", Bucharest and becomes a Study Centre in Vernacular Architecture. The joint project was realized in time periods between the end of 2004 and the beginning of 2005. It will be referred to from now on as "*Schönberg*";
- the interior of the church St. Michael in Munich chosen due to its geometric complexity, further on appointed as "*St. Michael*";
- the church of the University of the Bundeswehr Munich and a small statue of the goddess Athena are used as test objects to describe several processes involved in this thesis;
- the old Hohenburg castle ruins. The ruins of the medieval castle situated in Lenggries, Germany are study objects in a virtual reconstruction project generally defined as "*Hohenburg*".

The above case scenarios are used to investigate the level of involvement of laser scanning technique as main spatial data acquiring method. Furthermore the level of information that can be gathered versus the needed data for a complete model generation and the amount of work needed to bring the projects in a comparative stage are investigated.

The initial case scenarios evaluation from Table 2.1 emphasizes the methodical differences between the selected projects and the distinctive approach needed for their solution. The table is organized in sections of different levels to be interpreted in a large subjective scale as follows:

- the physical state of the building varies from a symbol "-" (poor) to a group of symbols "+". A group of four "+" symbols denotes a construction in a good or very good condition;
- the object complexity reflects on a scale from "+" to "+ + + +" the geometry complexity of the building and the amount of work requested for data acquisition;
- the model complexity level defines the geometry of the computer model and can be quantified in the number of model faces or the time needed for its realization. A comparison between the object and model complexity is not reflected by the below table. The levels were assigned in order to reflect the differences between the case studies;

- the virtual reconstruction level defines the amount of data and other information that is generated directly on a computer having non or a small amount of spatial data recorded. The level assigned to the Schönberg project is not referring to the current state of the construction but rather to past instances creation;
- the "combining different recording methods" section reflects the needed level of mixture between laser scanning technology with other spatial or non-spatial data acquiring methods;
- the digital documentation section is referring to the availability and the form of the final deliverables. The available 3D environment for the projects "St. Michael" and "Test objects" can be consulted at the enclosed multimedia CD.

Case study / Aspect	*Maximilian Str.* Chap. 7.1	*Schönberg* Chap. 7.2	*St. Michael* Chap. 7.3	*Test objects* Chap. 7.4	*Hohenburg* Chap. 7.5
Physical state of the building	+ + + +	+ + +	+ + + +	+ + + +	-
Object complexity level	+ +	+ +	+ + +	+ +	+
Model complexity level	+ +	+ +	+ + + +	+ +	+ +
Virtual Reconstruction level planned	-	+	-	-	+ + + +
Combining different recording methods	+	+	+	+	+
Digital documentation	yes	yes	yes + 3D environment	yes + 3D environment	yes

Table 2.1 Case scenarios evaluation

The next chapters will clarify the methods used in the case scenarios and also other possible approaches in order to provide the spatial information for the cultural heritage documentation.

Chapter 3

Data Acquisition

As stated in the previous chapter this thesis will concentrate on methods or techniques used to record, investigate and provide spatial information for the cultural heritage documentation. The architectural investigation and data acquisition generally starts with a simple reconnaissance, advances to surface and subsurface non-destructive and destructive examination and often ends with required laboratory analysis [Travis C. McDonald, Jr, 1994].

The simple reconnaissance usually consists in a visual overview and provides the most limited type of investigation. The first step in a systematic investigation is the examination of all surfaces. The purpose of the surface data acquisition is to observe every visible detail of design and construction and to reveal possible alterations, structural and environmental problems. With respect to the intended level of detail, different techniques like visual inspection, traditional surveying, photography, close range photogrammetry and terrestrial laser scanning are used in surface inspection.

The next level of data acquisition consists in sub-surfaces investigation using non-destructive methods. Results derived from the surface inspection could supply information about the areas that present interest for sub-surface investigation. There is a number of techniques that can be used in a manner that provides none or minimal damage to the object of study. These include impulse radar or ground penetrating radar (GPR), endoscopy, ultrasonics, X-ray computed tomography, magnetometry, infra-red thermography, ground conductivity, ground resistivity, microgravity survey, electro detection, metal detection, micro-drilling, video camera, fiber optics, etc. [Robert Demaus, 1996].

The last step in data acquisition is represented, if needed, by the laboratory analysis. Extracted sample from in-site investigations are examined in the laboratory using different methods in order to establish the material's chemical components, material age, material characteristics and properties, etc. [Travis C. McDonald, Jr, 1994].

3.1 Geodetic Measurements

3.1.1 Traditional Surveying

Traditional surveying implies the employment of one of the classical measurement techniques starting with the simple measurement tape or laser distance meter devices and ending with high-tech tachymeters. The techniques are used to survey the general structure of the building and could supply quality information needed to increase the measurement's accuracy for other spatial data acquiring methods.

The efficiency in employment of the geodetic instruments as a singular method in surface recording is directly connected with the entity's complexity. More complex surfaces make the method ineffective. However, the high measurement accuracy makes the method

valuable in the single point determination, often used as constrain or datum for other data acquiring methods like close range photogrammetry or terrestrial laser scanning.

As sorting criterion their deployment the surveying data can be categorized in:

- data describing the geometry, the shape and the state of the object of interest: measured points located directly on the object's surface, elevation data, tape measurements, etc.;
- data describing the neighboring area of the object of interest: measured points and other data used only to generate the surrounding environment;
- reference points used for geo-referencing the surveying data with/or other type of data (point clouds, photographs, etc.): measured points located directly on the object's surface or in the neighboring areas.

The data processing is generally realized with a specialized software or CAD application, manually using the digital tracing technique or automatically using the data attributes, and consists in the creation of specific 2D or 3D drawings, profiles, sketches, etc. Measuring tape or laser distance meter data are used mainly to generate 2D information referring to the dimensions of the object of interest or surrounding objects. Robust area or volume information could be obtained only in specific cases (straight angles, low tolerances or combined with other measurement methods). 3D models could be realized combining the generated 2D prints with elevation information. Leveling data are used mainly to determine accurate elevation profiles and networks, slopes or digital terrain model (DTM). The point data acquired with tachymeters is used to generate 2D plans, façades and 3D models of the object of interest and surrounding objects, and also to determine information referring to the object's structure and their condition. The tachymeter point data is used also to reference or connect other type of data (point cloud registration, combine laser scanning data with photographs, etc.). In this way, the registration of two different point clouds can be performed even without having point clouds overlapping (the tachymeter network defines the fixed "point cloud" and the scanned data is floating). The GPS data is used mainly in geo-referencing, but for larger areas it can be also used to generate the surrounding area of the object of interest.

3.1.2 Image Processing and Close-Range Photogrammetry

Image processing

The image processing operations of photos of the object are used to restrict undesired distortions or to improve image proprieties for further processing in 3D model generation and/or texture mapping of 3D models.

The image processing operations are classified in point, local and global operations. The point operations are referring to the single pixel transformation. In local operations the output value at a specific coordinate is returned with respect to the neighborhood input values at the same coordinate and the global operations return the output value at a specific coordinate dependent on all the values in the input image [Mc Glone et.al, 2004].

A basic method to interpret the quality of an image is by analyzing its histogram. This displays the gray value distribution in a grayscale image or the individual color value in a RGB image. An image with all gray values occupied and equally distributed denotes a better contrast and a higher quality. A common technique used to improve the image appearance is *the histogram equalization*. The process transforms an image with a non-uniform histogram like the one in Fig. 3.1. a into one with a uniform histogram, thus an image with better contrast, brightness and uniform coloring is obtained.

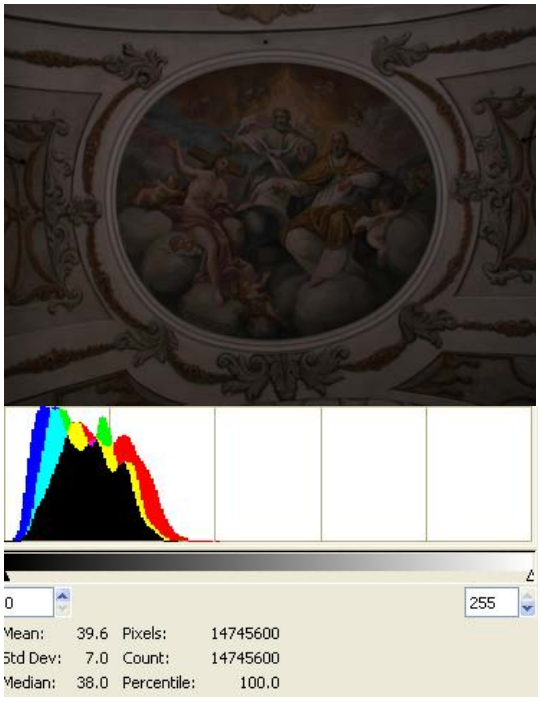

a. Non-uniform histogram

b. Uniform histogram

Fig. 3.1 Histogram equalization using Gimp 2.2

(see project *St. Michael,* Chap. 7.3)

Another point method is *the thresholding*, used to separate the regions of image corresponding to the objects of interest from unwanted regions. The process can be performed on a grayscale image when a threshold T is defined and gray value bigger than T are equaled to 1 (black) and smaller to 0 (white).

The acquired images may be affected by a various type of "noise" generated for instance by temperature effects in the semiconductors (dark noise), the sensor signal reading process (readout noise), the differences in arrival time of light to the sensor (photon noise), voltage fluctuations, electromagnetic interference etc. (random noise) [Medkeff, 2004], [Schowengerdt, 2003]. The presence of noise in digital photographs could be reduced by using *low pass filters* that are smoothing the image appearance. They are using a defined neighborhood around a pixel in the input image to generate a new brightness value for a pixel in the output image. The results are acceptable as long as the noise in the input image has smaller size than the smallest entities of the object of interest [Mc Glone et.al, 2004]. If the noise has a higher value than the output image contains blurred edges.

Other procedures like high pass filter or edge extraction, unsharp masking filters, brightness and contrast modifier, color balance, color levels, tonal range, gamma correction, motion blur reduction, etc. are used to enhance the image appearance quality. Furthermore morphological based operations (dilatation and erosion, opening and closing, boolean convolution, skeleton, etc.) are used to find the contour or the skeleton of an object, the filling regions, to remove or separate objects. When the acquired image requires a larger storage space, images compression methods are used to compact the image while preserving its quality.

The described and many other image processing filters are integrated in most of the image processing software like Adobe Photoshop [www29], Corel Photo-Paint [www30], GIMP [www28], etc.

The above described processes could be applied also to the film-photographs after the conversion to the digital format. The conversion is usually realized using a scanning device. The scanning process is directly performed using the film or the developed images. The information contained in a film-image is noticeably larger than the one taken with a digital camera. Since most of the digital cameras offer a sensitivity equivalent to ISO 100, a comparison between analog and digital imagery can be made on this format [www54].

Rectified and orthoimages

Currently, the façades of the object of interest are the main component in an architectural documentation. They can be easily generated using rectified or orthorectified images. The rectified images have modified pixels to a vertical projection where errors due to the non-verticality of the camera are corrected. The orthophotos are images with modified pixels to an orthogonal projection with tilt errors corrected, variations in scale and displacement minimized. They are generated using a planar projective transformation with at least four control points as input data [Mc Glone et.al, 2004].

a. original image b. rectified image

Fig. 3.2 Rectified image using MatLab (see project "*Maximilian Str.*", Chap. 7.1)

Due to the camera tilt some regions of the object of interest can be occluded and appear in the orthophoto as shadows or black regions. The effect can be eliminated using images that contain the missing data and generate other orthoimages. When more than one orthophoto is available, a larger region can be created using the mosaic or stitching method. The main disadvantage of the method is that the orthorectified image or the orthomosaic has been resampled from the original image and it might have lost some of the original resolution and accuracy [Mc Glone et.al, 2004]. Besides their photogrammetrical usage, the orthoimages are ideal to be used as mapping textures for 3D models (see Chap. 3.3).

Photogrammetric restitution

Using an analog or a digital camera with know characteristics (lens focal length, image size, number of pixels, position of principal point and the lens distortion) at least two pictures of an object have to be taken. Using at least three common points in two different pictures, 3D coordinates can be determined for other points in the images. In this way the photogrammetry techniques convert the images in 3D models.

Photogrammetry is used with good results in areas that imply the non-contact investigation, high accuracy measurements, large site measurements, congested site environment, short field time, moving or vibrating sites. In addition to maps and models, photogrammetry provides also objective information and a photographic documentation of the inquired object.

The process of photogrammetric restitution is used to identify and generate points and edges using orientated stereo-images. It can be realized semi-automatically by digital tracing with a mark or automatically using different image segmentation methods. Using the digital tracing method the user follows and marks different details on the images of the object of interest.

When working with large and complex objects, an enormous interactive work is required for digitally tracing all important details (e.g. [www2]). To minimize this disadvantage automatic feature extraction tools can be involved. The resulted features can be further employed in image matching or in object recognition methods. Extraction operators like Förstner, Deriche, or Harris are currently used to identify points features or corners in images. The algorithms identify the points that are distinct and seldom with the neighboring points [Mc Glone et.al, 2004].

Corresponding features or parts identified in different images are used to perform the image matching procedure used further to determine the 3D model or to perform a surface reconstruction. The matching principles are commonly classified in area-based matching (cross correlation method, least squares) and feature matching [Mc Glone et.al, 2004].

3.1.3 Terrestrial Laser Scanning

The newest technique used for surface investigation is the terrestrial laser scanning method. The measurement principle is simple: an emitter sends a laser wave to a surface and a receiver collects the reflected beam. The distance from emitter to the surface is computed as a function of the travel time from emission to reception or from phase difference between the emitted and the received signal. The resulted distance in combination with angle measurements given by special mirrors, prisms or motor axes, supplies the 3D position of the intersection point between the laser beam and the investigated surface. The 3D position can be obtained also from triangulation of the emitted laser beam [Fröhlich, 2004], [Curless, 2000]

The specifications of the laser scanners make them a powerful tool in areas where highly detailed and accurate models are required. Other main keys of the laser scanning technology make it suitable for large site measurements, non-contact measurements, on-site results, low staff request and others. The main impediment for a larger usage of the laser scanner technology is represented by its costs at this moment.

A digital representation of the entity surface can be obtained using each one of previous techniques. The factors that define the choice of one of these methods are the complexity of the studied object, the detail and accuracy of the resulted model, the time needed for object capturing and model creation.

The laser scanner data can be used as the main method for capturing large or small sites, low or complex geometry, non-contact measurements and for capturing detailed elements of the object. The photogrammetry techniques can be used in congested spaces that do not allow the use of the laser scanner, for acquiring sites with low geometry detail, moving or vibrating sites and as mapping techniques for laser scanner data. Often, however, a combined usage will be the ideal case.

3.2 Non-Geodetic Measurements

The next level of data acquisition consists in sub-surfaces investigation using non-destructive methods. There is a large number of techniques that can be used in a manner that provides none or minimal damage to the object of study.

Infrared thermography can measure and record variations in infrared radiation which is emitted by all structures. As the radiation level varies, the infrared thermography can provide a large amount of information regarding the structure and condition behind the surface, within the fabric. However, this technique is very sensitive to weather conditions and does not have good results in case of highly reflective surfaces [www3].

Geo-electrical measurements are based on the measurement of the electrical resistance of the subsoil. The resistance measurements are taken by applying a current to the ground along two electrodes and then measuring the potential difference between these two. The result is represented by a 2D or 3D image [www1]. Fig. 3.3 displays the geo-electrical measurements realized by Bayerische Landesamt für Denkmalpflege at the ruins of old castle Hohenburg. The middle part shows in black color the presence of an old structure.

Impulse radar or ground penetrating radar works by transmitting pulsed radio energy from an antenna. As the signal wave passes through different layers its velocity changes and a part of the signal is reflected and received by the other antenna. The strength of the reflected signal depends mainly on the difference in the dielectric constant of the adjacent layers. A data conversion is performed for translating the travel time into the depth. Interpretation of the resulted information requires a high level of expertise and the assessment by impulse radar is relatively expensive [www5].

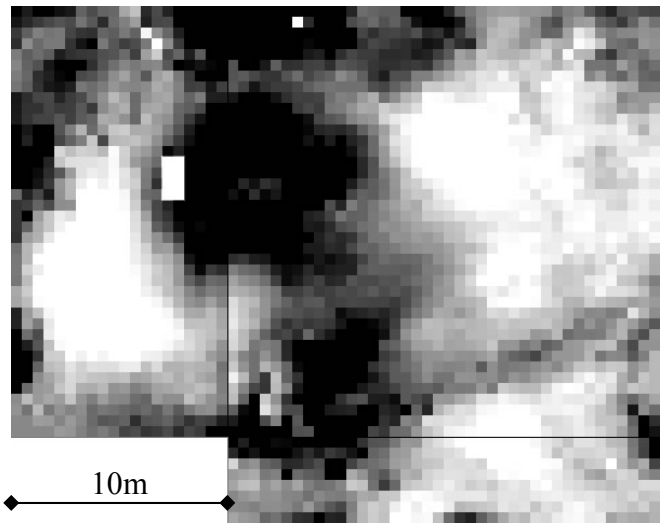

Fig. 3.3 Hohenburg ruins, geo-electrical resistivity – image provided by Bayerische Landesamt für Denkmalpflege (see Chap. 7.5)

Endoscopy is the extension of the visual survey in areas inaccessible to the naked eye. The equipment ranges from relatively simple lighted small diameter tube called endoscope to more complex systems [Robert Demaus, 1996].

Ultrasonics or UPV (Ultrasonic Pulse Velocity) are used to asses the density and elastic mechanical properties of materials and to investigate defects in the integrity and crack depth into materials. A very general description of the operating process of the ultrasonic equipment is the sound propagation throughout materials, velocity measurement and its conversion [T. Shaji et.al, 2000].

X-ray computed tomography thermal neutrons are radiographic inspection methods that use specialized software to reconstruct 2D or complete three dimensional images from cross-section views through an object [www51]. The main advantage is that the resulted image represents accurately the internal and external geometry of the object and provides information about object materials (Fig. 3.3) [Lehmann, et al., 2005]. The technique is used for larger objects investigation as well [www52].

Magnetic surveys include several techniques used to measure variations in the magnetic field. Application areas include ordnance detection, pipe and cable location, mineshaft detection, archaeological surveys and geological fault location. Good quality magnetic data for ferrous objects may be difficult to obtain in areas with a high density of ferrous surface debris or in areas of “live” electrical cables.

Microgravity surveys are effective in determining the nature and extent of underground voids and cavities by measuring very slight variations in the earth's gravitational attraction at points across a site [www53].

3.3 Combining Laser Scanning Data with Surveying and Close Range Photogrammetry Data

The merging between geodetic measurements like tachymetry or GPS and laser scanning data is realized during or after the data processing operations. Usually, points acquired by tachymeter or GPS methods can be used as datum to register and to geo-reference point clouds or/with pairs of stereo-images. The geodetic point data is also used to connect non-overlapping scan and photogrammetric data, thus inaccessible regions to the laser scanner could be modeled with stereo-images. The geodetic data could be used also to control the quality of the laser scanning or close range photogrammetry results.

Currently, available scanners have incorporated (HDS 3000, [www55]) or mounted external (LMS-Z420i, [www56]) digital cameras that provide the RGB information for the scan data. Combining the 3D geometry quality of the scan data with photogrammetry is realized by using targets or entities that can be acquired by both of the measurement methods. The scan data can be used to describe the geometry of the site and high resolution images are used to map different geometric data. True orthophotos can be generated by combining the geometry of the scan data with color information obtained from registered digital images.

A common method imported from computer graphics is the texture mapping of the 3D model. The textures for the 3D objects are generated from acquired images using an automatically projection method or an UVW map editor. The UVW are called mapping or texture coordinates which are equivalent to the XYZ coordinates in the 3D spaces. Basically, the texture mapping specifies the connection between the points in a 3D object with the position of the image on the object. In other words, it specifies that to a point (x,y,z) in the mesh corresponds a pixel (u,v,w) in the given image. The first method uses common types of planar, cylindrical and spherical projections. There are two methods used to match the image with the UVW coordinates. The image is imported as background and the UVW's position is modified on the image or the UVWs are exported as a template image and used as background to match or paint the texture on it. The planar projection and the UVW mapping editor used to position a texture for a stained-glass window can be vizualized in (Fig 3.5). The planar projection automatically arranges the texture that contains also the pixels from the neighbouring wall. This can be corrected by applying a scale factor to the texture or manually editing the position of the UVWs.

After processing, the 3D or 2D data resulted from different methods is integrated into a complete model using export/import functions. Usually the model is exported as *.dxf or *.vrml file formats compatible with most of the CAD or modeling software. Accuracy losses might occur during the export/import operations due to the complexity of the model. When the different components are previously orientated the complete model is constructed directly after importing. If not, a geo-referencing procedure is required.

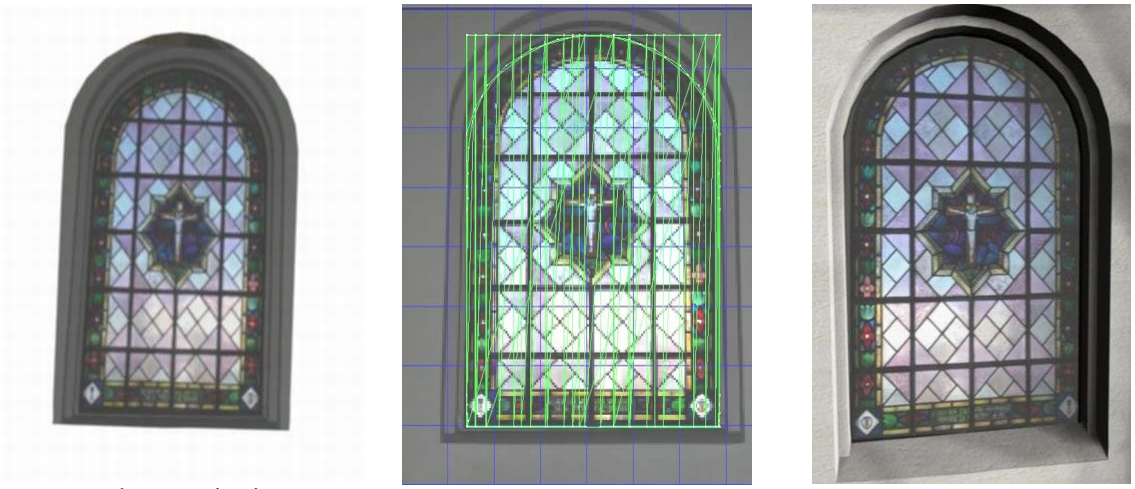

a. planar projection b. UVW map editor c. rendered image

Fig. 3.4 Texture mapping (e.g. stained-glass window, see Chap. 7.4)

3.4 Thermography Data Processing

Thermographic data processing, generally, leads to generation of reports containing temperature information referring to the object of interest. Two main groups of operations can be identified: one is used to visualize and enhance the thermograms and the other is used to obtain qualitative temperature information.

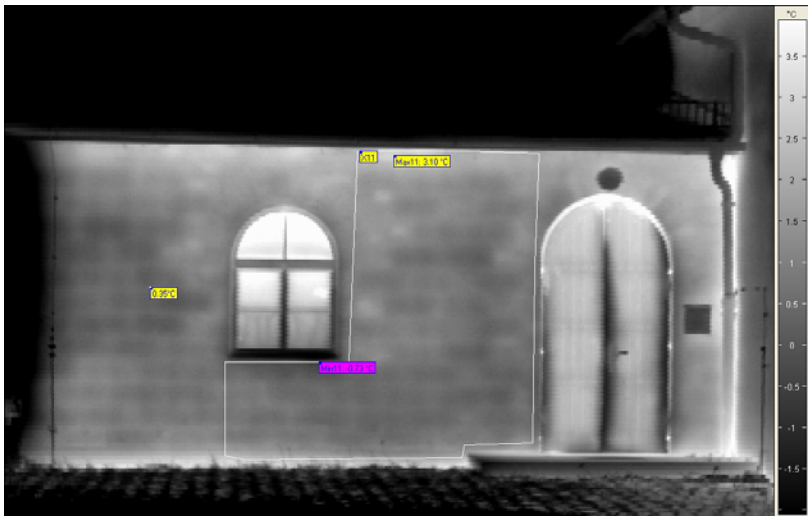

Fig. 3.5 Thermogram displayed in a black and white color palette (see Chap. 7.4)

Different color pallets or temperature intervals and levels are used to better visualize a phenomena or regions of the object. The temperature data is obtained visualizing the image accompanied by a legend or by digital tracing points, lines, circles or polygons on the image.

Other common operations are:

- the generation of profiles of the image or along a line;
- the computation of the histograms with temperature distribution;
- isotherms visualization;
- temperature correction using corrected emission level or other parameters specific to the object or to the measurement path;
- time analysis and animation when more thermograms were acquired at different intervals [www3].

There are two methods to integrate the thermographic data into the 3D model. One is to export the thermographs as image data format and using them as textures for mapping the 3D model. The second one implies the division of the 3D model in smaller individual parts and coloring or painting them corresponding to a temperature legend. The results of both methods have a more informative than a graphical character usually due to the low resolution of the thermographs. One solution is to merge or stitch more low resolution thermograms in order to obtain a high resolution one [www4]. It has also to be considerated that, when exporting the thermograms as image files, they contain only the information visible when exported. Images with different temperature level or intervals or other color palette can not be obtained directly in the CAD software. However, normally no accurate temperature measurements can be performed using the resulted 3D model.

In some cases both digital and thermographic exported images are mapped on the object in order to enhance the important regions from a thermography point of view (see e.g. Fig. 3.6).

Fig. 3.6 Building 3D model mapped with thermographic and digital images (see Chap. 7.4)

Chapter 4

From Point Cloud to 3D Model

This chapter deals with standard operations performed to generate a 3D model from point cloud data acquired by a terrestrial laser scanning instrument. The processes are described in an order that could form a general but not fixed working algorithm. Usually, more than one scan station is used to acquire data which covers the object of interest. A point clouds registration process is used to combine all the point clouds from different scan positions. This can be performed using one of the three types of registration or a combination of them: with targets, point cloud similarity and feature registration (see Chap. 4.1). Due to the systematic errors, hardware limitations, shadowing objects and other environmental factors in most of the cases the acquired data contain unwanted, missing and/or erroneous data. The impact of this data to the point clouds can be reduced using one of the point data treatment operations (see Chap. 4.2). The creation of a 3D model from a point cloud could be performed using for instance 3D geometric primitives fitting and CSG (Constructive Solid Geometry) operators, 3D curves fitting and low polygon generation, and 3D polygonal mesh creation (see Chap. 4.3). A list with the tested software and their capabilities related to the processes described in this chapter can be consulted in Annex II. The reminded algorithms are mostly semi-automatic and request the user intervention in order to evaluate the results returned by the software to the user inquiries regarding the quality of point clouds or the geometric objects.

4.1 Point Clouds Registration

Registration	▪ Target oriented registration	+ increased accuracy + allows geo-referencing - time request for target mounting and scanning
	▪ Point clouds or meshes similarity registration	+ reduces the on-site work + the resulted point cloud presents a consistent geometry (depending on the situation) - the accuracy has acceptable values only in conditions of a small scan raster - the geo-referencing is commonly not presented - requests extra processing time for large amount of data
	▪ Feature registration (spheres, cubes, cylinders, etc.)	+ similar to registration using point cloud and geometry similarity + reduces the processing time in the cases of large data sets - the accuracy has acceptable values only in conditions of a small scan raster - the geo-referencing is commonly not presented

Table 4.1 Point clouds registration types

4.1.1 Point Clouds Registration Using Targets

It is the most commonly used type of registration. Targets with different shapes or fabrics are mounted on site, on a tripod or directly on the scanned object. There are more advantages conducting the user to perform the point clouds registration with the help of the targets:

- the targets can be acquired also by using traditional surveying methods. In this way the geo-referencing of the point clouds can be achieved;
- the targets can be identified automatically or semi-automatically by the scanning software and their center point is identified and acquired with a better accuracy than a single point measurement. Generally, the range-scanner's accuracy for the single point measurements is in an interval of 10 to 5mm (at 1m to 100m distance from the scan head) and the target acquisition accuracy is increased by the algorithmic fit to 1-2mm or better.

When performing the registration of two different point clouds, one of them is considered fixed (home scan) and the other is considered to be floating (Fig. 4.1). The registration process consists in finding a set of parameters that can be applied to the floating point cloud in such a manner that will oriented it in the same coordinate system as the fixed point cloud. Usually, the set of parameters consists of three translations and three rotations corresponding with the coordinate system axes.

a. Fixed point cloud (Home scan)

b. Floating point cloud

A minimum of three identical targets in the point clouds fix-floating pair is needed in order to compute all six parameters. The transformation between the two coordinate systems shows the classical Helmert form with three translations along the X, Y and Z axes, three rotations about the X, Y and Z axes and the scale factor equal to 1 (unitless).

After the transformation parameters are determined, coordinates are computed in the fixed point cloud system for each point in

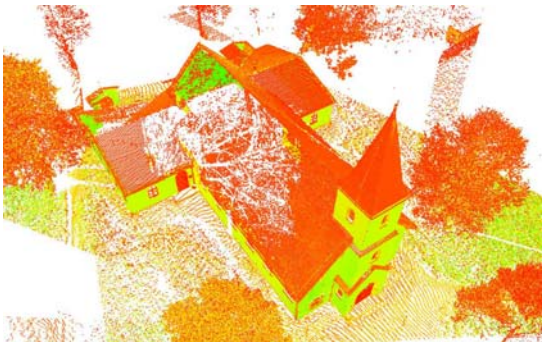

c. Merged point clouds

Fig. 4.1 Point clouds registration using targets (see Chap. 7.4, "Test objects",)

the floating point cloud. Another method is to consider the floating point cloud as singular geometry entity, computing its centroid and the corresponding coordinates in the fixed point cloud system.

The main disadvantage of this method is that only a small number of identical points from the overlapping region of the point clouds is used in the registration. Therefore, a visual inspection of the point cloud could reveal errors in cases of a bad geometry arrangement of the targets on site, even if the scripted result suggests a good registration.

These situations can be avoided if a number of more than three identical targets are used for the registration of the point clouds. Furthermore better results are obtained when these targets are forming a good geometry in the overlapping region.

For a reliable result, the targets arrangement on site has to be shaped in such a way that no details will be shadowed. This implies a good planning of the measurements campaign. Finally, the registration using targets is known as a time consuming method for mounting and scanning each target. In some cases, the regions where the targets are installed are rescanned with a higher resolution in order to be acquired automatically by the scanning software.

4.1.2 3D Similarity Registration

Several efforts have been made concerning the registration of point clouds without the need to use special targets. One of the developed methods is to use all points from the overlapping area of the point clouds pair. First steps were made with the design of the Iterative Closest Point algorithm (ICP) by [Besl and McKay, 1992] and [Chen and Medioni, 1992].

The ICP algorithm is an iterative descent procedure generally described in three steps:

- search for pairs of the nearest points in the fixed and the floating point clouds;
- estimate a rigid transformation that better aligns the floating point cloud with the fixed point cloud;
- apply the transformation to the floating point cloud.

The process is repeated until convergence is concluded. With a good initial estimate the ICP gives acceptable results. Problems could appear due to fact that the algorithm is assuming that one point set is a subset of the other [Fusiello et al., 2002] and due to the exhaustive search for the nearest point. In order to overcome these problems, several variants to ICP are proposed by [Zhang, 1992] [Masuda and Yokoya, 1995], [Bergevin et al., 1996], [Chetverikov et al., 2002] and [San Jose et al., 2004].

[Roth, 1999] developed a method that uses the intensity information supplied by most of the laser scanning devices and automates the feature matching process. Firstly, points of interest are computed in the intensity data of each of the two range images and then 3D triangles are constructed and matched by 2D points of interest. [Kim et al., 2002] proposes an iterative registration of multiple 3D data sets using the covariance matrix, and [Akca, 2004] uses a method to minimize the Euclidian distance between the surfaces by least squares (Least Square 3D Surface Matching, LS3D).

This registration method has several advantages:

- it does not require targets thus the on-site time is reduced;
- in contrast to the first type of registration, this method uses all points in the overlapping region of the two point clouds and the merged point cloud has a more consistent and reliable geometry.

The problems that could appear when performing this type of registration are within the used algorithm. The obtained result is far from being reliable when scanning with a small resolution or a larger raster data. Visible errors can easily be observed in the merged point cloud. Due to the lack of targets the geo-referencing of the point clouds can be realized by using a minimum of three known scanner positions.

4.1.3 Feature Registration

The previously described registration can be simplified by using only points from the overlapping region of two point clouds that can estimate different geometry primitives. The steps involved in the point clouds merging are:

- searching for pairs of correspondent points that can best-fit objects like patches, cylinders, spheres, etc.;
- estimate a transformation to better align a geometry primitive from floating point cloud to its correspondent in the fixed point cloud;
- applying the transformation to the floating point cloud.

As the previous one, the method does not require special targets. Points from the objects of interest are used and no extra scanning operations have to be performed. To eliminate a pointless search for points that better map geometry primitives, the method is semiautomatic. The user has to select from the fixed and floating point clouds only the points that can be used to estimate a primitive. The points are selected by simply defining a region of points or by using a region grow method.

Beside other facts, the accuracy of the method is a function of the primitive's best-fit accuracy. When a higher resolution is used in the scanning process, a better accuracy for fitting geometry objects to the point clouds could be obtained.

Used in practice, all the above described methods have their pros and cons (see Table 4.1) and they can give good results used as a singular technique for point clouds registration. However, a combined method using the geometrical shape of the site and scene features for combining point clouds and targets to validate and optional to geo-reference the results, is in general recommended to obtain complete and reliable results.

Merging point cloud process is complementary and optional to the registration and it is used to join previously registered multiple point clouds into a single point set. The resulted unified point cloud can improve the visualization performance and it is used for surface reconstruction.

4.2 Point Cloud Treatment

Point cloud treatment operations have to be applied to the point clouds before starting with the model creation. These processes are done before or after the registration procedure. They help to remove useless or erroneous data from the scanned point clouds or to improve the point quality.

4.2.1 Remove Unwanted Points

Other neighboring regions or objects could be captured also during the scanning process of the area of interest. Points that are not used for future registration or modeling are entering the category of unwanted entities and they have to be removed in order to clarify the scene and to have a better view of the objects of interest.

a. Unwanted points (e.g. tree and car) **b. Unwanted points removed**

Fig. 4.2 Unwanted points removal

In the above sketch (Fig. 4.2) position a. reveals the presence of two categories of unwanted points:

- points that do not disturb or influence the area of interest (e.g. the tree);
- obstacles in the area of interest (e.g. the car).

If in the first category, the removal of the unwanted points causes no changes to the object of interest, the elimination of the points from the second category could reveal missing points in the object of interest. If the area is also scanned from other positions, the unwanted points could enter the first category.

The process is so far not automatic, the user has to select and remove the unwanted points manually. Problems can appear due to the subjective type of the process. If unwanted points are near or intersect with the wanted points, often the later ones could be erroneously eliminated.

4.2.2 Detect and Remove Outliers

Outliers are points that statistically do not fit the pattern that describes most of the point cloud. They are introduced during the scanning process and could produce errors when the point cloud is modeled. Generally algorithms for outlier detection can be compressed in the following steps [Förstner, 1998], [Kraus, 1997], [www6]:

- compute a global solution (e.g. plane, shere, etc.) using all the points;
- test the normalised residuals;
- remove the points that are most likely to be gross errors based on the previous test;
- stop if no such points occur or iterate the algorithm omitting the points removed in the prior step.

Some of the alternative robust estimators algorithms are:

- the Danish Method uses so-called M-estimators and equivalent weights that are computed after the first least square estimation. The least square adjustment and the reweighing process is repeated with these weights until the algorithm converges [Wieser, 2001];
- the L_1 norm minimization method estimates the parameters by minimizing the sum of absolute residuals. A iterative process of exchanging basic and non-basic variables is used until the objective function reaches a minimum [Marschall and Bethel, 1996];
- the Fuzzy logic method assigns fuzzy membership values to acquired data and the outlier data is given according to the magnitudes of these values [Gökalp, 2005].

Due to the complexity of the detection algorithm, the process is a semi-automatic one. The user has to set a sensitivity value (significance level) for the outlier search and to decide if the returned points are erroneous or not.

a. Outlier detection using a larger significance level

b. Outlier detection using a smaller significance level

Fig. 4.3 Outlier detection and removal

A section of a point cloud is represented in Fig. 4.3. The “circle” is the geometric primitive that can be fitted to the point cloud. If a larger value for the significance level is used, only outliers situated farthest from the main body of the model (circle) are selected. If the process is repeated and the significance level is lowered (sensitivity value

increased), points situated nearby the main body are also selected and the user has to decide if these points are also errors or not.

4.2.3 Detect and Remove Disconnected Components

Disconnected components are satellites of the main body of a point cloud. A process for their detection and removal can be described in some main steps:

- set a value for the size of the components that will be identified as disconnected;
- set a value for the distance between the components and the main body of the point cloud to establish if they are disconnected;
- evaluate the point clouds and the results with respect to the a priory knowledge of the site and the modeling goal;
- remove the disconnected component if not necessary.

In Fig. 4.4 the upper view of the point cloud of a building and neighboring objects are represented. Fig. 4.4a illustrates the selection of the disconnected components by size, ignoring the distance to the main body. Fig. 4.4b shows the selection with respect to the distance between satellites and main body of the point cloud. The main body is represented by the area of the scan were most of the points are concentrated.

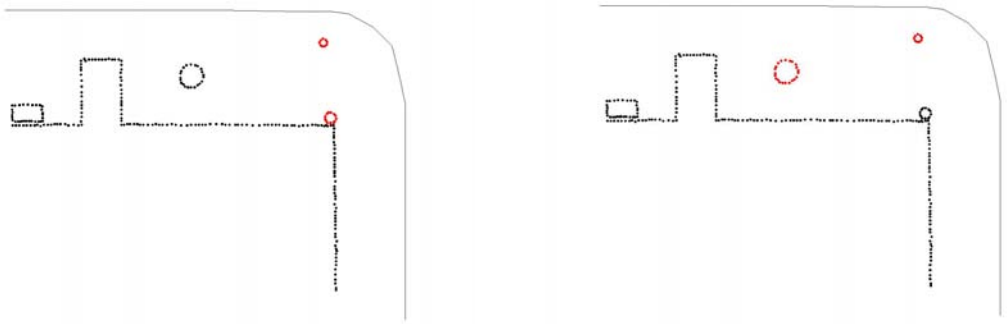

a. Disconnected components by size **b. Disconnected components by distance**

Fig. 4.4 Detection and removal of the disconnected components

4.2.4 Noise Reduction

The noise reduction process eliminates or reduces the noise in a point cloud and smoothes the scan data. The combined physical characteristics of the laser beam and the scanned object can cause false points acquirement due to an incorrect evaluation of the distance between laser head and object. The laser beam divergence, the incidence angle between laser beam and the object, object's color, texture, surface reflectivity, laser type, scan resolution, etc. are components that might introduce false or unwanted data in the point cloud like "phantom points", "jumping points" or "in depth points".

Fig. 4.5 "Phantom points" (project "Test objects", see Chap. 7.4)

The main cause of the „phantom points" appearance is the incidence angle between the laser scan beam and the object's edges [Cheok et. al., 2002]. The process is amplified by the distance between laser head and object, and laser beam divergence. A splitting signals effect occurs when scanning the edge and two incidence points are reported. The recorded range is an interpolation between two ranges, thus, a „phantom point" is created (Fig. 4.5).

The detection and removal of this category of false points is to be performed manually by an operator during the point cloud inspection or later during the inspection of the triangular mesh. An automatic process is difficult to be applied due to the fact that the errors of these points are too small to consider them as outliers or disconnected points.

The „jumping points" occur due to the surface reflectivity and the falsely recorded points have an offset from the real object surface. The false points could be revealed after a visual examination of the point cloud or of the triangular mesh (Fig. 4.6):

- some of the points are clearly not in the correct position on the object surface;
- the acquired object has clearly different dimensions than the real one.

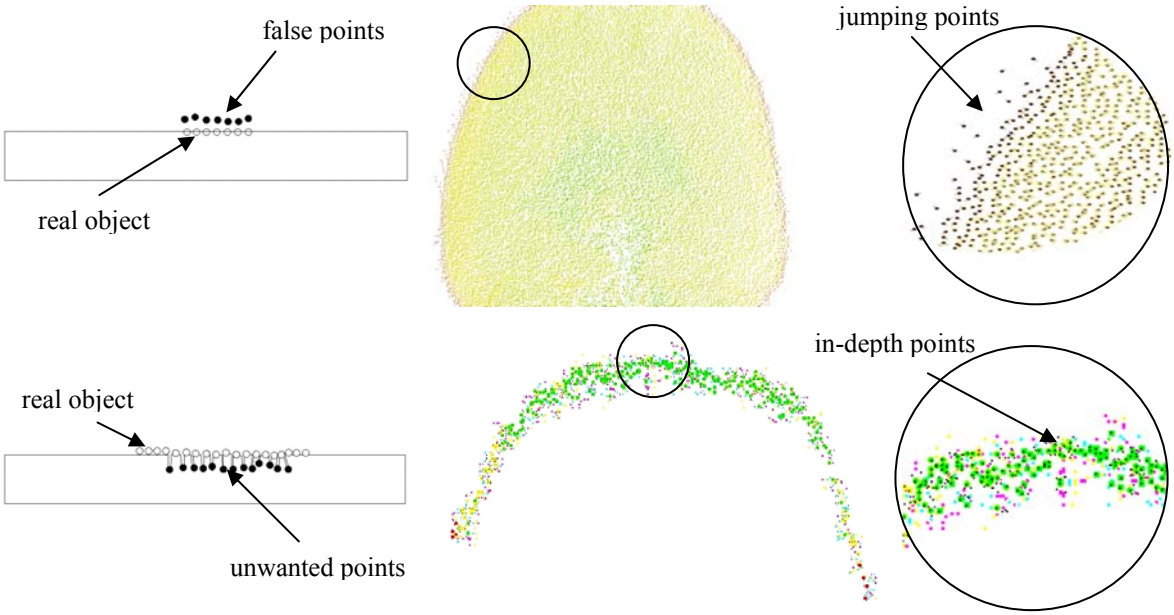

Fig. 4.6 "Jumping" and "in-depth" points (see project "Test objects", Chap. 7.4)

Scanned objects with a porous surface could lead to a different type of noise data. So called „in-depth points" appear when the laser beam penetrates the scanned object's surface (Fig. 4.6). Usually, a time consuming visual inspection of the point clouds reveals the affected regions (areas that appear thicker than in reality). Sometimes, viewing the point cloud in sections helps to detect them.

The reduction of the noise data is performed by best-fitting a form to the point clouds, and determining the points that are deviating from this form. The user has to consider that:

- if the algorithm computes the best-fit form, it uses also the noise data and thus the resulted shape has an amount of uncertainty;
- the amount of noise data has to be estimated correctly; an overestimated noise level can lead to point cloud alteration and an underestimated one could lead to false results.

4.2.5 Redundancy Reduction, Point Clouds Sampling and Decimation

During the registration process points from the overlapping region are used to orient two different point clouds and thus the resulted cloud displays areas with redundant data. The extra amount of data could increase the point cloud processing time and optionally can be reduced using a redundancy filter. A mean value for the distance between points is computed or set by the user and within this value points are eliminated automatically. The mean value is used to determine if two points can be identified as identical, in such case, one point can be removed (by erasing one of the identical points or by computing a mean point).

The sampling and decimation processes refer to a systematic reduction of the extra point data without changing the shape of the point cloud. Basically, it decreases the number of the points in a scan. As a direct effect it has a lower computation time for further operations.

The uniform sampling operation eliminates point data according to a ratio to original percentage or point count.

In the grid sampling operation, a vertical and horizontal point spacing value is used to divide the model space into a identically sized cells, and all but one point are eliminated from every cell.

The curvature sampling operation is used to reduce points based on curvature. The process preserves points from regions with high curvature and reduces the point number from flat regions.

- Initial point cloud
- 208,798 points

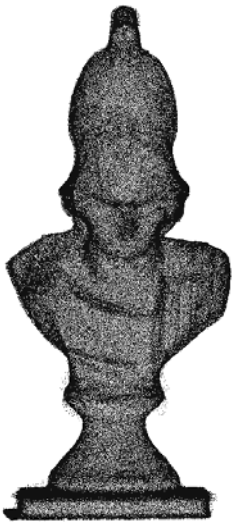

- Uniform sampling
- 66,579 points

- Grid sampling
- 66,758 points

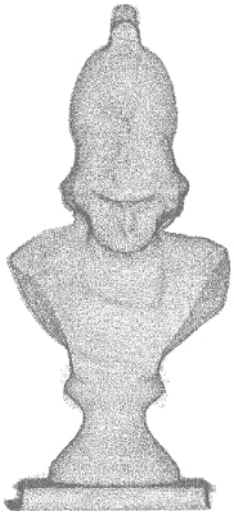

- Curvature sampling
- 75,247 points

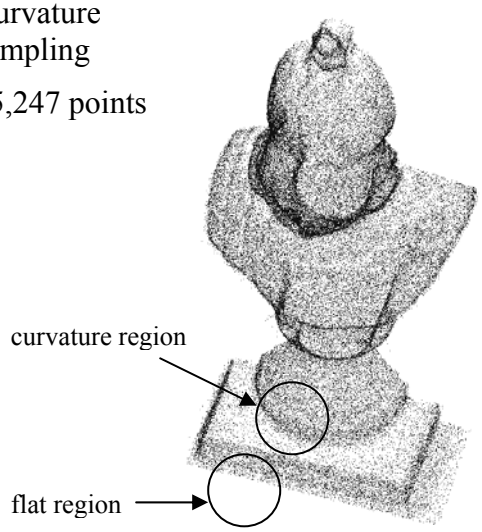

Fig. 4.7 Point clouds sampling: uniform sampling (performed with Cyclone 5.1), grid sampling (performed with Geomagic Studio 6[2]), curvature sampling (performed with RapidForm 2004[3]), (see project "Test objects", Chap. 7.4)

4.2.6 Adding Points

Adding points operation is used mainly in generating automatically new point data in order to fill the holes in the point clouds or to refine the point cloud.

Regions with missing data are more visible after the removal of all the unwanted points from the scan data. If the missing data can not be completed by scanning the object from other positions, a filling holes procedure can be performed. The process can be performed at the stage of the point cloud treatment, otherwise during or after the surface reconstruction phase.

[2] Raindrop Geomagic Studio 6 demo version license in the period 22. Oct – 21 Nov. 2004

[3] RapidForm 2004 demo version license in the period 08.Jun. - 08. Aug. 2003

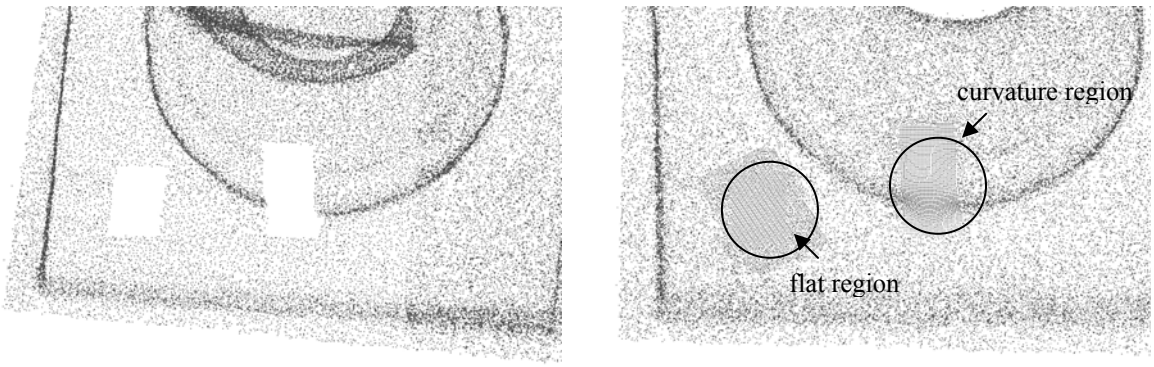

a. Point cloud with missing data **b. Point cloud after filling holes**

Fig. 4.8 Hole filling process performed with Geomagic Studio 6 (see project "Test objects", Chap. 7.4)

Some of the factors that drive the user to perform the hole filling operation during the surface reconstruction stage are described as follows:

- on the point stage small or medium holes are hard to be detected;
- small or medium holes in the point cloud do not imply automatically future problems for surface reconstruction (flat surfaces can be reconstructed with a small number of point data);
- the surface reconstruction process can reveal or generate extra holes not detectable in the initial point data;
- the filling holes algorithm on the surface reconstruction stage offers more reliable results;
- some algorithms have problems if a large raster was used to scan the object;
- the holes in the curvature regions are treated better in the surface reconstruction stage;
- in most of the cases a hole filling operation during the surface reconstruction stage is not avoidable.

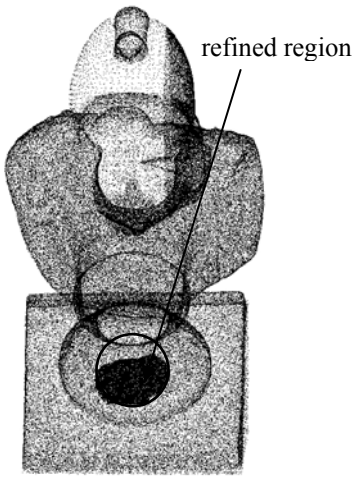

Fig. 4.9 Refining point cloud (performed with Geomagic Studio 6)

A refining operation is used to increase the number of points in the scan data by subdividing the scan grid. It is used in order to obtain a denser and smoother model during the surface reconstruction process.

The user has to consider that:

- the process does not improve the quality of the point cloud;
- for scans with large acquisition raster the process does not smooth the model;
- the process does not replace the fitting holes operation;
- usually, the process generates more computation time to construct surfaces.

4.3 Create 3D Geometry from Point Clouds

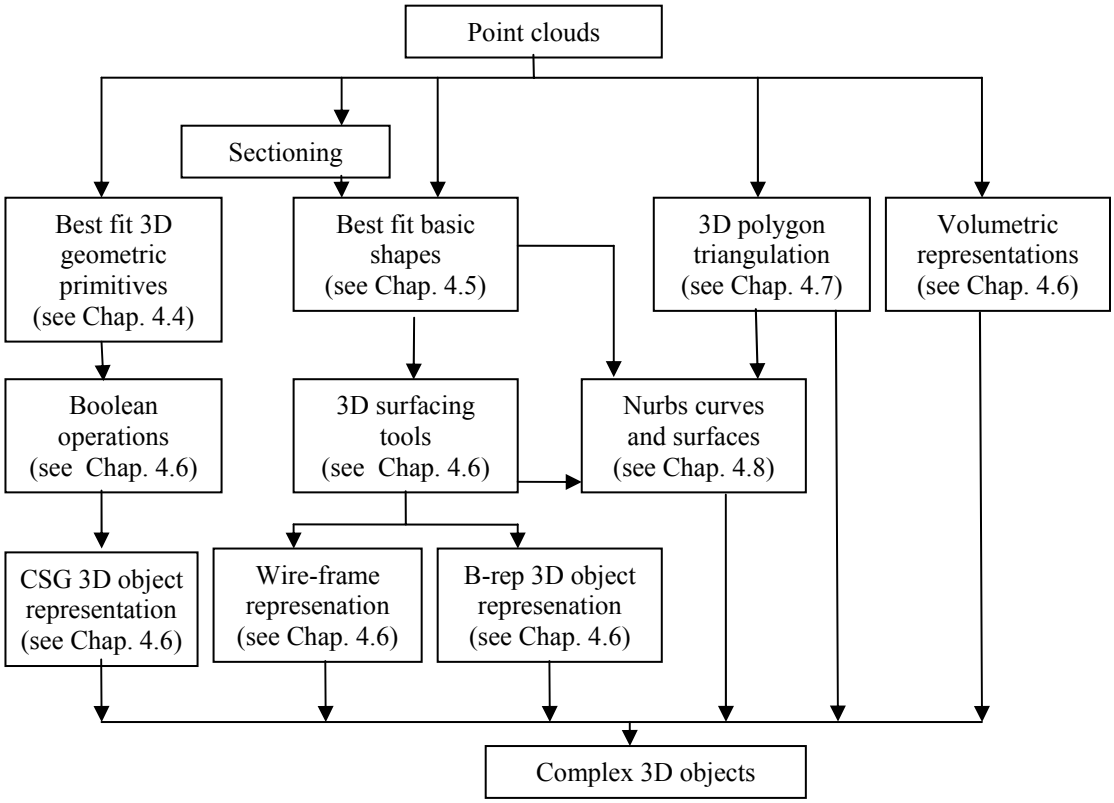

Fig. 4.10 Create complex 3D objects from point clouds – generic scheme

The following sections describe the methods that can be inquired in order to create complex 3D geometry starting from point cloud data. As represented in Fig. 4.10, the user has a large spectrum of tools that can be involved when performing this task. The methods for 3D object creation are divided in categories highly subjective to the ones used in the case scenarios. This explains why volumetric representations (voxels, octree, etc.) are just reminded and not treated in more detail. The chosen method for 3D object creation is highly depending of factors like the available software, the form of the final product, accuracy request, the end user compatibility, etc. Also it has to be considered that depending on the project nature and accuracy request, parts of the final product can be realized involving different methods and in the end connecting them together. For example, the point clouds of a building flat wall with bas-relief elements can be modeled as a basic primitive plane estimate for the flat wall and a triangulation mesh for bas-relief elements. In these cases the user has just to avoid non-compatibility problems due to the involved software.

4.4 Create and Fit Basic Geometric Primitives

One of the methods to obtain the reconstructed surface of a scanned object is by creating and fitting basic objects to the point clouds. Geometric primitives like planar patches, spheres, cylinders, cones and other objects like pipes, elbows, steel sections, etc. can be gradually fit to the point data in order to obtain a completely reconstructed scene (Fig.

4.11). Also sections made through out the point clouds could reveal basic geometrical shapes like line segments, circles, ellipses, curves etc. which are used in basic CG (computer graphics) operations and in 3D surfaces construction (4.6)

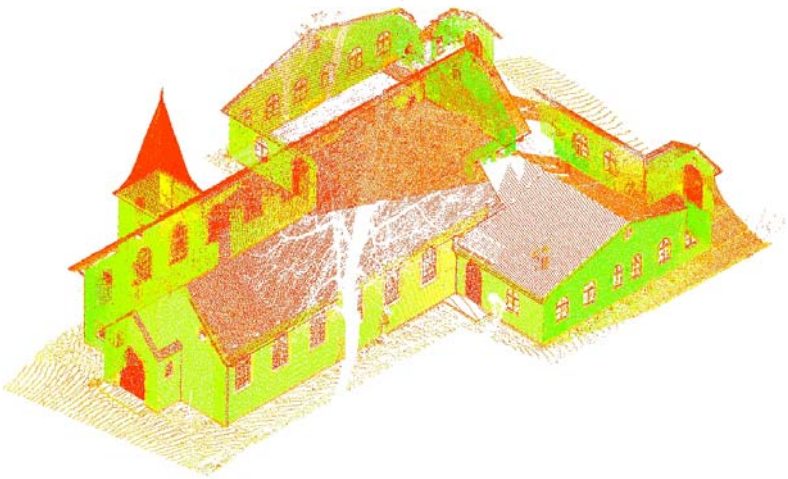

a. Point cloud

b. Reconstructed model

Fig. 4.11. Reconstructed model with geometric primitives
(see project "Test objects", Chap. 7.4)

To fit a geometric primitive to a point cloud implies two main actions:

- find the best geometric primitive to be mapped by the point cloud;
- compute the estimation parameters to best-fit the geometric primitive to the point data.

Sub-sets of point data resulted from manual or automatic segmentation of the point cloud are used to search the model library for the geometric primitive that best matches the sub-selection. A set of parametric estimators are used later to best-fit the found geometric primitive to the point data.

The next sections are describing the fitting procedure for geometric primitives as the planar patch and the sphere.

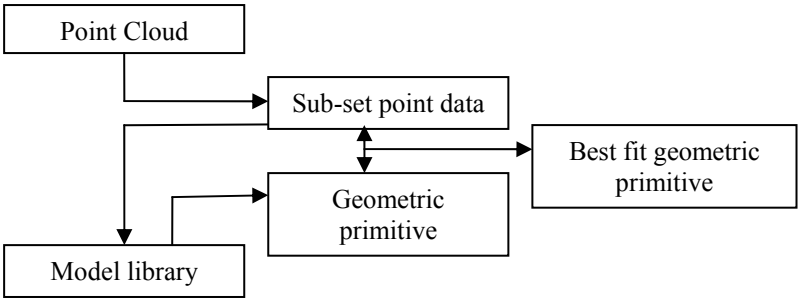

Fig. 4.12 Fitting a basic object to a point cloud

4.4.1 Fitting a Planar Patch to 3D Point Sets

To fit a planar patch to a set of 3D point data can be translated in minimizing the distances D_i between the given points and a planar patch. The *a*, *b*, *c*, *d* parameters that give the plane equation $ax + by + cz + d = 0$ are estimated so that the distance D_i is minimized, where

$$D_i = \frac{(ax_i + by_i + cz_i + d)^2}{a^2 + b^2 + c^2} \tag{4.1}$$

with x_i, y_i, z_i as the 3D point data.

Basically, three methods can be used to fit a planar patch to a 3D point cloud:

a) create a planar patch from three selected points;

b) create and fit a planar patch using a region grow procedure;

c) fit a planar patch to a set of 3D points.

a) Creating a planar patch from three selected points

The equation of a plane defined by three points is given by e.g. [Bourke, 1989], [www57]:

$$A_1 x + A_2 y + A_3 z - A = 0 \tag{4.2}$$

where

$$A = \begin{vmatrix} x_1 & y_1 & z_1 \\ x_2 & y_2 & z_2 \\ x_3 & y_3 & z_3 \end{vmatrix} \tag{4.3}$$

and A_i (i=1:3) is the determinant obtained by replacing x, y, or z column vectors with a column vector of 1.

The planar patch boundary is given by the line segments defined by the points.

b) Creating and fitting a planar patch with a region grow procedure

The procedure assumes the selection of one or more points from the point cloud and the definition of two tolerances:

- one tolerance gives the maximum distance between two adjacent points that defines if the points are to be included in the fit calculation;
- and one tolerance defines the surface planarity.

To create and fit the planar patch the Random Sample Consensus Algorithm [Fischer and Bolles 1981] can be used. Unlike other methods, RANSAC uses only a small set of points as data to obtain the initial solution, and then enlarge this set with consistent data.

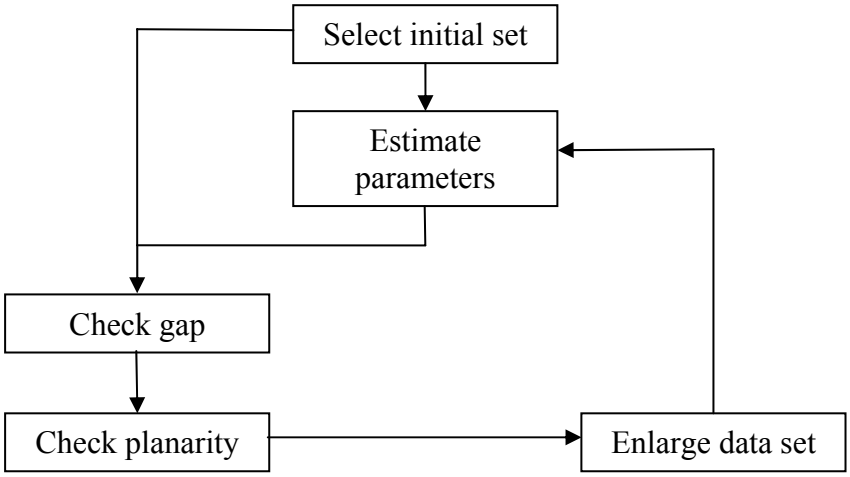

Fig. 4.13 Fitting a planar patch to a 3D set of points

The fitting algorithm can be resumed in the following steps:

- select a random set of points;
- if there were less than three required points selected, the number of required points is completed with adjacent points that satisfy the assumed tolerances;
- estimate the parameters with current data set;
- search for compatible points adjacent to current data within tolerance;
- if no points are found, the algorithm is stopped and current solution is accepted, else enlarge the data set;
- repeat last three steps.

The distance or the gap tolerance is used to search for points in the point cloud that are close enough to the current point set, in order to consider them included in the current planar patch computation. If the distance tolerance is not qualifying, this does not suggest that these points are not coplanar with the current point set (e.g. see Fig. 4.2a). It implies that they are not included in the current fitting solution. The situation can appear in practice, e.g. while scanning a wall that is shadowed by neighboring trees. One solution is to compute different planar patches for the individual coplanar regions and then to merge them into a larger planer patch. Another solution for initial estimation is to select points

from different regions and the planar patch will be estimated with points from all selected regions.

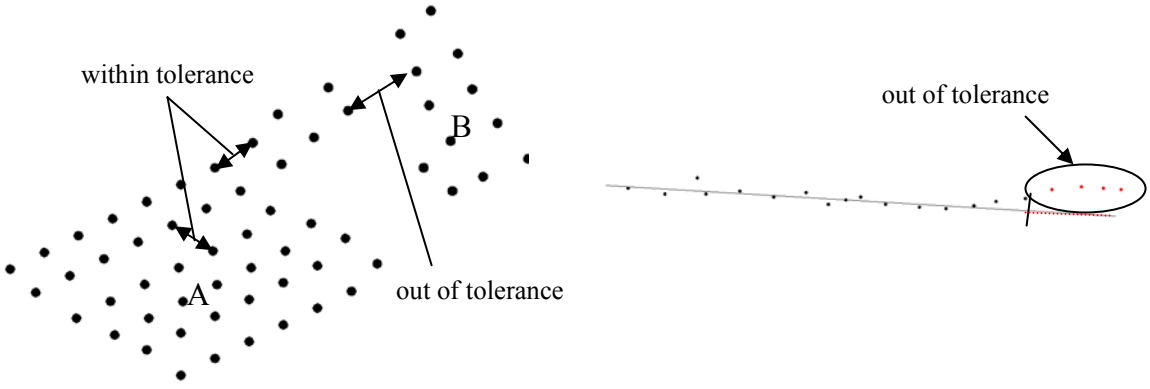

a. Gap tolerance **b. Planarity tolerance**

Fig. 4.14 Tolerances in planar patch region grow algorithm

The planarity tolerance decides if the points found in the neighboring areas of the current data set are coplanar or not with the current solution.

The next step implies the computation of plane parameters using the current data set. For a three points data set the solution is given by the formulae 4.2 and for data sets larger than three points, a least square algorithm is used.

c) Fitting a planar patch to a set of 3D points

This is usually accomplished by a least square fitting procedure. The plane parameters *a*, *b*, *c*, *d* are estimated with the condition:

$$f(a,b,c,d) = \sum d_i^2 \rightarrow \min . \qquad 4.4$$

It is assumed that the least-square plane contains the centroid of the data. This gives:

$$d = -(a \cdot x_0 + b \cdot y_0 + c \cdot z_0) \qquad 4.5$$

where x_0, y_0, z_0 are the coordinates of the centroid. With this assumption the plane equation is written as:

$$a \cdot (x_i - x_0) + b \cdot (y_i - y_0) + c \cdot (z_i - z_0) = 0 , \qquad 4.6$$

with i=1: n, where n is the number of points.

The point to plane distance condition equation rewrites as:

$$f(a,b,c) = \sum \frac{(ax'_i + by'_i + cz'_i)^2}{a^2 + b^2 + c^2} \qquad 4.7$$

where:

$$x_i' = x_i - x_0 \qquad y_i' = y_i - y_0 \qquad z_i' = z_i - z_0 \qquad 4.8$$

are the normalized point data.

And in matrix form:

$$f(x) = \frac{\boldsymbol{x}^t \cdot \underline{\boldsymbol{N}} \cdot \boldsymbol{x}}{\boldsymbol{x}^t \cdot \boldsymbol{x}}, \tag{4.9}$$

where $\boldsymbol{x}$ is the unknown vector and $\underline{\boldsymbol{N}}$ the normal matrix.

$$\boldsymbol{x}^t = \begin{bmatrix} a & b & c \end{bmatrix} \tag{4.10}$$

$$\underline{\boldsymbol{N}} = \underline{\boldsymbol{A}}^t \cdot \underline{\boldsymbol{A}} \tag{4.11}$$

$$\underline{\boldsymbol{A}} = \begin{bmatrix} x_1' & y_1' & z_1' \\ x_2' & y_2' & z_2' \\ . & . & . \\ . & . & . \\ . & . & . \\ x_n' & y_n' & z_n' \end{bmatrix}. \tag{4.12}$$

After SVD (Singular Value Decomposition) of $\underline{\boldsymbol{A}}$ is computed:

$$\underline{\boldsymbol{A}} = \underline{\boldsymbol{U}} \cdot \underline{\boldsymbol{\Sigma}} \cdot \underline{\boldsymbol{V}}^t \tag{4.13}$$

where $\underline{\boldsymbol{\Sigma}}$ is a $n \times 3$ matrix containing the singular values of $\underline{\boldsymbol{A}}$ and $\underline{\boldsymbol{U}}$ is an $n \times n$ matrix, $\underline{\boldsymbol{V}}$ is an 3×3 orthogonal matrix having as columns the singular vectors of $\underline{\boldsymbol{A}}$. The normal matrix becomes:

$$\underline{\boldsymbol{N}} = \underline{\boldsymbol{V}} \cdot \underline{\boldsymbol{\Sigma}}^2 \cdot \underline{\boldsymbol{V}}^t. \tag{4.14}$$

In the end, the least-squares plane contains the centroid of the data, and its normal is the singular vector of $\underline{\boldsymbol{A}}$ corresponding with the smallest singular value [Golub, 1989].

Quality parameters of the computed estimators like the maximum and the medium offset or an empirical deviation value could be determined using the distances D_i from the points to the estimated plane:

$$s = \sqrt{\frac{D_i^2}{n-3}}. \tag{4.15}$$

The algorithm can be simply written in Matlab:

X=[x;y;z];	% input 3D point set
X0 = mean(X)';	% find centroid
A = [(X(:, 1) - x0(1)) (X(:, 2) - x0(2)) (X(:, 3) - x0(3))];	% form matrix A
[U, S, V] = svd(A);	% compute SVD of A
[s, i] = min(diag(S));	%find the smallest singular value in S
n = V(:, i);	%extract from V the corresponding right singular vector
d=A*n/sqrt(n(1,1)^2+n(2,1)^2+n(3,1)^2)	%distance from point to plane
MaxE=max(abs(d)); MeanE=mean(d)	%determine the maximum and medium offset
sizeX=size(X); sizeX=sizeX(1,1);	
s=sqrt((d'*d)/(sizeX-3))	%compute empirical deviation

Table 4.2 Best-fit plane using singular value decomposition – Matlab code

An alternative to the SVD approach is the classical polynomial regression where the z coordinate is computed as function of x and y coordinates:

$$z = a_0 + a_1 x + a_2 y \qquad 4.16$$

X=[x;y;z];	% input 3D point set
x1=X(:,1);	
x2=X(:,2);	
y=X(:,3);	
X = [ones(size(x1)) x1 x2];	%write design matrix $\underline{A}$
a=X\y	%compute polynomial regression parameters
ys=X*a; u=y-ys;	%compute deviation
s=sqrt(u'*u/(sizeX-3))	%compute empirical deviation

Table 4.3 Best-fit plane using polygonal regression – Matlab code

The above algorithms are tested successfully using large point data sets (over 300000 points) and respond with similar solutions in calculation time of few seconds. It can be considered that the PR (polygonal regression) algorithm has a slight advantage over then SVD algorithm due to the memory usage. The PR method stores a design matrix with $n \times 3$ elements while the SVD algorithm stores two more large matrices ($\underline{\mathbf{\Sigma}}$ and $\underline{\boldsymbol{U}}$). To minimize this disadvantage the "economy size" decomposition can be used that computes the matrix $\underline{\mathbf{\Sigma}}$ only with the first 3×3 elements [Matlab help]. The advantage of the SVD method in comparison with the polynomial regression is given by the fact that direct solution is obtained and the estimates are computed considering the errors on all three coordinates.

Another alternative approach to SVD is to consider, at first stage, the plane as a slope-intercept form [Wang and Tseng, 2004] and calculate the initial estimators. Then by linearizing the point to the plane equation the corrections $\Delta a, \Delta b, \Delta c$ are computed. The best-fit plane is determined if the computation converges.

4.4.2 Fit a Sphere to a 3D Point Sets

Three methods can be used to fit a sphere to a 3D point cloud:

a) create a sphere from four selected points;

b) create and fit a sphere using a region grow procedure;

c) fit a sphere to a set of 3D points.

a) Creating a sphere from selected points

At least four points are needed to define a sphere with unknown radius r and center point (x_m, y_m, z_m) uniquely:

$$(x_i - x_m)^2 + (y_i - y_m)^2 + (z_i - z_m)^2 = r^2, \tag{4.17}$$

with i=1:n, where n is the number of points.

In order to determine a sphere, four initial points have to respect the following conditions:

- no more than three of them can be coplanar;
- no more than two combinations of them can be collinear.

Starting with the sphere equation given by four points e.g. [Beyer, 1987], [Bourke, 2002]:

$$A = \begin{vmatrix} x_m^2 + y_m^2 + c_m^2 & x_m & y_m & z_m & 1 \\ x_1^2 + y_1^2 + z_1^2 & x_1 & y_1 & z_1 & 1 \\ x_2^2 + y_2^2 + z_2^2 & x_2 & y_2 & z_2 & 1 \\ x_3^2 + y_3^2 + z_3^2 & x_3 & y_3 & z_3 & 1 \\ x_4^2 + y_4^2 + z_4^2 & x_4 & y_4 & z_4 & 1 \end{vmatrix} = 0 \tag{4.18}$$

it can be proven that:

$$x_m = \frac{1}{2} \cdot \frac{A_2}{A_1},\ y_m = -\frac{1}{2} \cdot \frac{A_3}{A_1},\ z_m = \frac{1}{2} \cdot \frac{A_4}{A_1},\ r = x_m^2 + y_m^2 + z_m^2 - \frac{A_5}{A_1}, \tag{4.19}$$

where A_i are minors obtained by removing the first row and the column i from the determinant A.

b) Estimation of a sphere to a set of 3D points

The sphere parameters are estimated using a least-square approach (see also [Eberly, 2001]):

$$f(a,b,c,r) = \sum_{i=0}^{n} (d_i - r)^2 \rightarrow \min \tag{4.20}$$

where $d_i = \sqrt{(x_i - x_m)^2 + (y_i - y_m)^2 + (z_i - z_m)^2}$.

The above condition is respected if the partial derivates of 4.20 are equal to zero:

$$\frac{\delta f(x_m, y_m, z_m, r)}{\delta x_m} = 0, \frac{\delta f(x_m, y_m, z_m, r)}{\delta y_m} = 0,$$

$$\frac{\delta f(x_m, y_m, z_m, r)}{\delta z_m} = 0, \frac{\delta f(x_m, y_m, z_m, r)}{\delta r} = 0. \tag{4.21}$$

Setting these derivates equal to zero yields:

$$
\begin{aligned}
r &= \frac{1}{n}\sum_{i=0}^{n} d_i \\
x_m &= \frac{1}{n}\sum_{i=0}^{n} x_i + r' \cdot \frac{1}{n}\sum_{i=0}^{n} \frac{x'_m - x_i}{d_i} \\
y_m &= \frac{1}{n}\sum_{i=0}^{n} y_i + r' \cdot \frac{1}{n}\sum_{i=0}^{n} \frac{y'_m - y_i}{d_i} \\
z_m &= \frac{1}{n}\sum_{i=0}^{n} z_i + r' \cdot \frac{1}{n}\sum_{i=0}^{n} \frac{z'_m - z_i}{d_i}
\end{aligned}
\qquad 4.22
$$

The process is iterated until the solution converges. For the first iteration the center of the sphere can be determined as:

- the centroid of the point set if the point cloud is uniform distributed on the sphere surface;
- the center of a sphere given by four random points from the point set.

```
load L;
sizeL=size(L,1);
iteration='j';
Xm=sum(L)/sizeL;
Xc=Xm(1,1); Yc=Xm(1,2); Zc=Xm(1,3);                                   %compute
X=L(:,1); Y=L(:,2); Z=L(:,3);                                         centroid
for i=1:4  a(i,1)=X(i,1); a(i,2)=Y(i,1); a(i,3)=Z(i,1); a(i,4)=1;              end
M11=det(a);
for i=1:4  a(i,1)=X(i,1)^2+Y(i,1)^2+Z(i,1)^2; a(i,2)=Y(i,1); a(i,3)=Z(i,1);  a(i,4)=1; end
M12=det(a);
for i=1:4  a(i,1)=X(i,1)^2+Y(i,1)^2+Z(i,1)^2;  a(i,2)=X(i,1); a(i,3)=Z(i,1);  a(i,4)=1; end
M13=det(a);
for i=1:4  a(i,1)=X(i,1)^2+Y(i,1)^2+Z(i,1)^2; a(i,2)=X(i,1); a(i,3)=Y(i,1); a(i,4)=1; end
M14=det(a);
for i=1:4  a(i,1)=X(i,1)^2+Y(i,1)^2+Z(i,1)^2; a(i,2)=X(i,1); a(i,3)=Y(i,1); a(i,4)=Z(i,1);
end
M15=det(a);                                                           % determine the
Xn=0.5*M12/M11                                                        initial
Yn=-0.5*M13/M11                                                       approximation
Zn=0.5*M14/M11
r=sqrt(Xn^2+Yn^2+Zn^2-(M15/M11))
while iteration =='j'
for i= 1:sizeL  d(i)=sqrt((X(i,1)-Xn)^2+(Y(i,1)-Yn)^2+(Z(i,1)-Zn)^2);  end
for i=1:sizeL corX(i)=(Xn-X(i,1))/d(i); corY(i)=(Yn-Y(i,1))/d(i); corZ(i)=(Zn-
Z(i,1))/d(i); end
Xnew=Xc+r*mean(corX) Ynew=Yc+r*mean(corY) Znew=Zc+r*mean(corZ)
iteration=input('Iterate the process? j/n [j]: ', 's');
if isempty(iteration) iteration='j'; end                              % determine the
if iteration=='j'  Xn=Xnew; Yn=Ynew; Zn=Znew; rn=mean(d);  r=rn       estimators
else    for i= 1:sizeL  d(i)=sqrt((X(i,1)-Xn)^2+(Y(i,1)-Yn)^2+(Z(i,1)-Zn)^2);   v(i)=d(i)-
r;  end
MaxCorr=max(abs(v));  MeanCorr=mean(v);  vv=v*v';  s=sqrt(vv/(sizeL-4))  end end
```

Table 4.4 Best-fit sphere using iteration algorithm – Matlab code

The estimators' quality could be described by the distances from the points to the sphere surface. Thus a maximum, a mean offset or an empirical error could be determined by comparing the distances d_i from the points to the estimated sphere center with the estimated radius r.

The described algorithm has slight advantages with respect to the classical Gauss-Helmert method mainly due to the low memory usage and smaller response time. The algorithm can be written in Matlab code as in Table 4.4.

An alternative for the previous algorithm is the polynomial regression if the equation of the sphere is written as [Teubner, 1996]:

$$a_1x^2 + a_2y^2 + a_3z^2 + a_4x + a_5y + a_6z + a_7 = 0\,. \qquad 4.23$$

The above equation describes a sphere if the parameters a_1, a_2, a_3 are equal. If present the differences suggest the ellipsoidal form of the input data set. The coordinates of the sphere center and its radius can be determined direct from the parameters of the above equation:

$$\begin{aligned} x_m &= -\frac{a_4}{2a_1} \\ y_m &= -\frac{a_5}{2a_2} \\ z_m &= -\frac{a_6}{2a_3} \\ r &= \sqrt{x_m^2 + y_m^2 + z_m^2 + a_7}\,. \end{aligned} \qquad 4.24$$

To validate the different estimators a maximum deviation or an empirical deviation of the data can be computed. The tested algorithm in Matlab (see Table 4.5) showed a better handling for large set of data points than the one described previouslly. Problems arise if the point clouds are not defining a rigorous sphere and a correct radius estimator can not be identified (an incorrect or partial solution can be generated by computing a mean value for the parameters a_1, a_2, a_3).

X=[x;y;z];	% input 3D point set
x=X(:,1);	
y=X(:,2);	
z=X(:,3);	
A=[x.^2 y.^2 z.^2 x y z];	%write design matrix A
a=A\ones(size(x))	%compute polynomial regression parameters
x0=-a(4,1)/(2*a(1,1))	%compute center point
y0=-a(5,1)/(2*a(2,1))	
z0=-a(6,1)/(2*a(3,1))	
a7=1/a(3,1);	
R=sqrt(x0^2+y0^2+z0^2+a7)	%compute radius
u=A*a-1	%compute deviation for each point
MaxDev=max(abs(u))	%compute maximum absolute deviation
s=sqrt(u'*u/(n-7))	%compute empirical deviation

Table 4.5 Best-fit sphere using polygonal regression – Matlab code

c) Creating and fitting a sphere with a region grow procedure

The algorithm for creating and fitting a sphere to a point cloud using a region grow procedure is similar to the one of the planar patch. The difference is that the planarity tolerance is replaced by a spherical shape checking (Fig. 4.15).

The selection of the initial point data has an important aspect, due to the primary approximation of the sphere center with the centroid of the data. A weak selection can lead to an unwanted solution. Fig. 4.15 presents one example of a false identification of the shape due to the incomplete initial selection. Better results are obtained when manually selecting points uniformly distributed on the sphere surface.

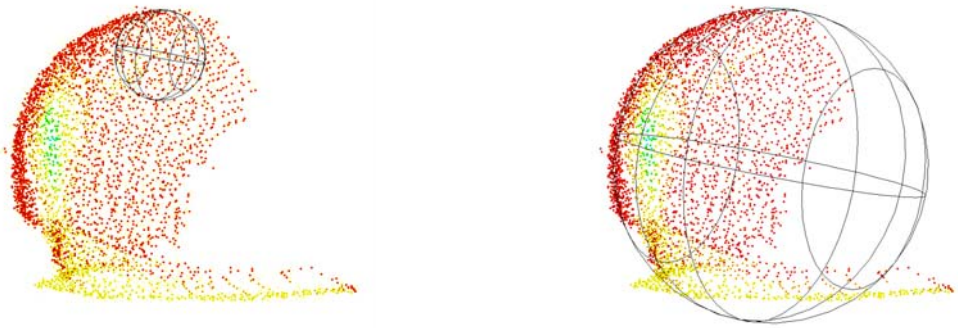

a. False sphere identification **b. Correct sphere identification**

Fig. 4.15 Region grow-sphere (example performed in Cyclone 5.3)

4.5 Create and Fit Basic Shapes

In this thesis a shape is defined by an object formed by one or more curved or straight lines. The shapes can be created and fitted either in 3D or 2D. The common techniques are:

a) automatic line detection;

b) semi-automatic line generation;

c) digital tracing.

a) Automatic line detection

The procedure enables the line creation from the point cloud without user intervention. High point density and regular object geometry are main requirements for a reliable shape generation. In practice, especially in architecture projects, an adequate point raster and a regular geometry are not always granted.

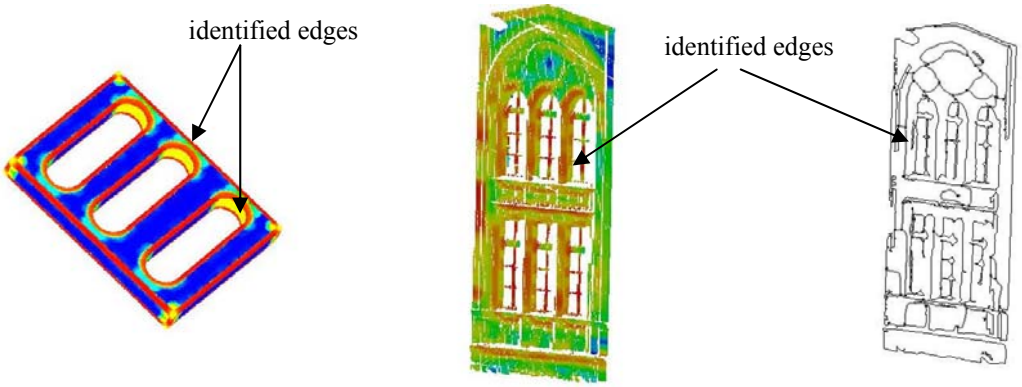

a. Machine part **b. Architecture model** **c. Automatic line generation**

Fig. 4.16 Automatic edge detection (examples performed with Geomagic Studio 6)

Common results are presented in Fig. 4.16. Objects with regular geometry and scanned with a high resolution are better candidates than objects scanned with a lower resolution. It is very unlikely to use the high resolution (sub-millimeter point raster) when scanning large sites due to the file capacity that will result from the scanning process and due to the large amount of time needed to scan the object. Objects like the machine part example have small dimensions and usually are scanned using a sub-millimeter resolution with a laser triangulation scanner.

Currently, most of the available commercial scanners have a high resolution digital camera incorporated or the capability to mount one on the scanning device. Also the scanning software is normally able to visualize the point cloud mapped with the acquired images. One of the approaches to automatic line extraction could be based on the image edge detection algorithms. Using one of the common edge detection operators like Roberts, Sobel, Laplacian, etc. [e.g. McGlone, 2004] lines can be automatically extracted and then digitized. Resulted lines are then fitted to the data using neighboring points.

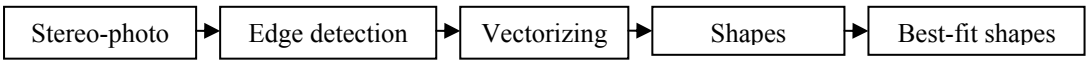

Fig. 4.17 Generic edge detection algorithm

b) Semi-automatic line generation

The process can be used to generate lines along of predefined cross-section templates. The user selects only the region where the lines will be generated from the point cloud. A template is created or selected from a library and lines are fitted starting from points (nodal points) picked out from the template.

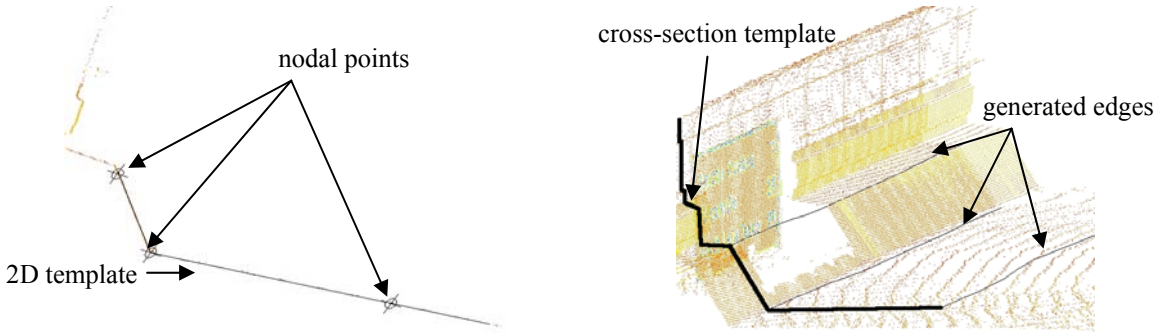

a. Template cross-section and nodal points selection

b. Edge generation

Fig. 4.18 Semi-automatic edge detection (performed with Cyclone 5.3)

c) Digital tracing

The procedure consists of the simple selection of points that define the shape. The manual tracing is then automatically adjusted by best-fit algorithms. Slicing or segmentation are tools used to visualize the areas where to trace over the points.

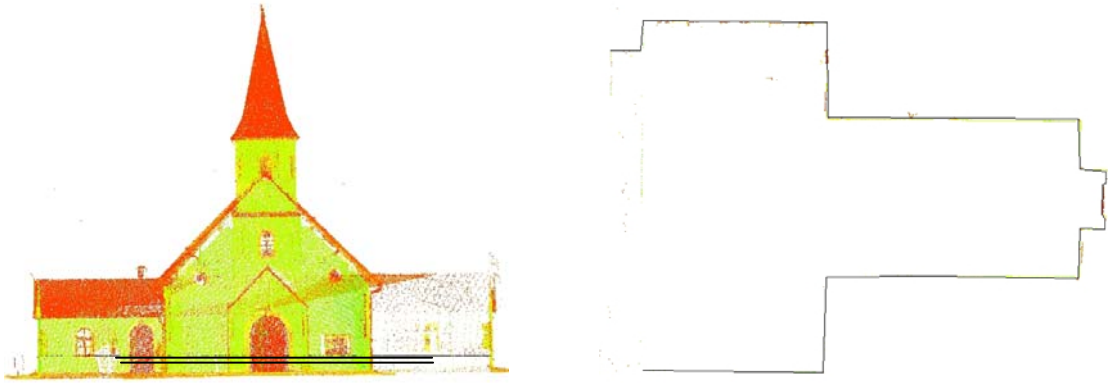

a. Viewed point cloud is reduced with slice tools (front view)

b. Tracing and best-fit line (ground plane)

Fig. 4.19 Data tracing performed with CloudWorx 3.1 (see project "Test objects", Chap. 7.4)

Even though the technique is time consuming, the digital tracing procedure is one of the main tools used to detect and fit shapes to the point cloud.

This is caused by the following aspects:

- the automatic edge detection algorithm is at this moment not robust enough to extract reliable data;
- reliable data can be extracted also from irregular geometry objects or objects scanned with low resolution;
- due to the irregular geometry of the architectural objects, the semi-automatic procedure can only be partially used.

The next sections are exemplifying the fitting procedure for basic shapes as a straight line and the circle.

a) Create and fit a straight line to a set of 3D points

A straight line described by a set of 3D points $X(x_i, y_i, z_i)$ can be concisely written as

$$X = X_0 + v \cdot t \qquad 4.25$$

where $X_0(x_0, y_0, z_0)$ is a point on the line, $v(a,b,c)$ is the direction co sinus of the line and *t* is a real number. The problem is reduced to 2D space when slicing tools are used to better identify the points on the line.

Like in previous cases, the mathematical technique to estimate a line to a given point set is by minimizing the sum of the squares of the point's residuals from the line. Due to the fact that the uncertainty is manifested on all three coordinates, finding a best-fit line is a orthogonal distance regression problem; the perpendicular offsets are computed and not the vertical ones.

As in the case of the best-fit plane, the centroid of the data is considerated to be a point on the best-fit line. This gives $X_0(x_0, y_0, z_0)$ as

$$x_o = \frac{1}{n}\sum_{i=1}^{n} x_i\,,\ y_o = \frac{1}{n}\sum_{i=1}^{n} y_i\,,\ z_o = \frac{1}{n}\sum_{i=1}^{n} z_i\,. \qquad 4.26$$

The algorithm is similar to the best-fit plane. The normal matrix is $\underline{\boldsymbol{N}} = \underline{\boldsymbol{A}}^t \cdot \underline{\boldsymbol{A}}$, where $\underline{\boldsymbol{A}}$ is the matrix of the translated points. The SVD of matrix $\underline{\boldsymbol{A}}$ is computed. It can be proven that the sum of squares of the residuals are minimized for the largest singular value [Golub, 1989], and the singular vector corresponding to this singular value is the line co sinus direction. The algorithm can be written simply in Matlab language:

X=[x;y;z];	% input 3D point set
X0 = mean(X)';	% calculate centroid
A = [(X(:, 1) - X0(1)) (X(:, 2) - X0(2)) (X(:, 3) - X0(3))];	% form matrix A
[U, S, V] = svd(A, 0);	% calculate SVD of A
[s, i] = max(diag(S));	%find the largest singular value in S
a = V(:, i);	%extract from V the corresponding right singular vector

Table 4.6 Best-fit line – Matlab code

b) Create and fit a circle to a set of 3D points

A circle *s* is uniquely defined in the 3D space by its center $X_0(x_0, y_0, z_0)$, a radius *r* and the normal vector $n(a,b,c)$ to the plane that contains the circle. The best-fit circle to a 3D point set is computed with a least squares procedure:

$$f(X_0, r, n) = \sum_{i=1}^{n} (p_i - s)^2 \rightarrow \min \qquad 4.27$$

where p_i-s is the distance from the point p_i to the circle *s*. Due to the complexity of its computation, the direct 3D solution is replaced with one using a reduction to the 2D space.

The procedure implies the following steps [Shakarji, 1998]:

- the computation of the best-fit plane of the point data. Centroid and normal vector solution are found;

- the data is rotated such as the best-fit plane is parallel with xy plane;
- the data is projected on the local x'y' plane and the 2D best-fit circle is computed:

$$r = \frac{1}{n}\sum_{i=0}^{n} d_i$$
$$x'_0 = \frac{1}{n}\sum_{i=0}^{n} x'_i + r \cdot \frac{1}{n}\sum_{i=0}^{n} \frac{x'_0 - x'_i}{d_i} \qquad 4.28$$
$$y'_0 = \frac{1}{n}\sum_{i=0}^{n} y'_i + r \cdot \frac{1}{n}\sum_{i=0}^{n} \frac{y'_o - y'_i}{d_i}$$

where $d_i = \sqrt{(x'_i - x'_0)^2 + (y'_i - y'_o)^2}$;

- the data is rotated to the initial orientation;
- a 3D minimization search of all the parameters is optional.

4.6 Create 3D Objects

Using specific procedures, 3D complex geometry can be generated from 3D geometric primitives or 2D/3D basic shapes.

A 3D object in the terms of the simplest 3D representation – a so called wire-frame representation – consists of a list with 3D points and edges. Generally, the wire-frame representation of a 3D object can be obtained by combining the best fit shapes like segment lines, curves, etc. of the point clouds sections (see Fig. 7.2). The main disadvantage of the wire-frame modeling is the ambiguous representation for determining quantities like the surface area or the volume of the object.

The solid representation technique that combines simple 3D geometric primitives to build more complex models using Boolean operators is called *Constructive Solid Geometry* (CSG) [e.g. www58]. The resulted model is a procedural model stored in a binary tree database, where the leaf nodes are the primitives and the branch nodes are the Boolean operators.

The Boolean operators are:

- the union operator joins all objects into a single shape;

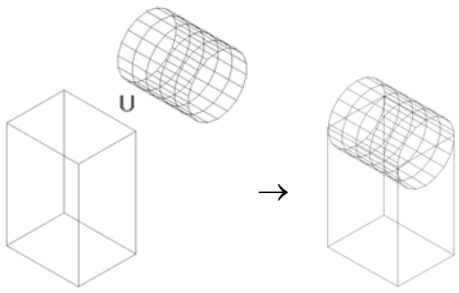

Fig. 4.20 The union operator

- the combine operator is similar to the union operator, with the difference that the overlapping region is removed. In some of CG applications the union operator is identified with the combine operator;

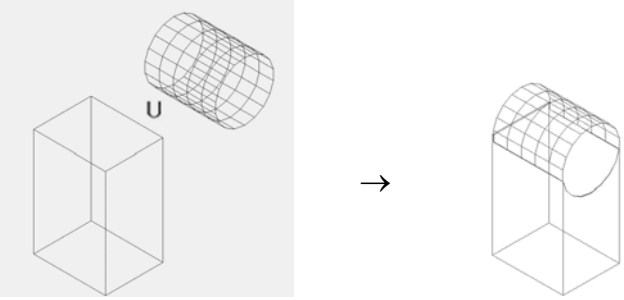

Fig. 4.21 The combine operator

- the intersection operator returns only the overlapping region of the operands;

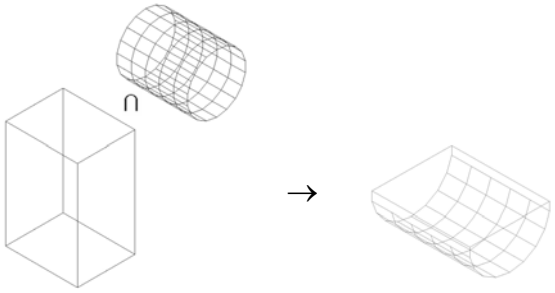

Fig. 4.22 Intersection operator

- the subtraction operator removes the overlapping region from one of the operands;

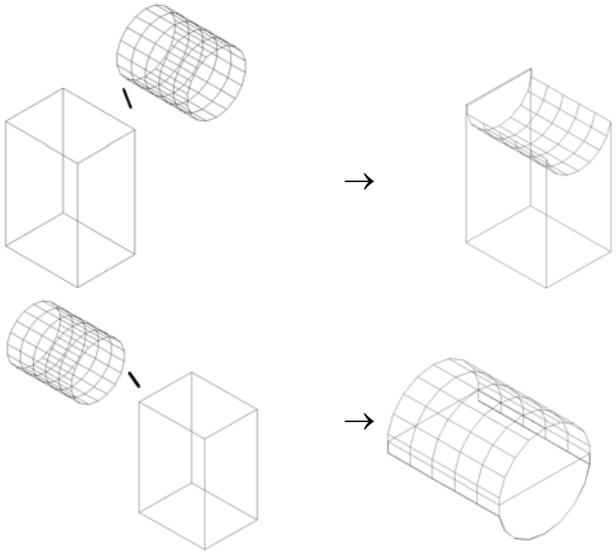

Fig. 4.23 Subtraction operator

- the fragment operator combines the intersection and the subtraction operator. It returns three new objects from two overlapping operands;

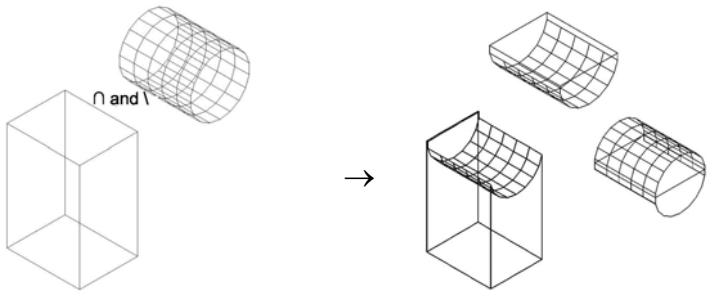

Fig. 4.24 Fragment operator

Another solid modeling technique is the *Boundary Representation* method (B-Rep) [e.g. www58], in which a solid[4] is represented by a collection of the bounding surfaces. The object geometry is defined by a combination of surfaces, curves and points, and represented by a set of topological entities (solids, shells, faces, loops, wings, edges and vertices[5]). In other words, the geometric description of the object specifies the form and the position of the surfaces, curves and points, and the topological description records their connectivity by means of pointers in a data structure.

The B-Rep and CSG object representation methods are implemented in most of the CAD and CG applications. Their specific advantages and disadvantages are mainly defined by the user's (modeller's) point of view. In most of the cases the 3D object can be represented using both methods. However, when choosing the adequate method to be used, some of the following should be considered:

- the level of detail or complexity of the final object defines the items that should be modeled and the ones that will be left away. A highly detailed or complex model could require more modeling time when using the CSG method and there are situations where the set of primitives is not appropriate for a given object;
- generally CSG requires small storage space;
- the accuracy of the resulted object enforces the chosen method. The robustness of the primitive's parameters determination gives an advantage to the CSG method, but this only in the cases of simple object's complexity;
- the Boolean operations are more suitable to use for the CSG representation;
- the topological correctness of the surface;
- the computer resources and CPU time;
- the model compatibility.

Spatial enumeration and cell decomposition are two other common methods for 3D object representation. In spatial enumeration or *Uniform Space Decomposition* (USD), the 3D space is decomposed into a set of identical cells, usually having the form of a cube [e.g. Manner, 2004]. The cells are named voxels or volume elements and their location is given by their center coordinates. The object geometry is defined by specifying if the cell is empty or full. For a highly detailed model the number of cells is larger, hence, a higher storage space is required. The accuracy of the USD for objects bounded by curvature surfaces is directly connected with the size of the cells used in decomposition.

[4] In CAD and CG software the term of solid defines a part of space bounded on all sides.
[5] In CAD and CG software the term of vertex identifies a 3D point.

The cell decomposition or *Hierarchical Space Decomposition* (HSD) method is a variation of the USD. The cells have different shapes or sizes, thus the storage space requirements are reduced [e.g. Manner, 2004].

The Octree representation is a HSD method in which the spatial volumes are sub-divided into a set of eight cells or octants [Tanimato, 1980]. The model is generated by recursively dividing each octant into eight sub-cells, starting with the single large cell bounding the object, using the following algorithm:

- the cells are labelled empty E, full F or partially full P, depending whether the cells are outside, inside or partially inside the object;
- the partially full cells are recursively sub-divided into eight cells until all the cells are either full or empty, or until the lowest level of resolution is reached.

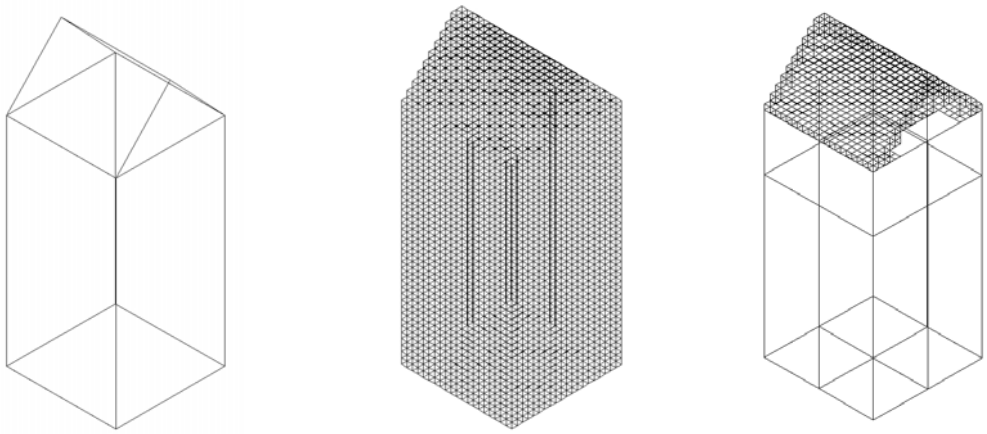

a. object (wire-frame representation) **b. voxel representation** **c. octree representation**

Fig. 4.25 Voxel representation vs. Octree decomposition [Manner, 2004]

Other HSD methods imply the decomposition in tetrahedral cells [Cutler et. all, 2002] or using hyperpatch representation [Joy, 1991].

Other representation techniques:

- Primitive Instancing (PI): an object is a set of pre-defined primitives, defined parametrically and located in space;
- Sweep representation (SWP) or generalized sweeps: an object is defined by sweeping a 2D or 3D shape along a trajectory. Could be considerate as a constructive method;
- Skeleton representation: an object is represented by idealized shapes that preserve the topology of an initial object;
- Generalized blob representation: an object is given by a collection of near-convex parts called sticks, plates and blobs. The object topology is defined by constrains that describe how the parts are connected [Shapiro et al., 1980];
- Spherical harmonic representation: the object's surfaces are defined as a set of function on the sphere [Büllow, 2001];

- Overlapping sphere representation: an object is described by a set of arbitrarily located and sized spheres (it can be considerated as a space decomposition method) [O'Rourke and Badler 1979];
- Generalized cylinder representation. Similar to the skeleton representation: an object can be represented as a set of cylinders;
- Hierarchical representation: an object is represented as a 3D prism or strip tree construction [Faugeras, 1983].

Currently, 3D complex geometry can be generated from basic shapes or curves in CG or CAD software using one of the above object representations methods as follows (a graphical representation of the following procedures can be found in Annex I):

- the *revolve* or *lathe* operation creates a surface by rotating a contour about an axis;
- the *lofting* process creates surfaces between cross-sections. If the surface is interpolated across one direction (given by the curves) the process is called U lofting, and if there is a set of curves in the V dimension as well as in the U dimension, the result is a UV loft surface. Loft surfaces can also be generated when sweeping a cross-section along a path;
- the *extrude* process creates a 3D volume by sweeping a fixed 2D shape along a path, usually a straight line. If a path is not specified, the extrusion direction is given by the normal of the 2D shape;
- the *boundary* surfaces are created by constructing a polygon mesh on adjacent curves;
- a *ruled* surface is generated by a straight line whose end points are sweeping two different curves that define the surface borders;
- the *cap surface* process is used to ceiling the edge of a closed surface;
- the *rail sweep* surface is similar to the loft surface. One curve defines the cross-section and the other the surface's edge (not the surface's path like in the loft surface). If the edge is not intersecting the cross-section the result can differ. In CG application, a *1-Rail* sweep surface is generated when at least two curves are used and a *2-Rail* or *Bi-rail* sweep surfaces are defined by a minimum of three curves (two curves define the two edges of the surface);
- the *blend* operator generates a smooth transition between two or more surfaces;
- the *extend* modifier is used to enlarge a selected curve or surface to another curve, surface or reference plane;
- the *trim* or *slice* operator cuts a curve or a surface creating a new boundary.

4.7 Create Triangular Meshes

The raw data supplied by the laser scanner systems are not always well suitable for a direct use in CAD systems. After the cleaning of the 3D point set, a simple and more direct way to produce a surface, that can be sufficient for some applications, is to generate a polygon mesh. A polygonal mesh is described by topology and geometry. The topology of the mesh is given by the neighborhood structure and the geometry is defined by the coordinates of the vertices. The topological structure of the mesh contains vertices, edges, triangles and other features like holes, genus and number of connected components. The relation between these elements is given by the Euler-Poincare formula:

$$V\text{-}E\text{+}F\text{-H}=2(C\text{-}G), \qquad 4.28$$

where V is the number of vertices, E the number of edges, F the number of triangles, H the number of holes, C the number of connected components and G the sum of the geni of all components [Karbacher, 2000].

The simplest type of polygon meshes, currently used in most of the commercial scanning or reverse engineering software, is the triangular mesh. This type of mesh is usually generated using the Delaunay triangulation method [Preparata, 1985].

The geometrical dual of the Delaunay triangulation is the Voronoi diagram. It essentially divides the space into convex cells by creating a region around each known site p_i such that every point ρ from the region is closer to the point p than to any from the other sites. [Preparata, 1985]. The topological elements of the Voronoi diagram are: the Voronoi point (the point located at equidistant distance from three different sites), the Voronoi line (given by the points which are equidistant to two sites in the plane) and the Voronoi cell or polygon [www9], [www10], [www11].

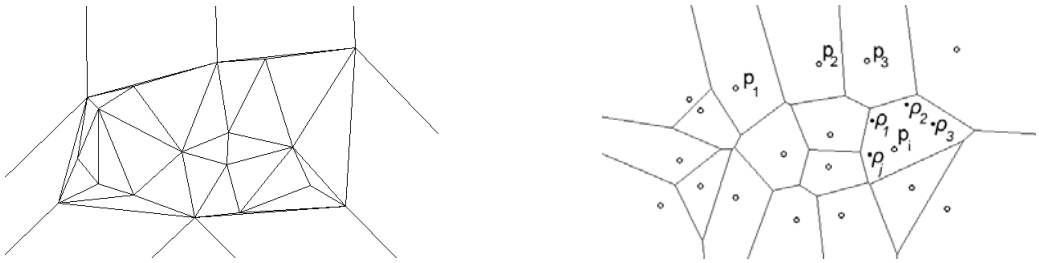

a. Delaunay triangulation **b. Voronoi diagram**

Fig. 4.26 Delaunay triangulation vs. Voronoi diagram (2D case) [www8]

The polygon mesh creation is a very dynamic research area; methods to increase the speed and robustness of the algorithms are continuously under development

4.8 Clean and Edit Triangular (Polygonal) Meshes

In order to process the polygonal mesh by producing a specific deliverable, a set of procedures should be performed to detect and fix topological or geometrical defects, to remove unwanted or unnecessary data and to create a complete mesh. This can be translated in methods for cleaning and editing polygonal meshes. Since the polygonal meshes can be converted in triangular ones by subdividing the polygons in triangles, the following methods focus on triangular meshes. A list with the tested laser scanning software and their capabilities related to the processes described in this chapter can be consulted in Annex II.

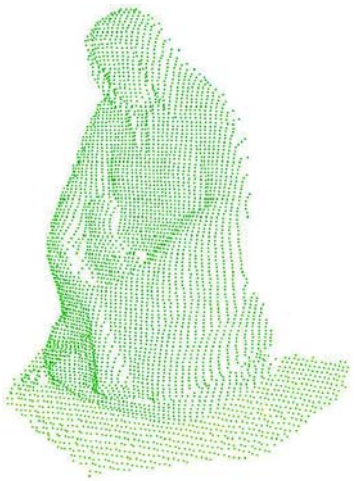

Fig. 4.27 Acquired point cloud data (see project "Test objects", Chap. 7.4)

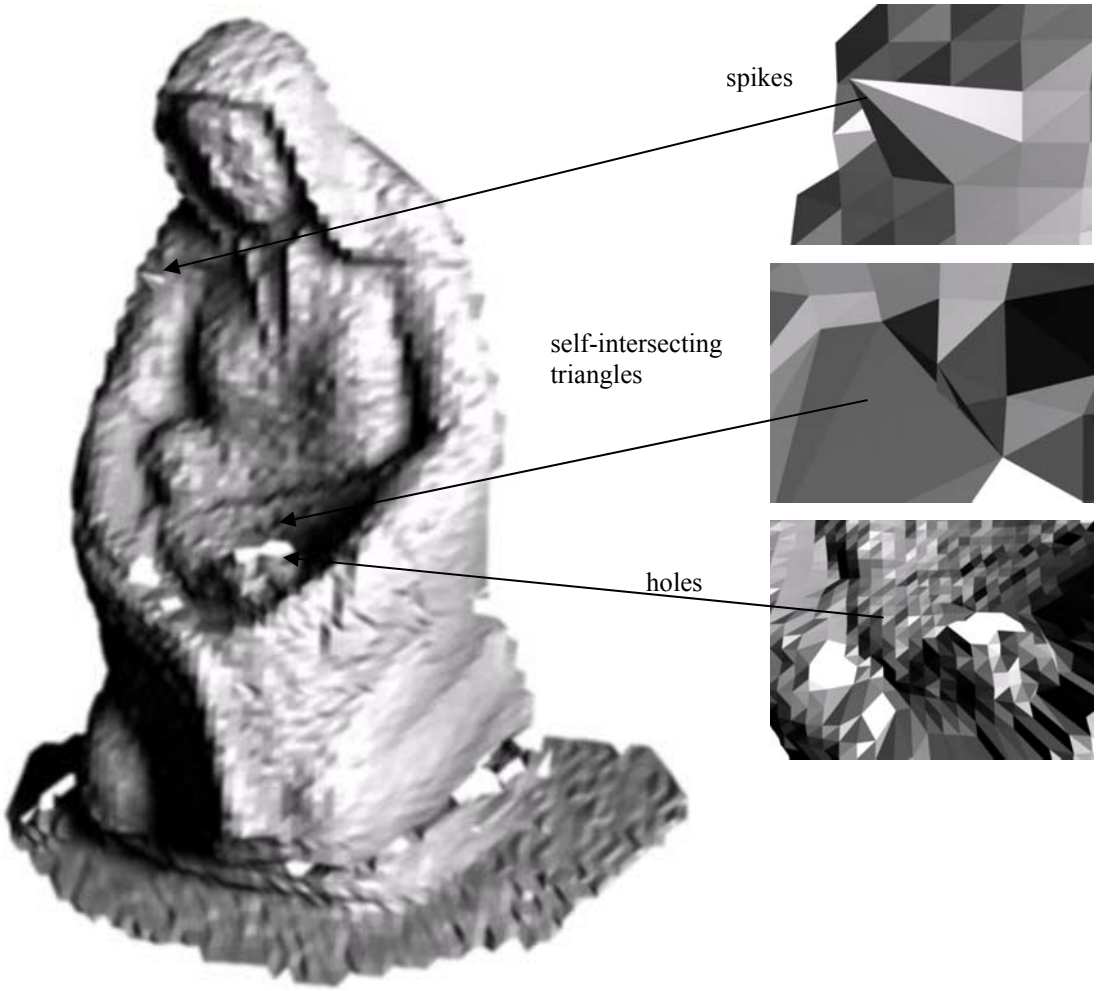

triangular mesh generated directly from point cloud data (see Fig. 4.27)

Fig. 4.28 Samples of topological and geometrical errors. (see project "Test objects", Chap. 7.4)

The first step that should be inquired is the search for topological and geometrical errors of the created polygon mesh. The procedures are mostly semi-automatic and involve the search for the following defects:

- self-intersecting triangles: non-adjacent intersected faces[6]. One fast method to detect these defects is a hierarchical approach using bounding boxes [Zomorodian, 2002]. The possible candidates for intersection are represented by their bounding boxes and the intersection of the boxes is tested. If two of these boxes are intersecting, a test for triangles inside the boxes is performed;

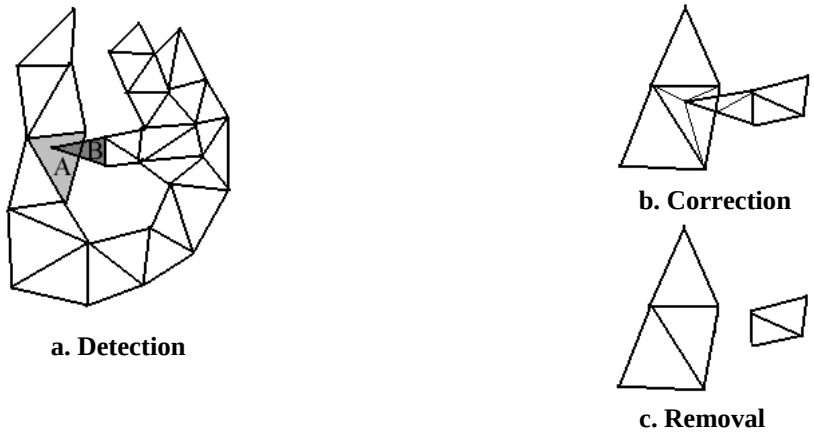

a. Detection **b. Correction** **c. Removal**

Fig. 4.29 Detect and b. correct self-intersecting triangles or c. remove self-intersecting triangles (2D case)

The triangular mesh represented in Fig. 4.29.a contains two non-adjacent intersecting triangles A and B. After the automatic or manual detection of the intersecting faces, the defect can be corrected either by cutting the triangles (new triangles are created) and removing the redundant part, either by removing one or both of them.

- crossing triangles: two edges with no common vertex are intersecting and the faces that contain these edges are called crossing faces;

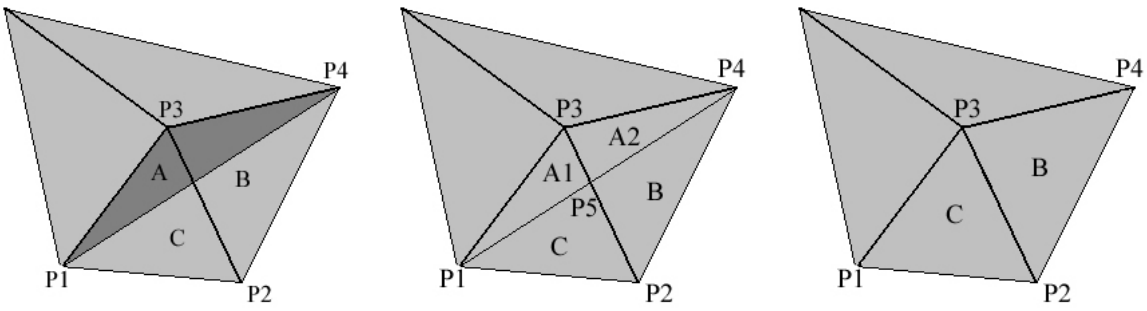

a. Detect crossing faces **b. Correction by cutting** **c. Correction by removing**

Fig. 4.30 Detect and remove crossing faces (2D case)

A crossing face can be generated by two edges that have a common vertex and their triangle intersect a non-component edge. The cleaning procedure can be accomplished

[6] In CAD and CG software the term of face denotes a surface bounding a solid.

by cutting the crossing faces and applying a smoothing function to them, or by removing the crossing faces and generate new faces.

- redundant faces within a mesh or in the overlapping area of two meshes. Within a mesh, an equal number of edges and faces defines a non-boundary vertex. A face disobeying this rule is a redundant one.

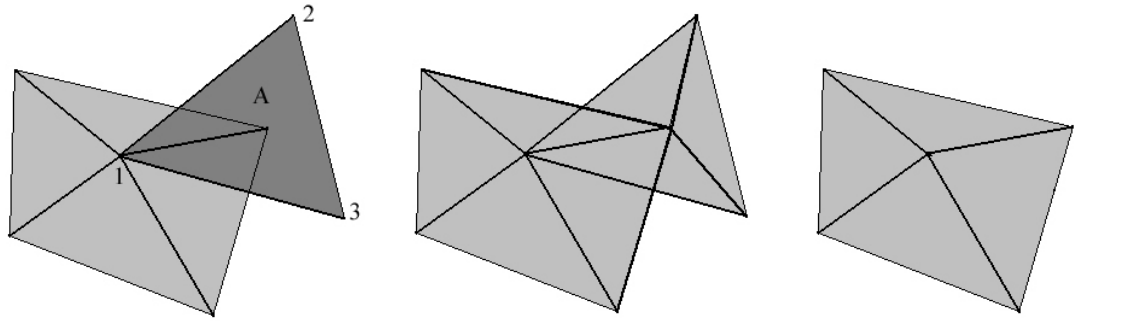

a. Detect redundant face (E=6, F=5) **b. Correction by cutting** **c. Correction by removing**

Fig. 4.31 Redundant face within a mesh (2D case)

The number of the edges *E* and the number of the faces *F* incident in the vertex *1* has to be the same, in order to define a topological correct non-bounding vertex. The cleaning procedure can be performed either by dividing the redundant face and generate a new triangle, or by removing it.

Redundant faces can appear in the overlapping area of two or more merged or connected meshes. A triangle is considered to be redundant if its vertices are located within a certain tolerance distance from the other mesh. Generally, this step is part of the connecting and merging meshes algorithm.

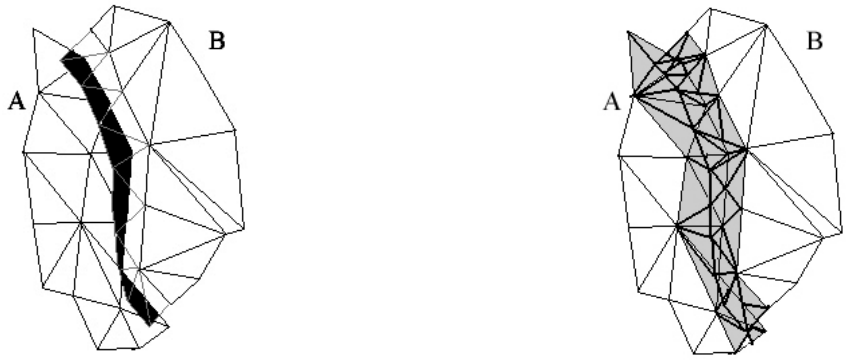

a. Two meshes with overlapping area **b. Remove redundant faces**

Fig. 4.32 Redundant faces of two overlapping meshes (2D case)

The redundant faces from the overlapping region of the meshes A and B are removed by adding new vertices at the intersection of the meshes, and generating new triangles.

- non-manifold triangles: one edge is contained by three or more faces.

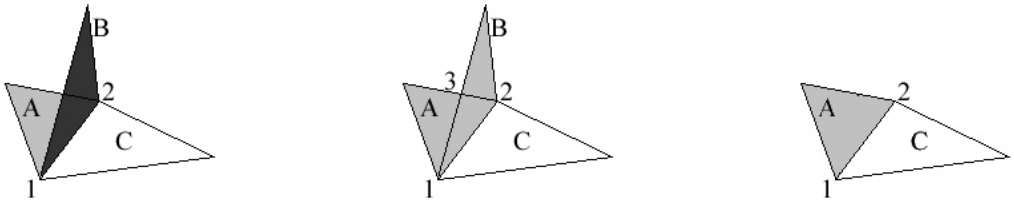

a. Detect non-manifold faces **b. Clean by cutting** **c. Clean by removing**

Fig. 4.33 Detect and clean non-manifold faces

To create a manifold topology, an edge can be shared by a maximum of two faces (a boundary edge is contained only by a face). In Fig. 4.33.a. three faces *A*, *B*, *C* are incident in the edge 1-2, the cleaning procedure can be performed by trimming the triangles and generate new faces or by removing one of the faces.

- bad normal faces are faces with the normal vector reversed. If not corrected, some holes detection algorithms can identify them as holes.

a**. Detect the bad normal faces** **b. Repair the normals**

Fig. 4.34 Detect and repair bad normal faces (2D case)

To determine if a face's normal is reversed or not, the reference normal direction of the neighborhood area has to be specified. In other words the direction for inside or outside has to be defined. The cleaning algorithm corrects all the normals whose directions are not matching the reference direction.

- open edges are a loop of boundary edges. Identifying the open edges is translated as detecting the holes in the polygonal mesh. A boundary edge is defined as an edge shared only by one triangle. Due to the duplicity of the boundary edges, the user's intervention is required, to assure whether the edges define a hole or not (Fig. 4.35).

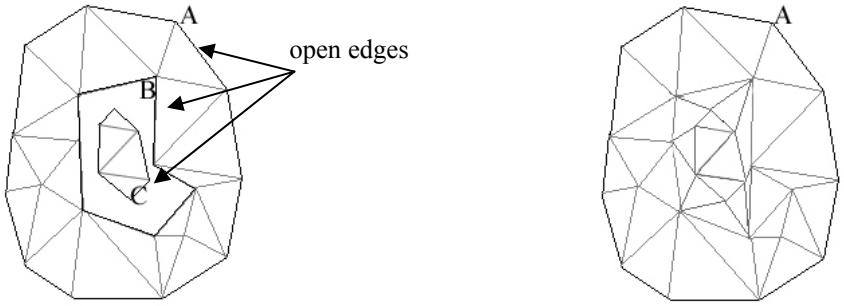

a. Detect open edges **b. Fill holes**

Fig. 4.35 Detect open edges (2D case)

The loop of boundary edges or simply the boundary is either internal (C) or external (A). The boundary A defines the limits of the polygonal mesh and C delimits an internal island inside the hole B.

If the available CAD or modeling software does not provide an automatic or semi-automatic set of procedures to identify and correct the above errors, a solution is to try to export as **.stl* (stereolithography) file format (available in most of the applications). The **.stl* files are used by a stereolithography machine to create 3D objects [www60]. If the exported data contains the above errors, defects will emerge when the physical model is created. To avoid these shortcomings, procedures were implemented to check if the 3D model is qualifying to be exported as **.stl* file.

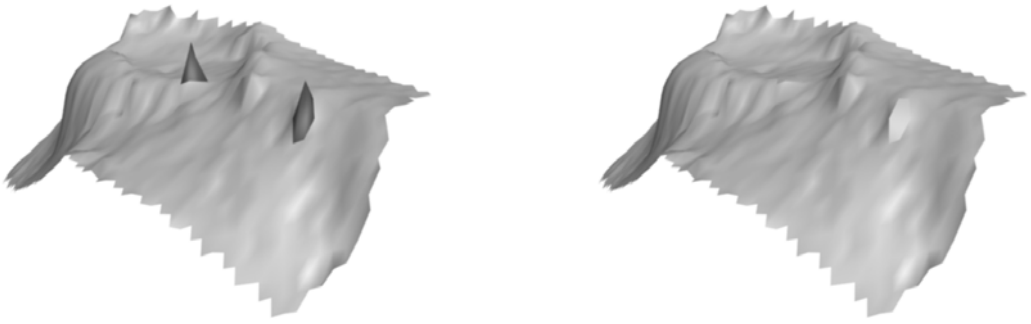

a. Detect spikes b. Remove spikes

Fig. 4.36 Detect and remove spikes (see project "*Hohenburg*", Chap. 7.5)

Outliers not removed during the point cloud treatment phase generate spikes when the polygonal mesh is created. The unwanted faces are detected using tolerance values for the maximum edge length, face area, deviation angle from a plane or between faces e.g. [Sun, 2002], [Pulli, 1997]. After their removal, a filling algorithm is applied to repair the holes.

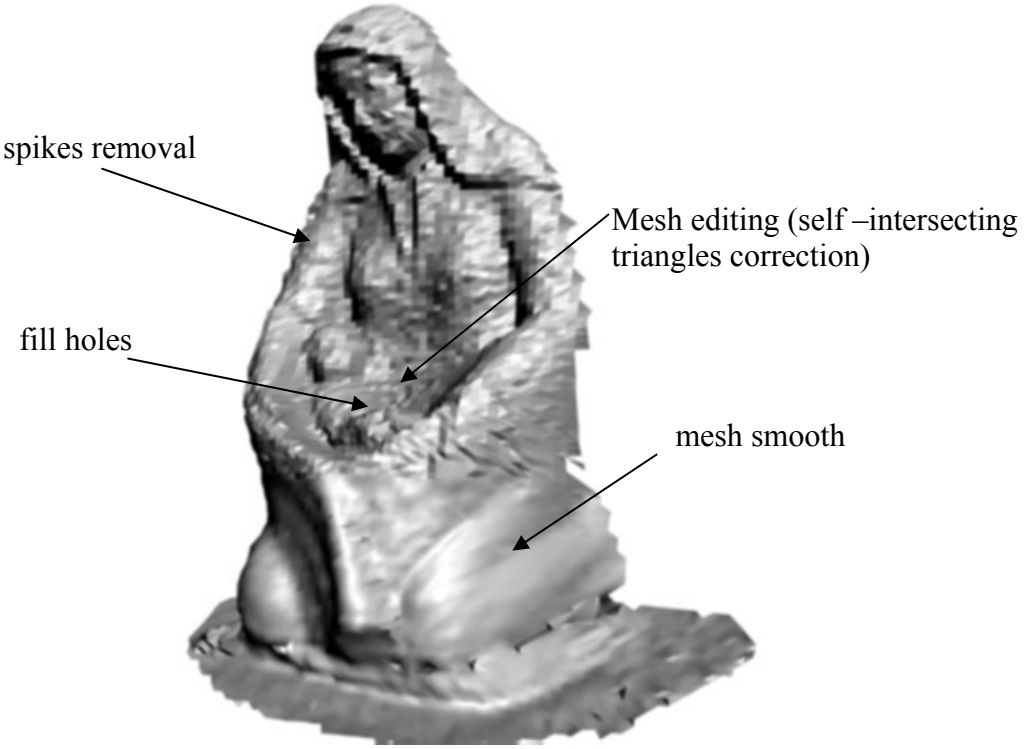

Fig. 4.37 Samples of basic topological and geometrical errors correction and mesh editing procedures (for initial mesh see Fig. 4.28 - project "Test objects", Chap. 7.4)

Two other mesh cleaning operations are the noise reduction and the smoothing procedures. Even they define two different actions, some applications use them as a group algorithm. The noise reduction algorithm removes the noise (error data) from the polygonal model and the smoothing operator reduces the mesh roughness. Two observations can be made. The procedures should be applied with respect to the shape preservation and/or surface curvature and if the noise reduction algorithm could reduce the mesh's face number, the smoothing operator will most likely increase this number.

Basic and advance editing procedures are used to generate a complete polygonal mesh that will satisfy the detail, accuracy and compatibility requirements:

- the final mesh should contain the required accuracy level. A more accurate model is translated as one with more details and that corresponds with the acquired data. If the modeling capabilities do not supply the wanted level of quality then the polygonal mesh has to be corrected restrictively to the significant constrains (for example defining a break-line into a mesh);
- the final mesh should not contain much more information than the required level of detail. If not so, more time will be involved in producing the model and the physical deliverables (e.g. printings) will contain details that will not be noticed, and even will worsen the access to the required data;

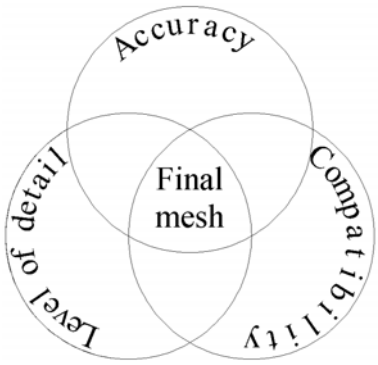

Fig. 4.38 Final mesh features

- the level of detail and accuracy of the final mesh should be reached not only by the model in the editing or modeling application, but mainly by the deliverable. Due to the conversion, some information may fail to be in the deliverables and so a higher detail should be provided before conversion.

The mesh basic editing procedures include operations for adding new triangles and editing current triangles:

- new triangles can be created manually by specifying the component vertices or the bounding edges;

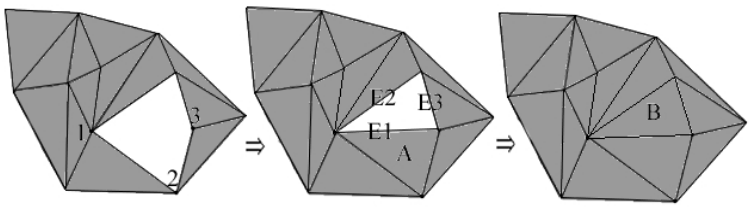

Fig. 4.39 Add new triangles (2D case)

The triangle *A* is generated by the vertices *1*, *2*, *3* and the face *B* by the bounding edges *E1*, *E2*, *E3*;

- current triangles can be deleted by manually selecting a face, an edge or a vertex;
- the location and the shape of a triangle can be modified by manually moving one of its sub-objects.

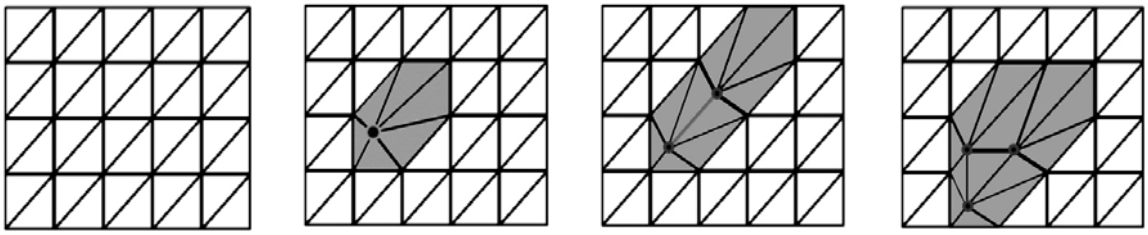

a. Initial mesh b. Move a vertex c. Move an edge d. Move a face

Fig. 4.40 Edit a current triangle (2D case)

Details that are not captured by the scanning devices or errors resulted from the scanning process can be represented and corrected by performing an editing operation on sub-objects level. The process can also be used to correct and complete the scanning data with data acquired by other measurement techniques, or to fill holes manually in the polygonal mesh. Due to the absence of the measured data, the editing process is considered to be more a modeling one than a reverse engineering one, and it is highly subjective to the modeller's point of view. When performed incorrectly or incompletely, due to its spread component, the editing-modeling process can produce highly erroneous results. Fig. 4.40 sketches the spread component of the editing process: when modifying the location of one sub-object, all other topologically connected sub-objects are deformed.

Due to the shadowing of the interest area during the scanning process, the polygon mesh could present some regions with missing data (holes). A hole is defined as a loop of boundary edges identified as abnormal topological elements during the mesh cleaning stage. If it is required, the mesh should be completed using a filling holes algorithm. One method (most laborious) is to edit the mesh sub-objects manually in order to cover the holes. Being one of the interest subjects in laser scanning technology, series of algorithms were developed and implemented in some of the modeling applications. For bounding holes a projection plane algorithm [Wang, 2003] or a volumetric diffusion method [Marschner, 2001] can be used to generate planar or curvature new faces based on the bounding vertices or the edges of the hole. Larger or unbound holes are converted to small bounding holes before applying the filling algorithm, using mainly a bridge method.

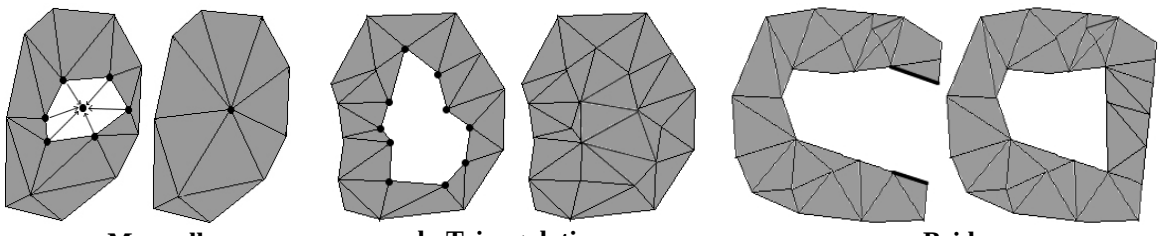

a. Manually b. Triangulation c. Bridge

Fig. 4.41 Filling holes

To construct a complete model, different meshes with an overlapping area are connected. In practice, two methods are used:

- mesh zippering: the overlapping region of two meshes is removed and a triangular network is generated using neighbouring boundaries [Turk, 1994];

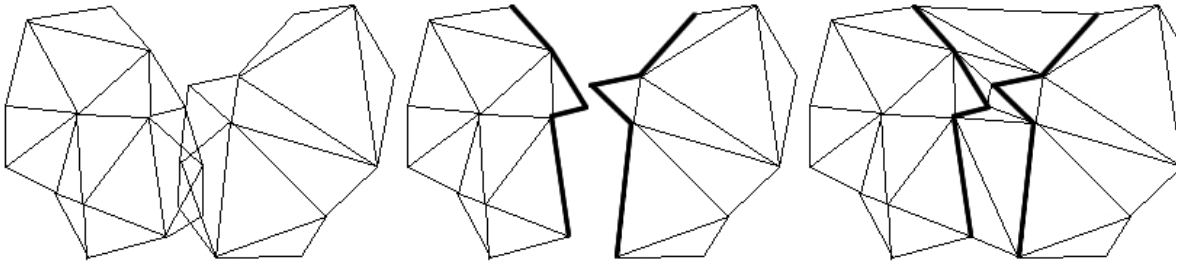

a. Identify the overlapping area **b. Remove the overlap and identify boundary** **c. Mesh zippering**

Fig. 4.42 Mesh zippering (2D case)

- mesh stitching: vertices and edges inserted at the intersection of two meshes are topological entities that generate new faces [www12].

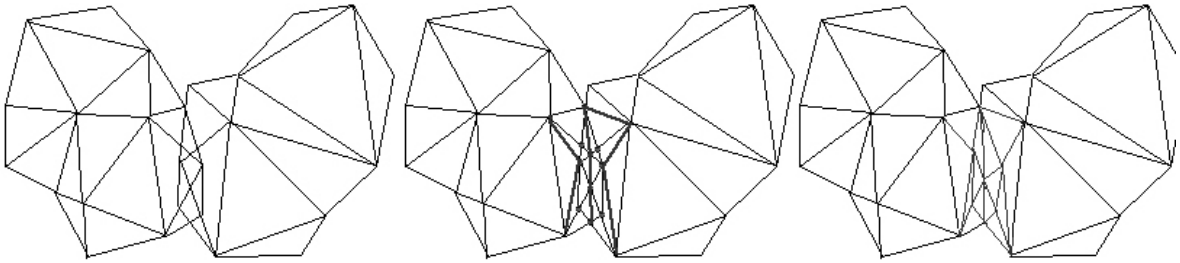

a. Identify the overlapping area **b. Insert vertices and edges** **c. Manifold extraction**

Fig. 4.43 Mesh stitching (2D case)

When the created polygon mesh does not fulfil the curvature continuity level between adjacent faces, or the current number of faces produces a rough surface, a subdivision or refining operator can be used to create a greater number of triangles with a smoother surface. The algorithm sub-divides each face into three or four new triangles by adding new vertices on each of its edges or at the centroid. The algorithm computes not only new vertices but can also adjust the coordinates of the existent vertices, thus the curvature continuity is improved. For prismatic objects the algorithm divides the faces without moving the current bounding edges. In CAD or modeling applications the mesh sub-division is achieved by co-called tessellation operators.

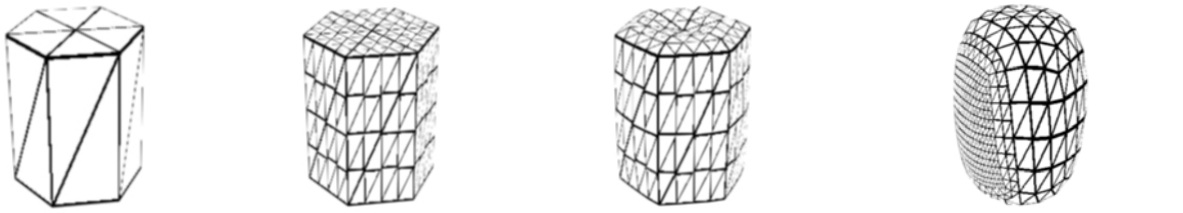

a. Geometric primitive (real object) b. Refine - keep edges c. Refine – adjust vertices d. Refine – improve curvature (geometry falsification)

Fig. 4.44 Refine mesh (generated using 3ds max 6)

The inverse operation to the refining procedure is the mesh decimation. The process reduces the number of triangles while preserving the surface integrity or detail.

Fig. 4.45 Mesh decimation (see project "Test objects", Chap. 7.4)

The decimation operation could be realized using one of the following common algorithms [www13], [Kobbelt, 1998]:

- vertex clustering: a uniform 3D grid is applied to the object and all vertices are removed from a cell excepting a main one defined as the most neighbouring vertex to all of them [Low, 1997];

a. Original mesh **b. Decimated mesh**

Fig. 4.46 Vertex clustering algorithm (2D case)

- vertex decimation: ranking all vertices and removing an unimportant vertex shared by a ring of triangles;

a. Original mesh **b. Decimated mesh**

Fig. 4.47 Vertex decimation algorithm (2D case)

- iterative contraction: ranking all edges with a metric cost and contracting the minimum cost edge.

a. Original mesh **b. Decimated mesh**

Fig. 4.48 Iterative contraction algorithm (2D case)

4.9 NURBS (Non-Uniform Rational B-Spline) Curves and Surfaces

NURBS geometry is one of the most important standard for object representation in several industries due to its capacity to represent both standard geometry like lines, circles, spheres, etc. and free-form geometry like human bodies, car parts, fuselage, etc. precisely in a unified database compatible with a large scale of CG or CAD programs.

NURBS geometry is given by the following components [Altmann, 2004]:

- the degree of the curve/surface is the order of the polynomial defining the curve/surface;
- control points are a set of vertices that do not lie on the curve/surface and define the control network that encloses the curve/surface;
- weights are positive values assigned to each control point. The weight defines the influence degree of the corresponding control point on the curve/surface. Modifying the weight influences the appearance of the curve/surface only in the neighbouring areas of the corresponding control point;
- knot vector is an array of values that specify the region of influence of the control points on the curve/surface.

The NURBS geometry is usually created and edited in computer software by the following methods:

- specifying the control points or the points on the curve/surface and then modifying their position or weight;
- converting geometric primitives, shapes or Bezier patches [Sederberg, 2005];
- using CG tools to generate solid objects from wire-frame models (see Annex I);
- using basic editing processes similar to the ones described in 4.8.

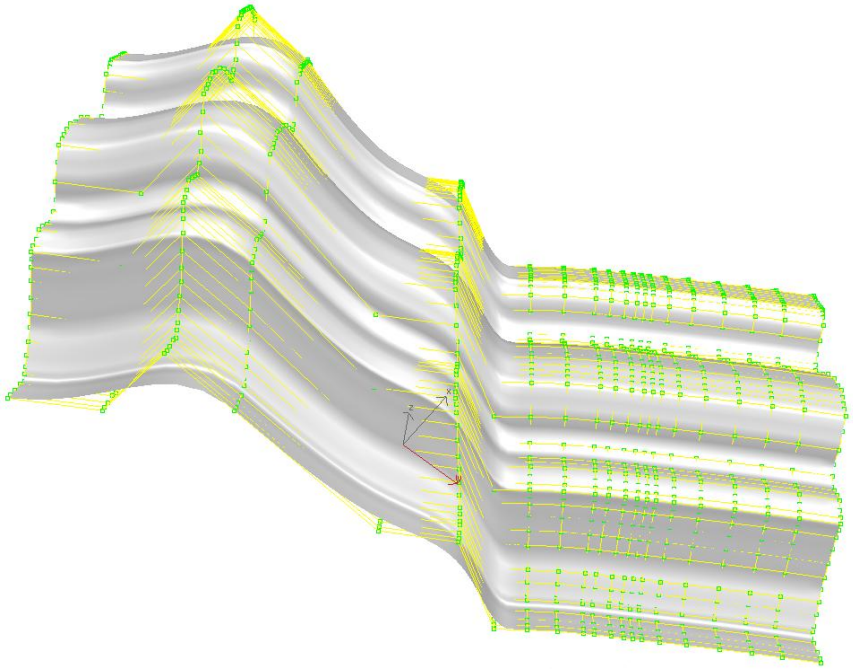

Fig. 4.49 NURBS surface with control points (green dots) and control network (yellow grid) (section wall element, see project "St. Michael", Chap. 7.3)

A detailed description of theoretical aspects of the NURBS representation can be found in common computer graphic books or at the internet [Piegl L., 1991], [www10], [Altmann, 2004].

Due to the fact that most of the 3D models from the case scenarios were created using software not primary based on NURBS geometry and the architectural models are not specific to NURBS modeling, this 3D object representation was used just at a low scale within the case scenarios.

Chapter 5

Virtual Reconstruction

5.1 Introduction

In the past, simply computer models were created usually just for presentation reasons or as help tools for low detail replica-model manufacture. Nowadays, computer techniques are used in a growing scale for virtual reconstruction of 2D or 3D complex models that are supporting high level virtual walkthroughs or highly detailed research, restoration or reconstruction processes.

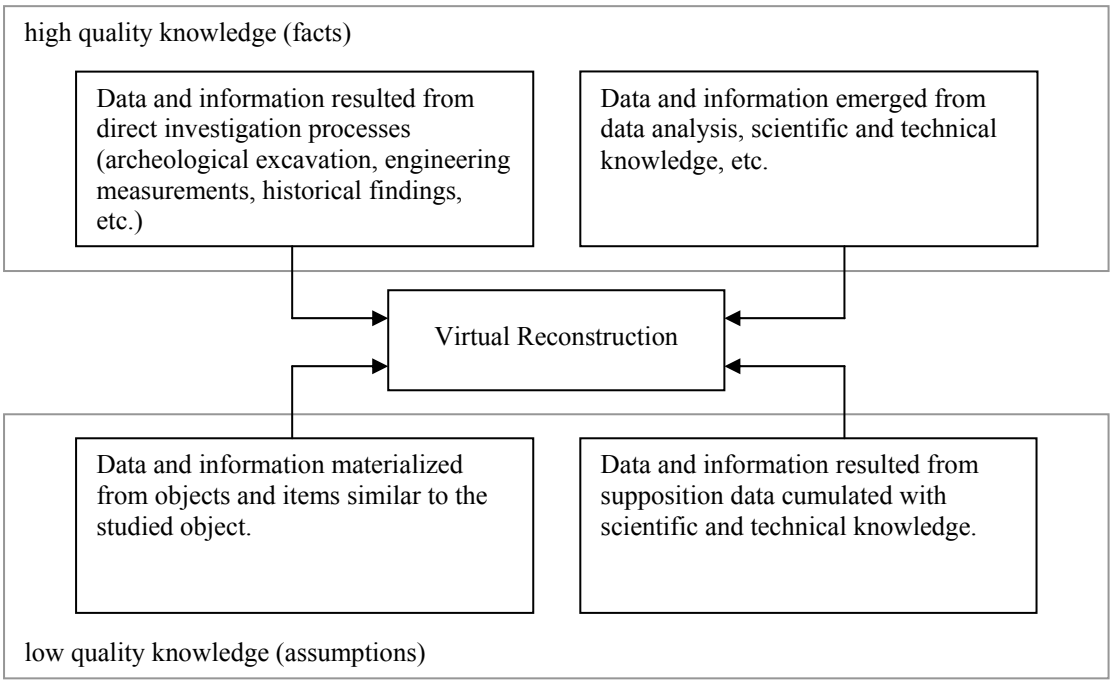

Fig. 5.1 Virtual reconstruction data sources

A schematic view over the virtual reconstruction process is given by Fig. 5.1. The main aspect that influences directly the accuracy and the reliability of the virtual reconstructed model lies in the high quality knowledge of the input data. The input data based on assumptions or low quality knowledge has only a secondary character. Input data with predominant high quality information emerge from findings from archeological excavations, engineering data or measurements and some of historical data. High quality data are also obtained from data and information derived directly from the above mentioned acquired data. Input data with a low quality nature materializes from resemblance data, where the missing data is replaced with data extracted from similar objects or from a similar time epoch. Furthermore, the missing data could be completed with supposition data and information emerged from logical deductions.

Following the above ideas, it is appropriate if not crucial to generate the virtually reconstructed model directly from acquired analysis data and information that incorporates existing evidence of the original structure. In addition, the virtual model is completed with resemblance and supposition knowledge. Furthermore, the reliability and accuracy of the virtual reconstructed model decreases with the increasing presence of the quantity data in the reconstruction process.

For a better understanding of the above statements a schematic preview of the virtual reconstruction process involved in the case scenario Hohenburg (see Chap. 7.5) is presented in the next sketch.

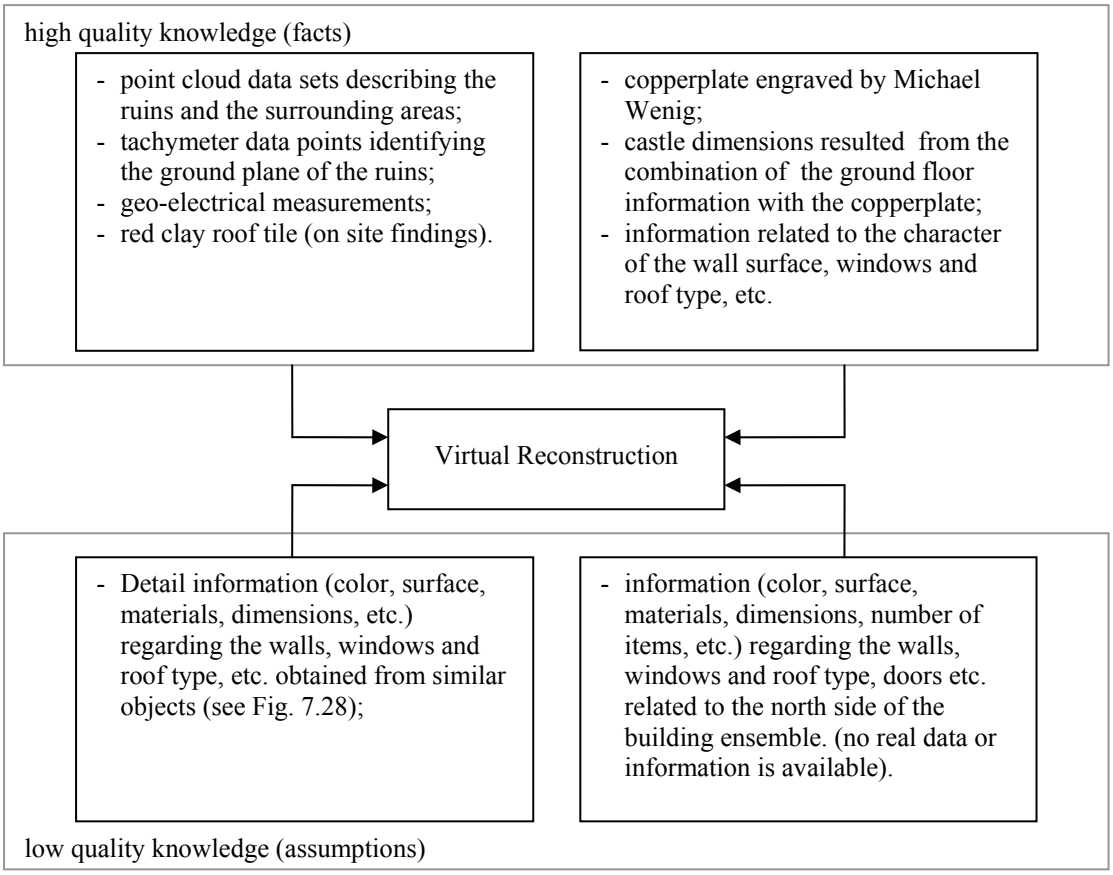

Fig. 5.2 Virtual reconstruction process related to the project "Hohenburg" (see Chap. 7.5)

The character of the output data can be discussed related to the specific demands of the target user. It is known that experts like architects or engineers are more comfortable with a technical output with non-photorealistic visualization, whereas other non-technical users like tourists or students yearn for a realistic as possible visualization. Thus, for the first type of users the work is mainly focused on the accuracy, reliability and the detail of the output model, whereas for the second category the main work is concentrated on the graphical and rendering methods. Generally speaking, every reconstruction has to be built in order to answer the questions and the needs of the end user. Moreover, some of the high quality knowledge input data may be intentionally left out and other inaccurate or incomplete data may have a bigger priority. This is also due to the fact that photorealistic models can be obtained through geometry not as accurate and complete as the photorealistic rendition may suggest (Fig. 5.3).

Fig. 5.3 Computer representation of an altar (see project "St. Michael", Chap. 7.3)

- **left view – detailed photorealistic rendering;**
- **right view wire-frame model, the golden details and the silver cross are not geometrically represented.**

Usually, end users of digital models generated from real data, like laser scanning measurements, are interested in the accuracy of the resulted model. This is computed using different mathematic methods, cumulating the differences between the digital model and the acquired data, the precision of the instruments and measurement technique, etc. In such a way the accuracy of the entire model or parts of it can be determined. In case of a virtual reconstructed model the above data is difficult to obtaine due to the absence or small percent of real data. As an answer to this situation, [Strothotte et al. 1999] propose an enhanced visualization of the reconstructed model with attributes that specify the uncertainty and design decision. The uncertainty level arises for two reasons [Kruse et al., 1994]: imprecision (the existence of a certain feature can be assumed but not its dimensions) and incompleteness (certain information is not available).

[Strothotte et al. 1999] are drawing non-photorealistic models using different line styles varying with the degree of uncertainty (Fig. 5.4 left view). The solution is suited for linear models and not for solids. The representation does not offer too many information about the uncertainty of the surface between the lines. The disadvantage might be reduced by representing the uncertainty of a reconstructed model using a color gradient map like shown in the right view of Fig. 5.4. The uncertainty level is represented as gradient color from green to red. Green symbolizes a lower level thus real data is presented (ruins) whereas red symbolizes a higher level of uncertainty and assumptions. Due to the absence of the quality data, the uncertainty level has larger values in the upper part of the building. The quality information is given by point data sets identifying the shape and the position of the ruins. Both methods do not give a certain value for the uncertainty level but only an informative one.

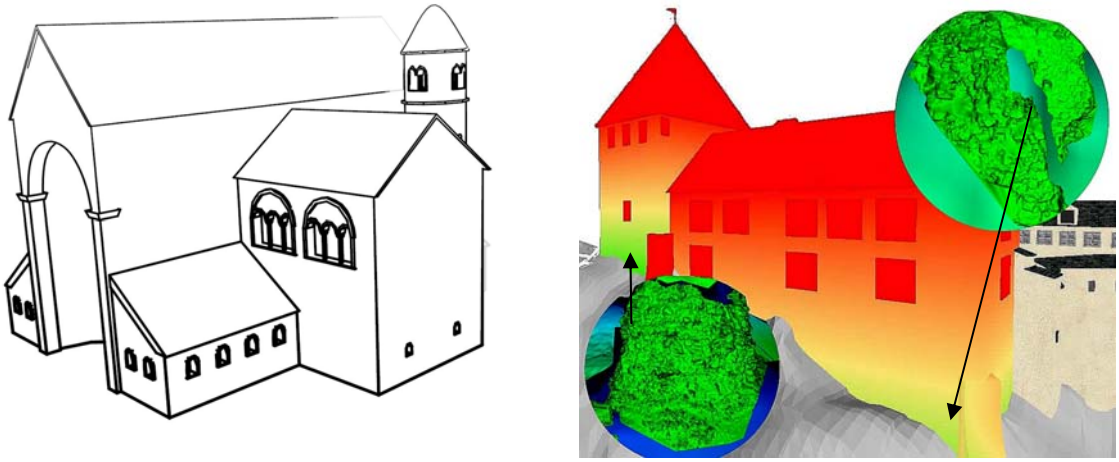

Fig. 5.4 Reconstructed model with uncertainty level representation

- **in the left view the uncertainty level is given by the thickness of the drawing lines [Strothotte et al. 1999]**
- **in the right view the uncertainty level increases with the distance from the ground that contains the only acquired data. The highlights from the left lower corner and right upper corner identify existing ruins represented as triangular meshes (project "Hohenburg", see Chap. 7.5).**

5.2 The Virtual Reconstruction Process

5.2.1 Data Collection

The virtually reconstructed model is the result of a process that starts with the data collection phase. This is represented by the acquisition of historical, iconographical, architectural, geometrical and other types of data that are suitable to be used in the reconstruction process. The acquisition phase is used to gather a sufficient quantity of data referring to the entity's history and condition including also similar entities. It can be divided into two main stages: one referring to the historical research and one referring to the current condition investigation.

The historical research uses specific methods to acquire information related to the object's earlier life periods covered in historical documents, yearbooks, account-books, historical descriptions, real estate registers, certificates, public records, interviews or testimonies, newspapers, magazines, pictures, drawings and other written or graphical data supported by real facts. The search for credible and useful data is the first and in some cases the only way to obtain essential data for an authentic and plausible reconstruction. A detailed description of occurred events from the object's life offers vital data for a better understanding of the actual state of the object and helps to create a chronological view of the object that can be used for a virtual introspective view in the object's history. This is one of the main advantages of the virtual reality: the ability to visualize features visible only in a certain period of time. Moreover, in case of an entity that suffered major or total deterioration, the historical research is the only way to gather data that can be used in the virtual model reconstruction.

The investigation of the entity current state is realized by methods specific to archaeology (excavations, age determination, material composition investigation, etc.), iconography,

ethnology or other anthropology subdivisions and engineering methods like the ones specified in chapter 3.

The data resulted from historical research and current state investigation has to contain information regarding the object and its components geometry, materials (fabrics, colors and characteristics), light sources (natural or artificial) and the time period of their appearance.

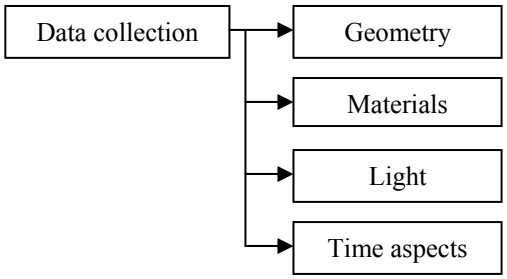

Fig. 5.5 Data collection for virtual reconstruction

5.2.2 Process Design

The process design defines the methods and tools that are used to virtually generate the above components in accordance to the needs of the end-users.

Firstly, the data collected in the previous steps is divided in proper categories (Fig. 5.5) and has to be analyzed in order to determine the level of suitability to the current request. The level of suitability is defined as the degree of appropriateness of the given data or information for a particular use. Following this, the data is identified as general data used to generate the environment of the reconstructed model or as data of interest that give the wanted detail of the reconstructed model.

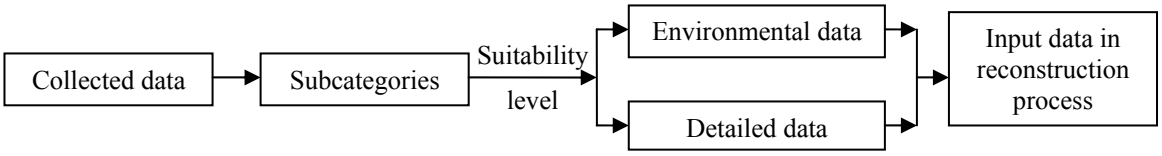

Fig. 5.6 Input data for a virtual reconstructed model

It might be possible that next to the virtual reconstruction a prior restoration or improvement of the available data has to be performed. Also at this stage the scale and the impact of the missing data in the reconstruction process can be observed.

After categorizing the input data, the available and needed reconstruction methods and tools are analyzed. These are also categorized in accordance with the input and output data. To generate the geometry, the materials, the lights and the time aspects different methods are inquired and the best suitable one or a combination of them is chosen to generate the virtual model and its environment.

5.2.3 Virtual Reconstruction Aspects

The virtual reconstruction process involves procedures related to the categories of data and information (Fig. 5.5) acquired in order to generate a virtual representation of a given object.

a) Geometry
When reconstructing the geometry of the model, the modeler has to choose from manual, automatic and semi-automatic methods and tools the ones that are leading to the desired output.

Aspects conducting in choosing or not the manual geometry reconstruction are:

- the working time increases with the complexity and the scale of the model;
- the form of the input data affects the process in equal measure. The reconstruction process can be performed directly with raster or vector data and a conversion is not imperative;
- the output data is influenced in a large scale by the designer's vision;
- the method allows an unstructured input data and reconstruction process. Unstructured data is defined by duplicate objects, objects on wrong layers, redundant or overlapping objects, etc.;
- all entities are individually positioned (translated and rotated) and calibrated (scaled) regardless of their similarity.

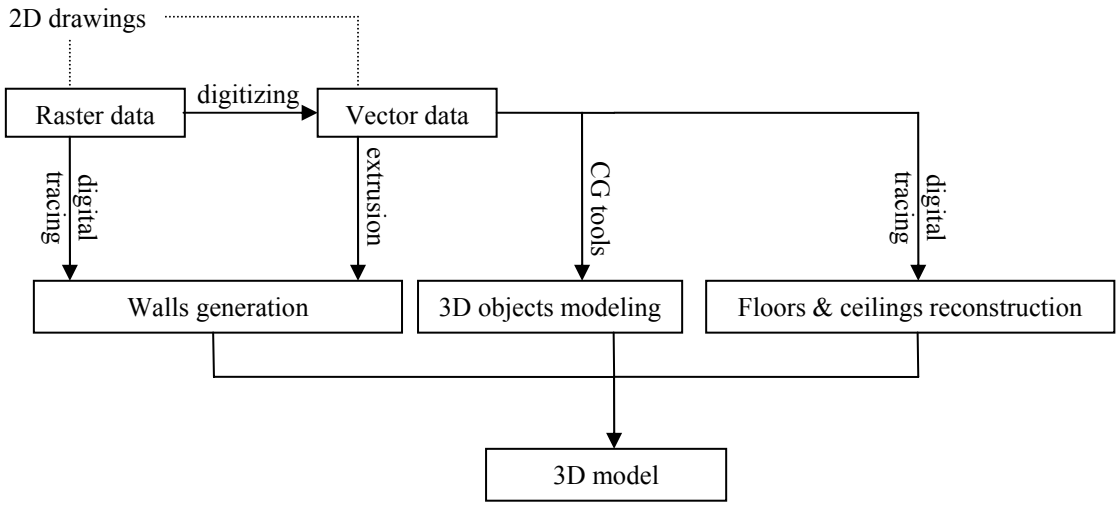

Fig. 5.7 The manual geometry reconstruction of buildings

Typically, the manual reconstruction process of buildings starts with the walls generation from 2D drawings in format raster or vector data using the digital tracing or extrusion tool. Other 3D details like doors, windows, etc. are constructed using computer graphics tools similar to the ones discribed in chapter 4.3. The floors and the ceilings are created by outling their perimeters using the digital tracing method. The 3D reconstructed model results by connecting the above entities.

There are a few characteristics to be considered when choosing the automatic or semi-automatic method to determine the 3D geometry of the reconstructed model:

- an object library is requested. For similar projects the library can be imported from previous ones;
- the complexity and the scale of the model influence the working time only in low scale. The working time is mainly influenced by the period needed to define the object library;
- the form of the input data influence the process in equal scale;
- it can successfully be used when using 2D floor or reflected ceiling plans. The elevations drawings are not yet fully supported;
- some errors could appear when dealing with irregular lines, but they could be corrected when using the semi-automatic approach;
- the method tends to idealize the virtual 3D model.

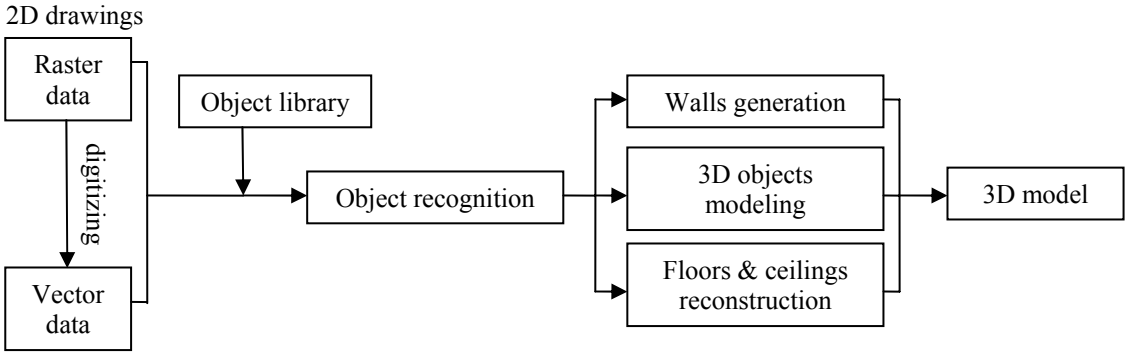

Fig. 5.8 The automatic geometry reconstruction of buildings

The automatic or semi-automatic conversion from 2D plans into 3D models is based on recognition algorithms of 3D entities from 2D drawing patterns. The object library has to be defined previously to the recognition process. The library sets a correspondence between the 2D drawing patterns (lines) and the 3D entities. The algorithm searches in the 2D drawing for a pattern or the set of patterns and replaces them with 3D objects. If some patterns were not identified they could be also replaced with their 3D correspondent by manually tracing the algorithm search position. Potential errors or unrecognized objects are removed, corrected and completed manually.

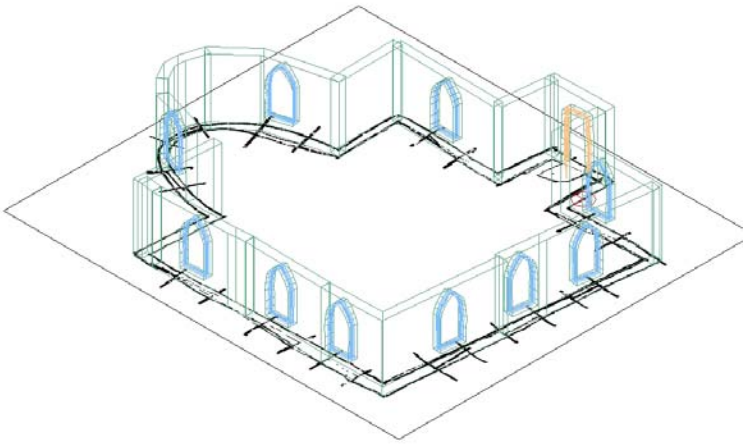

Fig. 5.9 3D Model generated automatically from a 2D hand sketch using PlanTracer [www59]

Currently, the automatic recognition algorithms are implemented in software like Plane2Model and PlanTracer [www59] that are running as plug-ins on ArchiCAD respectively AutoCAD (ADT) platforms, profiting of their large object libraries.

b) Materials

The way the human eye is able to distinct the appearance of different objects is influenced in nature by two factors: one is given by the surface of the object and the other is the light. The surface of an object defines also how an object reflects, absorbs and transmits the light.

In computer application the appearance of the real objects is reconstructed using materials or shaders. They can add details and increase the realism generally without adding complexity to the object's geometry.

Shaders are defined as functions that compute the way the object surface responds to light and as data applied to object's surface that determines its appearance. Some generally used shaders in computer graphics are described in Annex VII.

The material properties are defined by various attributes like color or physical elements. The attributes for a specific material are defined to a great extend by the shader type. The standard color elements of a material in CG software are ambient, diffuse and specular color. The ambient color is the color of the object in the shadow and defines how the ambient color influences the appearance of the object. The diffuse color is the color of the object in direct light and the specular color specifies the color of the highlighted areas.

1. Oren-Nayer-Blinn shader with diffuse and ambient color R:236, G:236, B:210, specular color R:229, G:229, B:229 and bump map;
2. Blinn shader with texture map in the diffuse color slot;
3. Architectural material, texture map, bump map and refraction index:2.5;
4. Translucent shader with translucent color R:35, G:35, B:35;
5. Blend material;
6. Multi/sub-object material.

Fig. 5.10 Generic materials in a VR (virtual reality) scene using 3ds Max 6 (see project "Hohenburg", Chap. 7.5); for a description of the used terms see Annex VII

Standard physical attributes are:

- opacity or transparency level;
- diffuse level (controls the brightness of the diffuse color);
- roughness level (defines the blending of the diffuse color into the ambient color);
- specular level (controls the intensity of the specular highlights);
- reflection level (defines the material reflection of the surroundings);
- refraction index (controls how the material refracts the light and how reflective the material is);
- self-illumination;
- glossiness level (controls how much a material is more or less glossy);
- translucence level (controls the level and color of the light scattered within the object), etc.

The above attributes are used to generate more or less realistic materials usually having properties distributed uniform on their surfaces. More realistic materials can be obtained by enhancing the previous ones with so called maps (see Annex VII).

The maps can be:

- 2D generally used to paint the surface of geometrical objects;
- 3D applied to create patterns in three directions;
- composite employed to combine and merge other maps;
- color modifiers, reflection and refracting maps and other types.

The most common ones, the 2D maps, are images used to describe the real appearance of the material in nature and to distribute the visual and physical material properties. The image can be the real image of the object in nature (e.g. see shader no.2 in Fig. 5.10) or a computer generated one.

The most common mapping method is the diffuse color mapping or the texture mapping which allows the painting of the object surface with an image. Other mapping techniques generally imply the use of a black and white or a gray level image to describe the distribution of a specific property in the material. Black and white pixels are used to reduce or increase some characteristics and intermediate values adjust it.

Some CG software support predefined materials other than standard ones like raytrace materials (material with enhanced surface shading supports advanced reflection and refraction computation), architectural materials (material with enhanced physical properties for 3ds Max 6), mental ray materials (materials for use only with Mental Ray renderer), etc. Also two or more different materials can be combined to create a superior one called compound material that contains the properties of all sub-materials. Furthermore customized materials could be created with most of the commercial CG software by advanced users.

c) Light

The light is the second main factor that influences how the human eye precepts the appearance of an object in nature. Even if the deliverable of the virtual reconstruction process is a non-photorealistic one, the way the objects are visualized is highly dependent on the illumination existent in the scene. If the reconstructed model is part of a scene without any light sources the returned object is always a black one. To prevent this, usually the CG software automatically includes a default lighting scheme in all scenes to illuminate uniformly all objects. Once a light source is manually configured, the default light is removed or turned off.

The light sources from CG software are simulating customs interior or exterior lights using algorithms with attributes that specify their distribution, intensity, light intensity distribution, color, temperature, attenuation, shadow parameters, etc. Some software also allow to import light characteristics using manufactures files, to simulate the sunlight on a given time and location (geographical coordinates) or to simulate atmospheric or ambient effects (e.g. shadows in Fig. 5.10).

The general algorithms used in CG to determine the light influence in the scene are the local illumination and global illumination solutions. The local illumination computes only how individual surfaces reflect or transmit light coming directly from light sources while the global illumination algorithms take in consideration also the light reflected or transmitted from other objects or surfaces in the scene. Although the computation time advantages the local illumination algorithms, the photorealistic result level recommends the global illumination solution for rendering highly realistic scenes. Common methods used for global illumination are the ray tracing and radiosity algorithms.

- one light source
- rendered in 3ds Max 6 with default Scanline renderer

- one light source
- rendered in 3ds Max 6 with MentalRay renderer with 5,000 photons (radius 0.025 m) and energy 500,000

Fig. 5.11 Local illumination (left view) vs. global illumination (right view) (see project "Test objects", Chap. 7.4)

The ray tracing algorithm computes the path of a ray from the view plane through a scene and calculates the light reflection, refraction, absorption and transmission whenever the

ray intersects a surface or object from the scene. For optimal time consumption the algorithm calculates backwards only the ray from each pixel of the screen to the 3D scene. The algorithm has to be repeated for each point of view.

The radiosity method computes the light propagation between all the surfaces from a scene using algorithms based on the theory of thermal radiation. The algorithm assumes that the amount of light energy is constant across a surface, thus, for an accurate computation the objects are divided into a mesh of smaller surfaces. The amount of energy that can be emitted by a surface is equal to the sum of direct (light source) and indirect (other surface) energy inherent to the surface. Finally, the radiosity results are stored for each small surface allowing the scene rendering from different points of view without repeating the algorithm.

Ray tracing	Radiosity
▪ Point oriented ▪ Resolves specular surfaces and omits diffuse reflections ▪ View dependent; algorithm must be repeated after changing the point of view ▪ Time consuming but memory efficient	▪ Surface oriented ▪ Resolves diffuse surfaces and omits specular and transparent surfaces ▪ View independent ▪ Memory consuming but can offer immediately results

Table 5.1 Ray tracing vs. Radiosity

Nowadays, more advanced global illumination algorithms are derived directly or combining the capabilities both of ray tracing and radiosity methods. Beam tracing [Heckberl, 1984] and cone tracing [Amanatides, 1984] algorithms are derivates of the ray tracing method that replace the light rays without thickness with polygonal beams or cones. They resolve some disadvantages of the conventional ray tracing algorithm related to sampling and aliasing, but due to their complexity they are not very popular. Recently due to the increase of the computer speed, methods based on Monte Carlo algorithm (approximate solutions are determined using random or pseudo-random numbers and are iterated until a solution is found) or photon mapping [Jensen, 1995] are becoming popular.

The photon mapping method based on ray tracing is able to simulate the direct lightning, refraction through transparent materials, effects due to the ambient and reflection between the objects from the scene, etc. Algorithms using this method are the distributed ray tracing [Cook, 1984] (the rays distributed over an interval are averaged), metropolis light transport [Veach, 1997] (bidirectional path tracing and path modifications), russian roulette [Kirk & Arvo, 1991] (multiple photon mapping) etc.

d) Time

The virtual reconstruction process generates virtual objects who's appearance is given by their geometry, materials and environment lights. One of the main advantages of the virtual reconstruction is capacity to represent the same object at different moments in time or during intervals of time. The CG software is also able to simulate environments changes or phenomena that affected the studied objects. The time is simulated in CG by modifying the object's geometry, material or light sources. The developer can chose to create different models at different time epochs or to simulate object degradation or

transformation during a time interval. If the first solution implies, usually, the methods reminded before, the second solution inquires the use of other algorithms like animation fading or object and/or material morphing.

Fig. 5.12 Simulated day light (Munich, 10:00 h left view, 14:00 h right view)

The simulated day light gives the actual church orientation on south-north direction and not the normal east orientation of the choir. The church was built by American troops after the WWII respecting the general south-north orientation of the buildings inside of the military base (see project "*Test objects*", Chap. 7.4).

The fading effect can be applied to images or animations and is generated by gradual replacing the original model with a secondary one by modifying the transparency of the initial one. As a result, the second model is visible and the original one is completely transparent. During the fading process the geometry, materials and the light from the scene are not suffering any modification, they are just being replaced.

The morphing method is defined as a gradual animated transformation of an object from one state to another. During the process the geometry and the materials of a model are modified generally by changing the position of the corresponding vertices during several stages. In order to function properly the original and all secondary models have to have the same number of corresponding points.

Chapter 6

Visualization

The visualization is classically defined as the formation of mental visual images, the act or process of interpreting in visual terms or of putting into a visual form [Scott, 1999]. Generally speaking, the visualization is the process of representing data as images that can assist in understanding the meaning of the data [www25], [DigiCULT, 2005]. More in detail, the visualization is a compact graphical presentation and user interface for manipulating large numbers of items, that enables the users to make discoveries, decisions, or explanations about patterns, group of items, or individual items [Shneiderman, 1999].

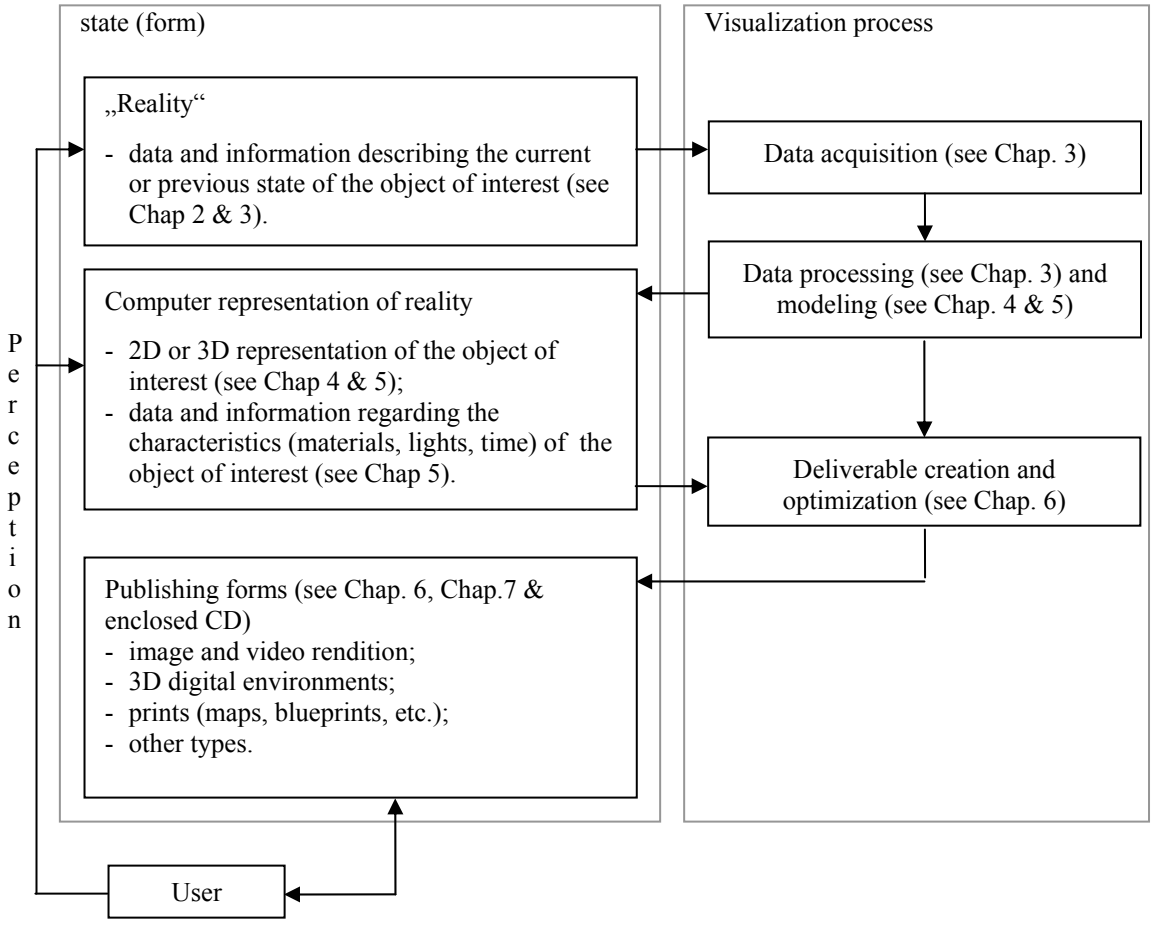

Fig. 6.1 Definition of visualization

Following the definitions given by various authors it can be assumed that one of the main aims of a visualization process is to enhance the human understanding and communication in relation to the represented or transmitted data or phenomena. This can be accomplished by visualization systems only after a clear understanding of the human perception. Such systems must have the ability to deliver proper data in order to identify (percept) the correct meaning of the transmitted data by the user. This requires a detailed knowledge of

color perception, cognitive issues, picture superiority effect, implicit/explicit memory, object perception, human visual system, etc. [Bedny, 2004], [Fleck, 2001] and [Salomon, 2000].

The visualization process includes primarily the following tasks (Fig. 6.2):

- data retrieval from previous data acquisitions operations (see Chap. 3) or post processing processes (modeling – see Chap. 4, virtual reconstruction – see Chap. 5, etc.) and/or data input from the current user/viewer (inquiries, log of the user actions to determine its area of interest, software/hardware profile, etc.);
- data filtering determines which information will be represented and how it will be visualized (e.g. level of detail);
- data analysis summarizes the quality of the data chosen for representation;
- data rendering computes the final deliverable that is visualized by the user.

Data retrieval or data input initiates the request for the needed data from a previously created database or for available data in the case of an individual or initial object. The returned data is organized in categories and data file types in order to response better to an eventually data filtering processes. In case of a returned user the previous data input log is analyzed in order to provide information more related to the user's previous actions. The access level defines the type of data, information and processes accessible to the current user. User's data input is used to formulate rules for data filtering processes (defines the user request, access level, etc.).

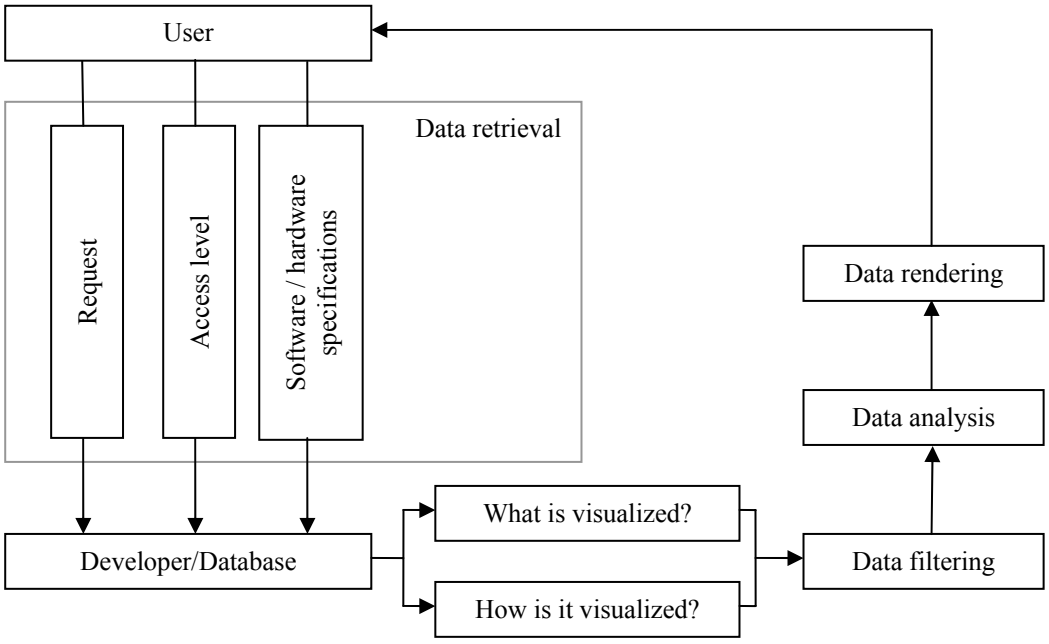

Fig. 6.2 Generic description of a visualization processes

Data filtering initiates an abstraction process that gradually removes details in order to emphasize the items corresponding with the user inputs, or a magnification process that enhances the visualization of the selected items. This is translated in the selection and the enhanced representation of the item which responds appropriate to the user inputs.

The next step is the conversion of the resulted data in a format compatible with the user's software/hardware profile. This is a mandatory stage due to the fact that in most of the cases the software and hardware accessible on the developer level is not accessible to the end-users.

If in case of written data the conversion might face some problems due to different symbols or signs recognition specific to various languages or writing font types, on the level of the graphical or 2D/3D spatial data the conversion could raise greater problems.

Nowadays, the image conversion to a file format suitable to the user/viewer specifications does not raise any problems. Not considering the professional tools such as Adobe Photoshop CS2 [www29] or CorelDraw [www30] there are also a series of freeware or shareware software available such as Irfanview [www26], ImageConverter [www27] or GIMP [www28] able to convert from large scale file formats (*.tiff, *.bmp, *.raw, *.tga, etc.) to more accessible types (*.jpg, *.gif, *.png, etc.) without loosing (too much) from the accuracy and the detail of the initial images.

For digital deliverables having the form of audio and video files, the problem of distributing the data to the user can be resolved by inquiring the viewer to install the suitable audio or/and video codecs [www31] necessary to decode the received data or to convert the available data to the user specifications [www32], [www33]. A short survey for the video formats used to create digital deliverables can be founded in Annex III.

Larger problems appear when dealing with 2D/3D geometric data. This refers to deliver to the end-users geometric data using a file format compatible to their specifications without or losing in a small scale from the accuracy and the detail of the items. This translates in simple words as too much data and not enough standardization.

Even at the developer level when dealing with geometrical entities modeled or created on different platforms, problems could appear due to:

- the incompatibility between platform native files format;
- the platform incompatibility with some geometrical shapes (for example just a small number of CAD software allow point cloud import or the NURBS geometry is not compatible with all software, etc.);
- not all features are supported (the geometry might be supported, but other features like texture mapping, lightning, etc. has to be redone on the import platform);
- incompatibility between versions of the same platform (for example *.max files from newer versions of 3ds Max can not be imported in previous versions of the same software).

Besides the software/hardware compatibility the distribution between developer and end-user is highly dependable on the data file size. The geometrical data has to be published in a format accessible to the user/viewer. For that it might be necessary to compress the geometrical data to a larger distribution file format.

Most of the problems related to the geometrical data transmission can be resolved using one of the following techniques:

- compatible direct export of a data file from the developer software platform corresponding to the user specifications (*.vrml, *.x3d, *.u3d, etc.);

- involvement of a geometrical conversion software like Deep Exploration™ [www38] or 3D Object Converter™ [www39]. Basically, these programs allow the user to visualize native data of most of the important CAD and CG software and data conversion between these formats. In cases of a complex geometry or with multiple items it might be helpful to convert individual items rather than the entire scene;
- using third party software to compress and visualize the geometrical content like Cult3D™ [www34], Lattice3D™ [www35], MyVr-software™ [www36], Walkinside™ [www37] or NGRAIN [www40]. Generally speaking, such software has three main components: an exporter unit installed usually as plug-in on the CAD platform, a publishing unit that converts and processes the data exported from CAD, and a viewer program for real-time visualization, animation, etc.

The user has to remember that the involvement of one of these methods and the migration of the original geometry from the initial processing platform could determine losses in accuracy and in detail.

Currently, there are numerous techniques used to visualize one- or multidimensional data (geo-spatial visualization, vector visualization, volume visualization, structural or tree representation, etc.) specific to the industry or to the area of applications. Independent of the method used to represent the data, all types of visualization systems have the following main aspects:

- the ratio between the amount of data and the quality of the represented data. The challenge of the visualization systems is to provide the amount of data and the quality specific to different types of information and user goals. The visualization system has to respond to the actual needs of the user and also a simply adaptation to new uses. The abstraction or the filtering process has to be controlled through out an easy-to-use and expressive manner that responds the needs of a basic or a advance user in equal measure;
- to represent the uncertainly level or the errors (information about the quality) of the visualized data (see Fig. 5.4);
- the accuracy of the filtering process shows the reliability and the accuracy of the data resulted from filtering (data conversion, approximation, extrapolation, etc.);
- the quality of the rendering versus the time needed to render. The display and the geometry resolution and the response time to the user interaction must be at a level of human perception;
- the perception of represented information or avoiding the false information perception. The visualized object might be enhanced with additional items or information needed to guide the user to a correct perception of the deliverables. For example Fig. 5.12 displays the north direction in addition to the main building and is accompanied by written information in order to emphasize the actual church orientation on south-north direction. Other additional elements like the legend or the scale in a map or an image (see Fig. 7.4) could offer more clear information about the dimensions of an object;
- the user interactivity level. The visualization systems have to response both to users that request a personal interaction (see enclosed CD / Test objects / Interactive

representation) and to users that find themselves more familiar with a guided representation (see enclosed CD / Test objects / Video).

A more detailed description of the aspects and the problems of the present visualization systems can be founded in computer graphics literature like [Hibbard, 1999], [Chen, 2005], [Johnson, 2004].

The data flow used to generate spatial data visualizations is generically described in Fig. 6.3. The deliverables related to the case scenarios (see Chap. 7.6 and the enclosed CD)are:

- common animation containing fly-around or guided walkthroughs: simple video data with or without audio component presenting the object of interest with or without the surrounding environment (see the enclosed CD if "video" menu is available);
- interactive free-orbit or fly-around visualization: common object inspection using tools like zoom/rotate/pan and measuring capabilities, sectioning, etc. (see the enclosed CD if "inspect" button is available);
- interactive guided or free walkthroughs: object inspection using first person perspective (see the enclosed CD if "interactive representation" menu is available);
- wire-frame or photorealistic image representation of the object of interest.

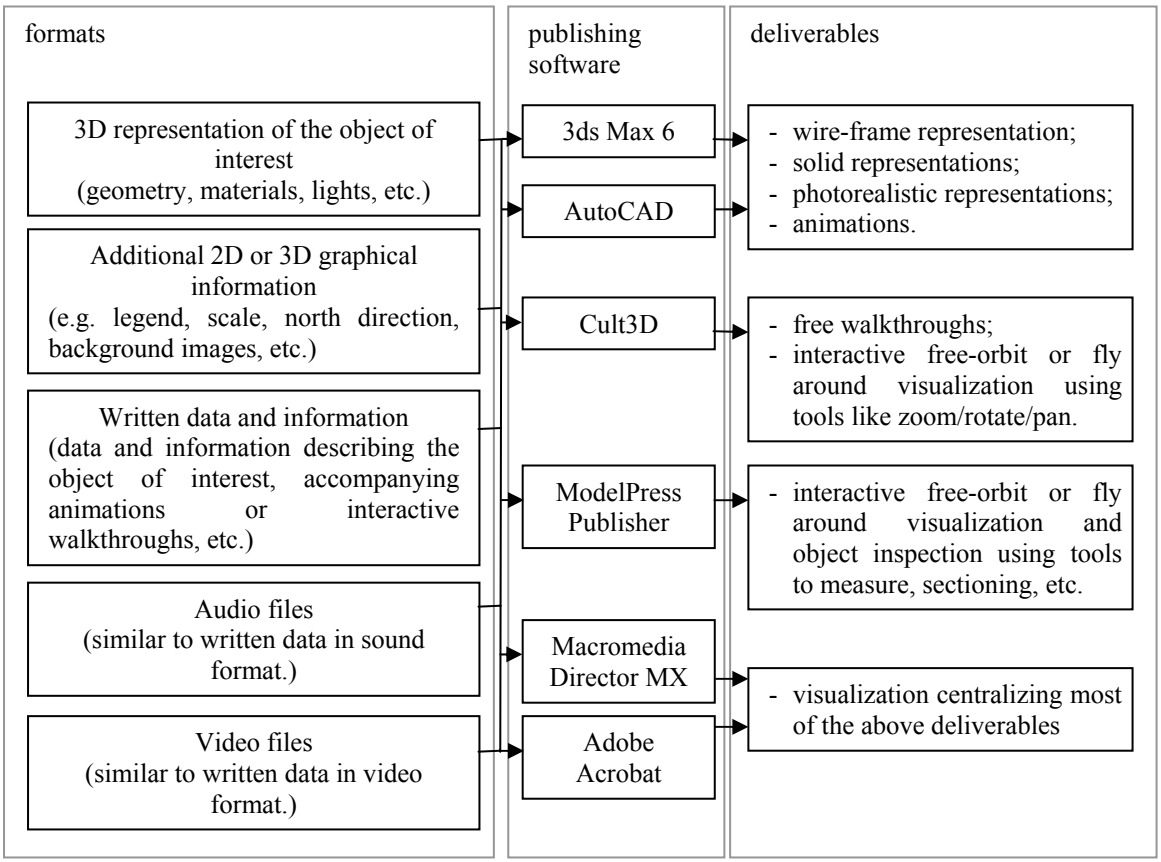

Fig. 6. 3 Visualization data flow

Chapter 7

Case scenarios

This chapter describes the main stages involved in creation of 3D digital documentation of cultural heritage sites based on the studied objects. The explanations are mainly concentrated around the creation of the 3D geometric state of the objects at the time of data acquisition with laser scanning technology and the virtual reconstruction process. The data flow used to generate the 3D geometric shapes for digital documentations can be examined in Annex IV.

7.1 Project Maximilian Straße

Location:
Munich, Germany
11° 34' 48" E, 48° 08' 19" N WGS84

Spatial data acquisition approx. 16 h
(4 persons - simultaneous laser scanning and tachymetry)
Data processing approx. 80 h
(1 person)

Point cloud approx. 9 millions
Final 3D object approx. 260000 faces

Fig. 7.1 Maximilian Straße 6, Munich

The architectural style of the building dates back to the middle of 19th century when the king Maximilian II gave the assignment to redesign and to enlarge the boulevard to the architect Friedrich Bürklein [www44]. During the Second World War, a large part of the street building ensemble, especially the west part (National Theater), was heavily affected by the Allies bombardments [www46] and a reconstruction was needed in the following years.

The project "*Maximilian Straße*" includes as object of interest the building situated at postal number 6 with its annexes (Fig. 7.1). As part of a renovation plan, the building was measured from 11 station points using a laser scanner Cyrax 2500. The final point cloud totalized a number of approximately 9 million points organized in 18 scans. A generic scan was performed with a vertical and horizontal raster of about 3 cm. Simultaneously, a tachymetric network was surveyed in order to determine constrains for the point clouds geo-referencing.

A combined target points and features registration is chosen to bring the point clouds in the same coordinate system, followed by a geo-referencing in the german grid (Gauß-

Krüger coordinate system). The registration performed in Cyclone using 24 targets points (6" circular targets) and 14 planar patches had a mean absolute error of about 8 mm.

After the point clouds are manually “cleaned” from all unwanted data (e.g. cars, people, traffic signs, etc.) several local coordinate systems are defined parallel to the building’s elements. This is performed due to the fact that the CloudWorx plug-in for AutoCAD generates sections of point clouds only parallel to standard planes (xy, xz, yz). Façades and floor planes of the building are drawn and a partial 3D wire-frame representation of the building is obtained using the fit section command in CloudWorx (Fig. 7.2).

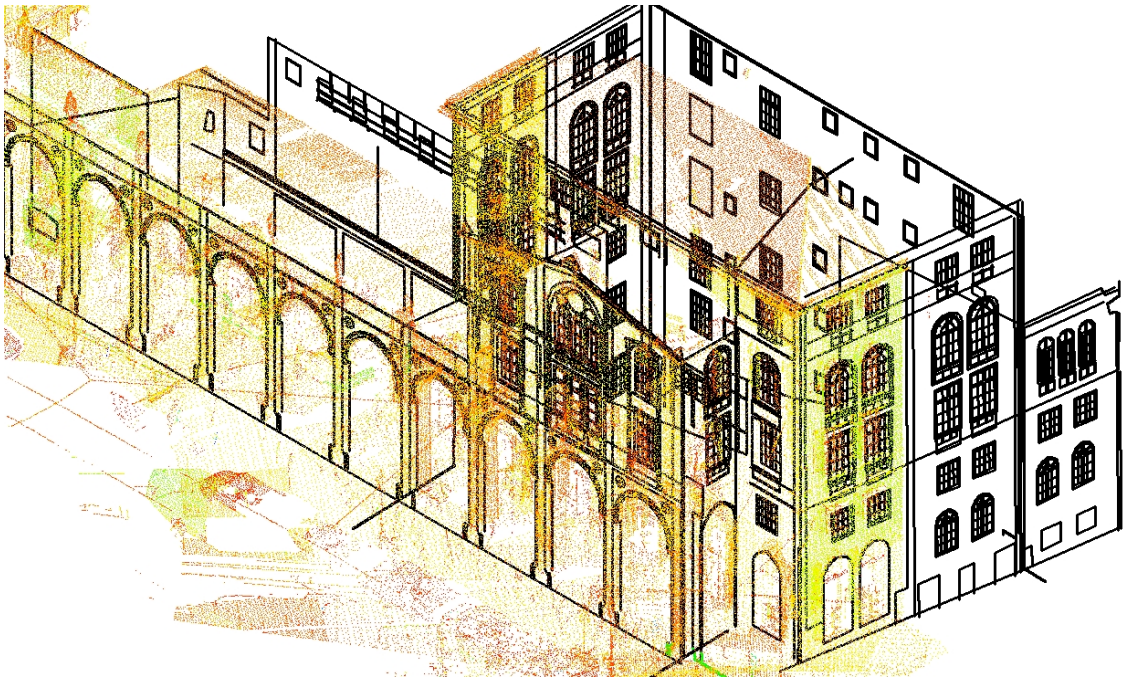

Fig. 7.2 Partial 3D wire-frame representation and point cloud comparison (AutoCAD with CloudWorx)

The wire-frame representation together with a triangulation mesh and the pipes geometry created in Cyclone are imported in 3ds Max 6 for further processing. Here, the first step is the creation of the wall’s geometry without any other components (windows, doors, arcades, etc.) followed by Boolean operations (see Chap. 4.6) that identifies the positions of above mentioned elements. Geometric components are manually created by digital tracing (see Chap. 4.5) and editing geometric primitives (boxes, cylinders, tubes, etc.) on the triangular mesh or on the wire-frame representation (see Chap. 4.6) of the building (Fig. 7.3). For a more detailed description of this process see Chap. 7.3.

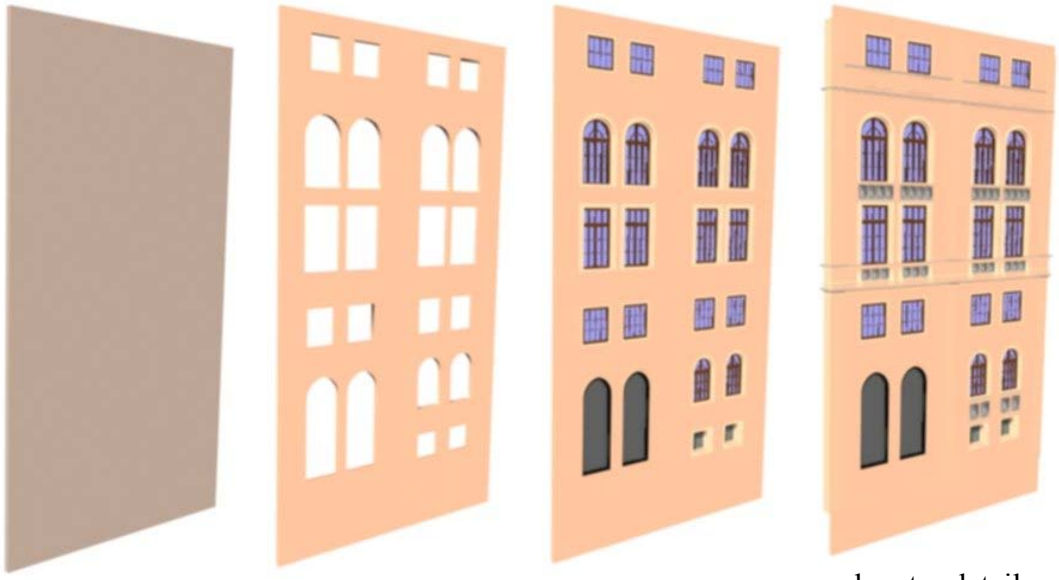

a. clear wall | b. Boolean operation | c. windows | d. extra details

Fig. 7.3 Geometry generation in 3ds Max 6 (west façade)

The geometric shape of the construction can be then combined with suitable materials and light sources (see Chap. 5.2.3) in order to obtain a photorealistic representation of the object of interest (Fig. 7.4).

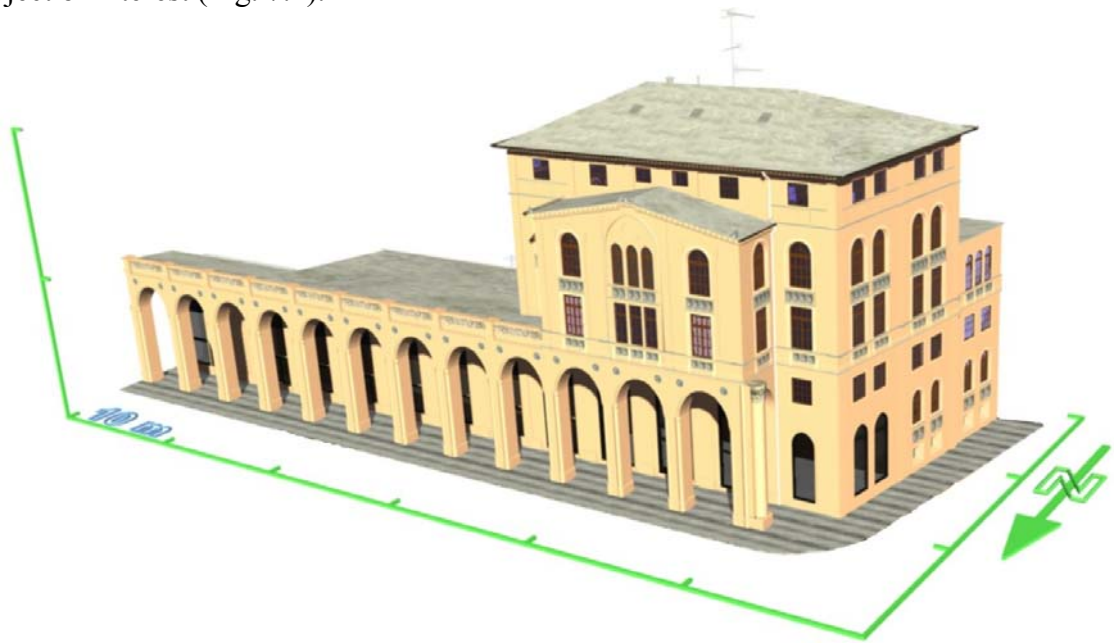

Fig. 7.4 Photorealistic rendition in 3ds Max 6
(view from north-west; for further views see the enclosed multimedia CD)

7.2 Schönberg (Dealu Frumos)

Location:
Dealu Frumos, Romania
24° 41' 33" E, 45° 59' 13" N WGS84

Spatial data acquisition approx 60 h
(4 persons)
Data processing approx. 160 h
(2 persons)

Point cloud number ca. 90 millions
Final 3D objects ca. 70000 faces

Fig. 7.5 Fortified church Schönberg, Romania (view from north – east)

The project concentrates on one of the fortified churches of Transylvanian villages. Some of these are already part of UNESCO world heritage since 1993 and 1999 (Biertan, Valea Viilor, Calnic, Viscri, Saschiz, Darjiu, Prejmer).

Dated around 13th century the church in Schönberg was constructed as a Romanesque basilica having three aisles with pillars and arcades, without tower and a quadrilateral space for choir. Around 1500 the church was fortified with surrounding walls and the side-aisles were lifted up in the style of the gothic churches. A 23 m height fortified bell tower with up to 2 m thick walls was constructed in the central aisle and a one floor smaller tower in the east side of the church. Both towers have timbered battlement parapets and pyramidal roofs. A well could be also found inside the church. Forward defense towers were built on the corners of the fortified perimeter. In the first half of 16th century the fortification is enlarged in the south side. The south-east tower is transformed in a pentagonal fortified tower and a two-storied entrance tower is constructed besides the north-east tower. Around 1647, the north perimeter wall is moved 5 m forward and on this side a rectangular building and a tower are constructed. In 1914 the pentagonal tower is transformed in church community house [www47], [Fabini, 1997], [www48].

Since 2003 the fortified church is under the patronage of the "Ion Mincu" University of Architecture and Urbanism, Bucharest and transformed in study centre of vernacular architecture in Transylvania.

The present project, part of an renovation plan, was performed in cooperation with "Ion Mincu" University of Architecture and Urbanism, Bucharest and Faculty of Geodesy of Technical University of Civil Engineering, Bucharest. The first part, the creation of a 2D surveying plan of the church and fortified perimeter, and a geo-referencing network was realized in two weeks practical work by the Faculty of Geodesy Bucharest.

The objects of interest within the project are represented by the fortified church and its surrounding annexes. Furthermore the roof truss of one of the buildings ensemble is under study due to the high interest over the wooden-frame junctions (see Fig. 7.9). The

measurement process was realized with a HDS 3000 instrument from 23 locations, thereof four for the truss. Finally, there were acquired approximate 90 million points. An acquisition horizontal and vertical raster of about 2 cm was used in the measurement of the fortified church and a raster of about 1-2 mm for the roof truss recording. Due to the large vegetation coverage some parts of the investigated items were not captured by laser scanning instrumentation. The missing data is replaced during the modeling stage by elements that could be seen in the photographic documentation or by completing the geometric shape (surface extend, cloning similar available items like windows or doors – see Chap. 4.5 and Annex I).

The modeling of the church ensemble is realized in two stages. A process similar to the one described in the project "*Maximilian Straße"* (local coordinate systems, sections in CloudWorx and fit section procedure – see Chap. 7.1) is used to generate a complete 3D wire-frame model of the central building. The usage of this method is encouraged by the presence of walls in good physically state with a simple geometric form. This was completed during a diploma thesis [Näher, 2005]. The 3D solid model is then generated by using the draw boundary surface option in AutoCAD (see Annex I).

For the fortified perimeter and the annexed building the above process could be involved just partially. In the areas were the fortified walls are suffering from degradation or having a non-uniform geometric shape, several sections are made and ruled or sweep surfaces are created based on these sections (Fig. 7.6).

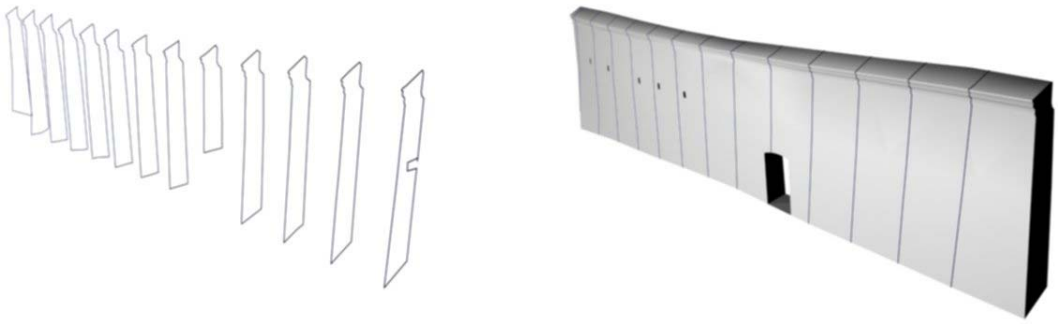

Fig. 7.6 Create 3D ruled surface from sections using 3ds Max 6 (see Chap. 4.6 and Annex I)

Other objects are created and corrected directly in 3ds Max 6 by digital tracing the mesh created in Cyclone. Fig. 7.7 (left view) shows the mesh in green color overlapping the generated objects at one of the modeling stage of the main entrance. The decision to modify the current shape of the objects is made by comparing the mesh and the information given by the digital image (right view) with the present geometry. Two common modeling issues are identified by this example. Firstly, the missing geometry represented by some small openings in the right tower's wall and secondly, the positions of the highlighted roofs relative to the mesh have to be corrected.

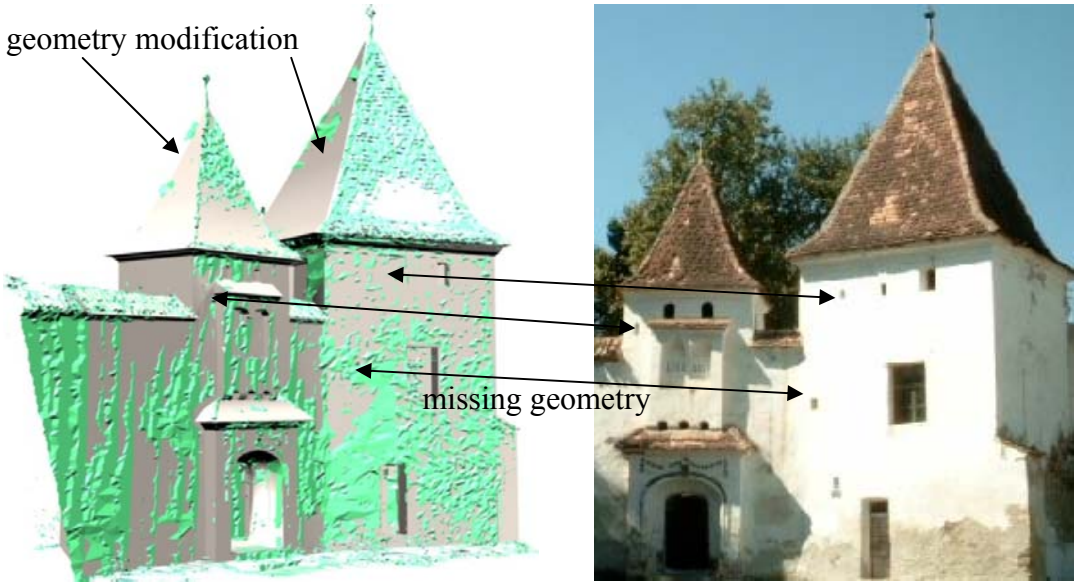

Fig. 7.7 Modeling decision stage - with arrows areas are identified which have to suffer modifications or improvements (main entrance view)

The model is completed in 3ds Max 6 using the above processes and the same procedures as in the previous case scenario “Maximilian Straße”.

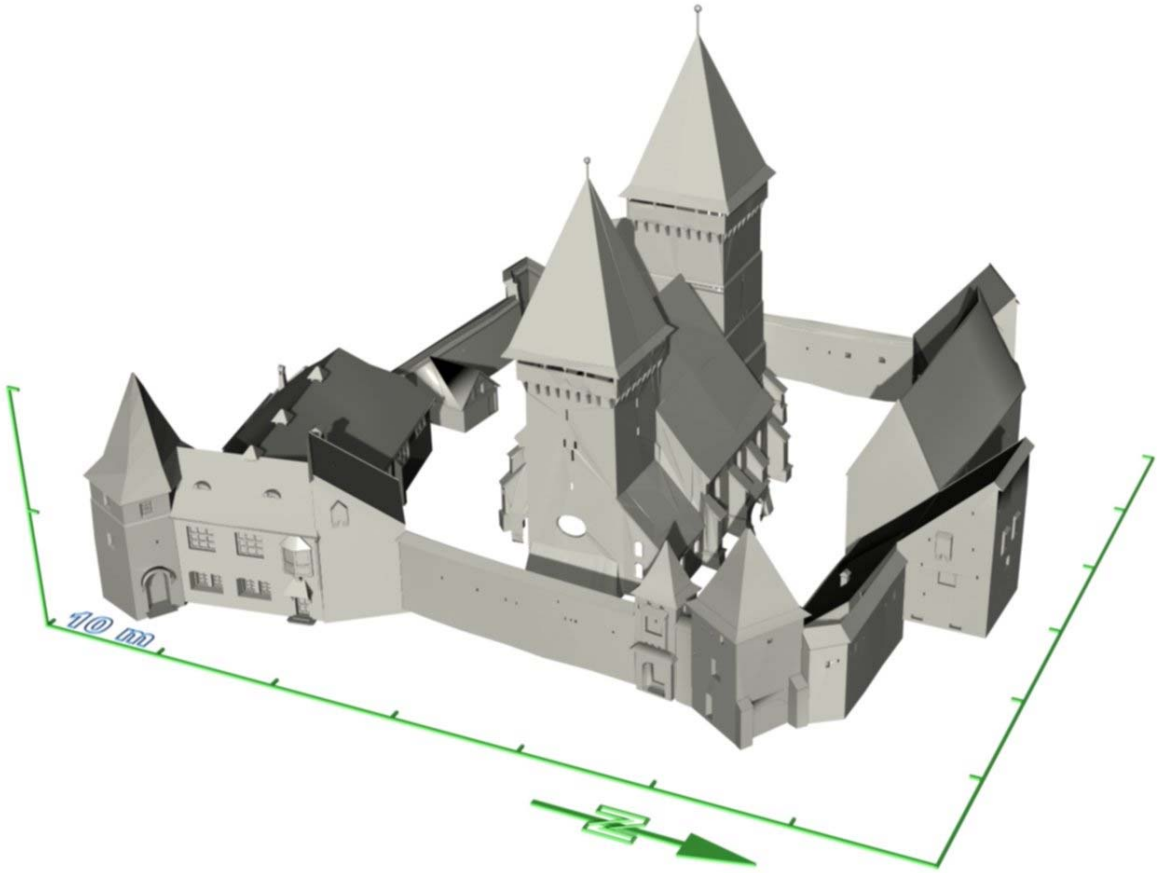

Fig. 7.8 Schönberg, 3D representation in 3ds Max 6

Initially the roof truss model was realized completely in Cyclone using piecewise the point cloud fit to box procedure. The resulted model shows the general distribution of the

wooden frame-work. For a detailed view of the wooden beams junction, a triangular mesh is generated direct in Cyclone and imported in 3ds Max 6, where a 3D model is manually created (Fig. 7.9). The 3D computer representation of the roof truss presents large significance in understanding the design of the wooden junctions by specialists from "Ion Mincu" University of Architecture and Urbanism, Bucharest.

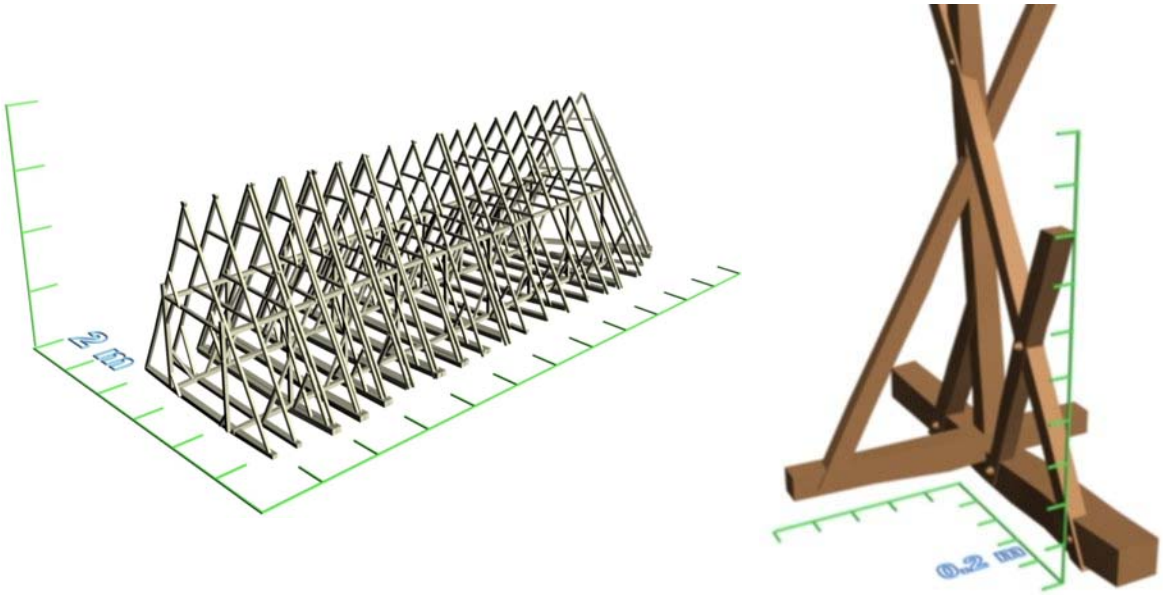

Fig. 7.9 Wooden truss: generalized model (left), detailed junction (right)

Beside the generation of 3D models based on data acquired with the laser scanner, the project also includes a virtual reconstruction of previous states of the fortified church. A number of six models are created based on isometric views found in [Fabini, 1997]. The representation of these virtual reconstructions can be found in Annex V and in the enclosed CD.

7.3 St. Michael church

Location:
St. Michael Church, Perlach, Munich
11° 37' 54" E, 48° 06' 05" N WGS84

Spatial data acquisition approx. 8 h
(1 person)
Data processing ca. 120 h
(1 person)

Point cloud number approx. 16 millions
Final 3D objects ca. 1502000 faces

Fig. 7.10 St. Michael Church, Perlach (Munich)

The project contains the interior of the St. Michael church in Munich and has as a main aim to generate a complex and detailed model from the acquired point cloud. If in the previous projects the work is concentrate on the building geometry and its elements, this case scenario also contains the geometry of all items presented at the scene.

For spatial data recording a laser scanner HDS 3000 was deployed in two scanning positions. The average raster scan is of about 2 cm in horizontal and vertical direction. The registration of the point clouds is made exclusively using circular targets and has an average error of 1-2 mm. The project also includes the usage of thermography methods for identification of the problematic areas within the building [Klingert, 2005]. The infrared information is included in the final 3D model as texture mapping.

With respect to the planned tolerances and object importance the following techniques are used to generate 3D computer representation of the acquired objects (for a complete view see Fig. 7.17):

1. Geometric primitives (patches – walls, boxes – wooden beams, cylinder – columns, etc.) are created directly in Cyclone using the "fit to cloud" or "region grow" commands (see Chap. 4.4). In order to maintain the quality of the final model in the wanted tolerance limits, most of the object's geometry is generated using automatic or semi-automatic tools and manual modeling is restricted as much as possible. It is recommended to involve other modeling tools in geometry creation just after the geometrical primitives are identified and modeled. This also improves the data access and the visualization of the final model;

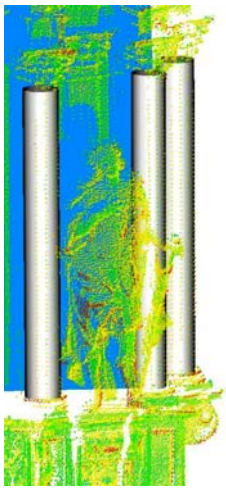

Fig. 7.11 Create basic geometry (cylinders and patches) in Cyclone 5.3

2. Sections and fitted geometry (lines, arcs) are generated in AutoCAD using CloudWorx (see Chap. 4.5). 3D objects based on these shapes are constructed in 3ds Max 6 or in AutoCAD using techniques like the ones in Annex I. The generic process consists in the creation of one or more cross-sections that are sweeping one or more paths. The quality of the constructed model is related directly with the number of the estimated cross-sections and has a larger reliability in the areas neighboring these cross-sections. The Fig. 7.12 shows the creation of a complex object by sweeping the curve *1* on the path *2*;

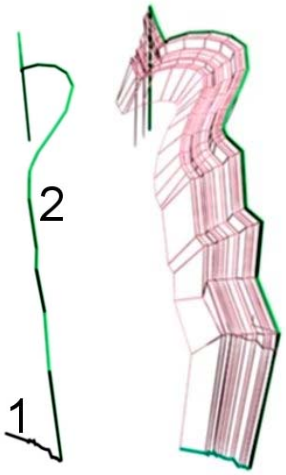

Fig. 7.12 Create a loft surface identifying a detail of the altar using 3ds Max 6 (see highlighted arrows no. 2 in Fig. 7.17)

3. Ornaments (statues, wall patterns, etc.) are created as triangular meshes in Cyclone (see Chap. 4.7) and mapped with textures in 3ds Max 6 (see Chap. 3.3). This method allows the creation of detailed and accurate objects. When dealing with complex sites, before proceeding with the mesh construction, it is highly recommended to divide the point clouds in areas that describe individual objects. This is made due to the hardware limits to render large numbers of polygons in an acceptable frame rate. This is also one of the reasons why the method is used to model only the significant objects from the scene that can not be suitable created with other methods. A mesh generated in Cyclone is shown in Fig. 7.13 (left view) and with the texture mapping in 3ds Max 6;

Fig. 7.13 Create textured triangular meshes (13846 faces occupying 1.66 MB)

4. The image processing (image enhancement, textures, opacity maps, etc.) is performed using the GIMP software (see Chap. 3.1.2). This method is used to represent objects with small importance for the quality of the entire scene, but will give a more realistic representation. The method is also used to reduce the geometric complexity of objects. The process consists in identifying and isolating wanted areas in digital images and creating different maps (see Annex VII) to use with the represented objects. Fig. 7.14 displays three types of maps used to represent a golden detail from the main altar table. The first image from left (diffuse map) is the one that gives the appearance of the object. The second one (inverted opacity map) determines which part of the images is rendered and the last one (bump map) gives a relief appearance for the represented object.

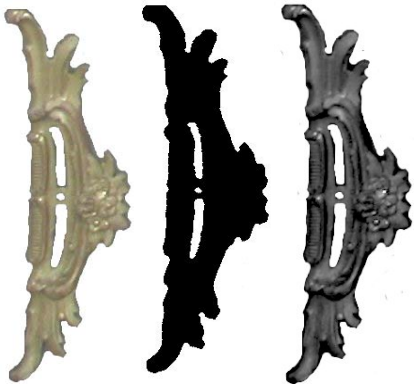

Fig. 7.14 Types of maps for object representation

5. The adjustment and missing data completion are realized in 3ds Max 6. Some objects are measured just partially during the laser scanning campaign mainly due to their low importance. Custom CG tools are used in order to obtain a complete representation of the scene. For example the candle holder from Fig. 7.15 (right view) is constructed by cloning and rotating the available part (left view). Other tools are used to edit and complete the available geometry: fill holes, correct shapes, etc. (see e.g. Chap. 4.8).

Fig. 7.15 Create a complete object (candlestick)

6. Extra items are created directly in 3ds Max 6 without direct spatial data information (e.g. tablecloth, chairs, candelabrum, etc.) using only the digital images captures on site. This method is used when the acquired data provides insufficient geometric information to generate partial or complete objects. Due to the fact that the resource data contains no quality metric information the resulted objects are used just to complete the scene and do not present any reliable geometry. The object is created starting from a geometric primitive (e.g. a box or a sphere) or by drawing poly-lines and using custom CG tools.

Fig. 7.16 Create an object from digital images (left – digital image, right – computer representation)

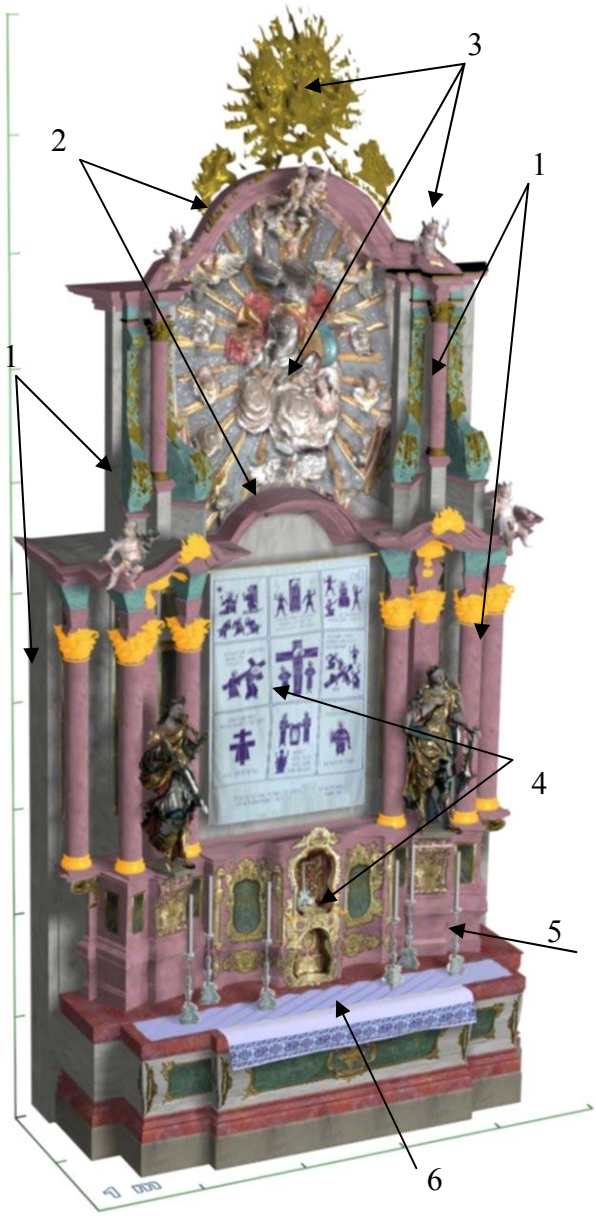

Usually, when creating a scene, firstly, the geometry of the objects is generated by combining the above methods and just in the end the shaders and the source lights (see Chap. 5.2.3) are introduced in the scene. Fig. 7.17 identifies with arrows the methods used to created different parts of the main altar. It can be observed that the distribution of the used methods does not have a uniform pattern. Usually, neighborhood areas are created with different methods in different applications. In order to maintain the original position of the component parts of the final model, a common (superior) coordinate system is used when modeling or just before the export of the model from the current application to the one that contains the final model.

Fig. 7.18 contains one view of the final representation of the St. Michael church. The image contains approx. 15 % of the entire scene. Further computer representations can be seen in the attached multimedia CD.

Fig. 7.17 Main altar – St. Michael church (default 3ds Max Scanline renderer). The numbers are identifying the above mentioned methods used to create the highlighted objects. The model contains approx 200000 faces and 40 materials (approx. 15 MB in *.max format).

Fig. 7.18 Representation of the St. Michael church. The image is rendered in approx. 12 minutes with the default 3ds Max 6 Scanline renderer.

The quality of the computer generated model is given mainly by aspects related to:

- the method used to generate the object representation. In most of the cases the triangular mesh and geometric primitive representations produce the most accurate results (restricted to the acquired data);
- the level of process automation. It is expected that a manual generation of a 3D model to produce a subjective representation;
- the proper usage of the modeling tools corresponding to the type of object. It has to be considered not only the type of technique used to generate the 3D model but also it's proper usage. For example, if is more appropriate to model an object having the shape of a cylinder using geometric primitives and not triangular meshes. The last ones may generate irregularities in the model surface due to the low raster scan;
- a quantification for the quality of an entire scene is difficult to be realized mainly due to the variety of the contained objects. Different methods are used to acquire data (see. Chap. 2 & 3) and create 3D models (see Chap. 4) in accordance with the importance level given to every object during the planning phase. Thus it is expected that objects with inferior importance level to be generated with a lower accuracy. In this case an overall quantification will be influenced in a negative manner and will provide false information about the significant objects from the scene. Therefore, a more suitable quality description can be given when analyzing individual objects (see for instance Fig. 7.22, gradient color information is used to investigate the quality of the represented model).

7.4 Test objects

Spatial data acquisition:
- statue of Athena approx. 2 h (1 person)

Data processing:
- statue of Athena approx. 20 h

Point cloud number:
- statue of Athena approx. 1.2 millions

Fig. 7.19 Small statue of the goddess Athena (object size 25 x 25 x 70 cm)

The case scenario "Test objects" includes the data acquisition and the modeling of a small statue representing the goddess Athena and of the church of the campus of the University of Bundeswehr Munich. The objects are previously mentioned in Chap. 4 to exemplify the processes specific to the laser scanning and modeling techniques.

Initially, the statue was used as test object to investigate the performance of the long range laser scanner HDS 2500 when dealing with small objects. A total number of approximately 1.2 million points were captured by scanning the item from 7 positions. Due to the presence of straight and curvature areas on its surface, the statue is proved to be a suitable object in testing the abilities and the performances of different laser scanning software in the point cloud treatment or in the creation and the editing of the triangular meshes (see Chap. 4 and Annex II). Due to the large number of triangular faces in the created mesh, the object is also used to determine the suitable software for publishing 3D geometrical models.

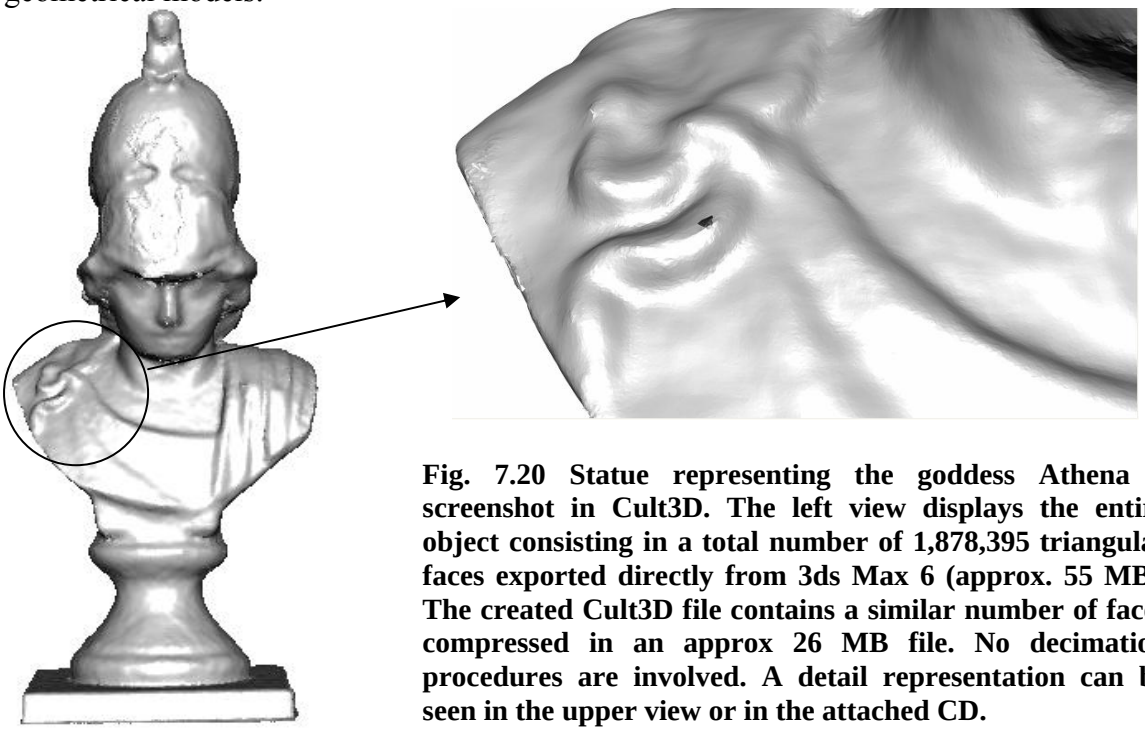

Fig. 7.20 Statue representing the goddess Athena – screenshot in Cult3D. The left view displays the entire object consisting in a total number of 1,878,395 triangular faces exported directly from 3ds Max 6 (approx. 55 MB). The created Cult3D file contains a similar number of faces compressed in an approx 26 MB file. No decimation procedures are involved. A detail representation can be seen in the upper view or in the attached CD.

Location:
Neubiberg, Germany
11° 38' 22" E, 48° 04' 44" N WGS84

Spatial data acquisition approx. 7 h
(2 persons laser scanning)
Data processing approx. 100 h

Point cloud number approx. 10 millions
Final 3D object: approx. 25000 faces

Fig. 7. 21 Side view of the church from the campus of the University of Bundeswehr Munich

The exterior and the interior of the church from the campus of the University of Bundeswehr, Munich are scanned using the laser scanner HDS 2500, respectively HDS 3000 with a sample raster of approx. 2 x 2 cm. The registration of the point clouds is performed in Cyclone using circular targets. During the data acquisition temporary positions for the registration targets are used and a connection between the point clouds describing the exterior and the interior of the object was not possible. The two parts are connected later using the geometrical position of the modeled components.

The object modeling is performed in a large scale using geometric primitives in Cyclone and completed in 3ds max 6 (see Fig. 4.11). An analysis of the accuracy of the created geometry is performed by importing the object into Geomagic Studio 6[7] and performing a point clouds to polygons deviation measurements (Fig. 7.22).

The object is also used for an initial integration of thermographic data within a 3D model. This is performed by texturing the 3D model with images captured with a thermo-camera (see Chap. 3.4).

The created 3D model is completed by applying materials in 3ds Max 6 and using different light arrangements in order to create a photorealistic representation (Fig. 7.23). A larger number of images representing both the interior and the exterior of this object can be seen in the attached CD.

The interior of the church was scanned and modeled after one year interval from the exterior data acquisition and constitutes the platform for a 3D cultural environment exemplification (see Chap. 7.6).

[7] The software Cyclone 5.3 allows point clouds to mesh deviation measurement only one at a time and due to this limitation the procedure is not used in this example.

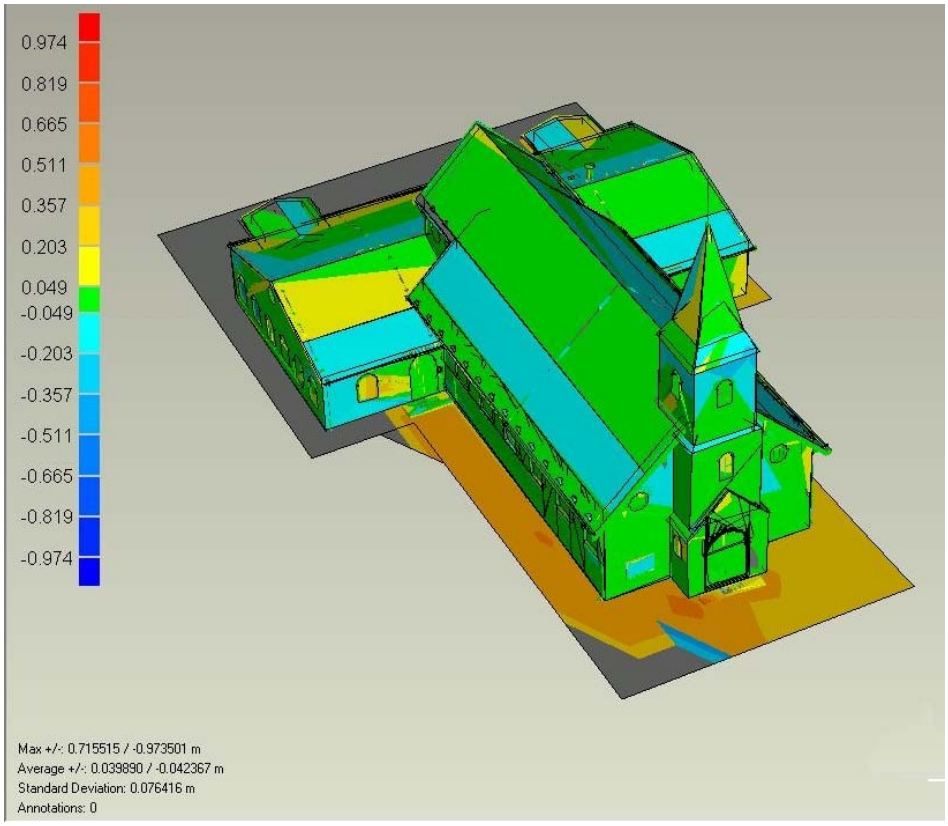

Fig. 7.22 Point cloud to polygons deviation in Geomagic Studio 6 (trial version)

Fig. 7.23 Detailed views over the exterior and interior of the church from the campus of the University of Bundeswehr Munich (see Fig. 3.6 for thermographic representation). The images (1160x1080) are rendered using default Scanline render in 3ds Max 6 (render time approx 15 seconds)

7.5 Hohenburg ruins

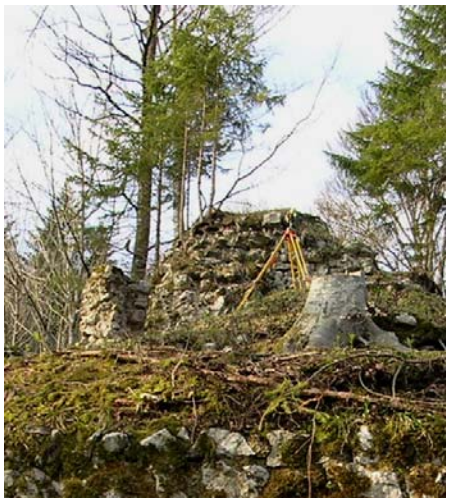

Location:
Hohenburg ruins, Lenggries, Germany
11° 34' 00" E, 47° 40' 60" N WGS84

Spatial data acquisition approx. 36 h
(2 persons laser scanning, tachymetry and GPS)
Data processing approx. 100 h

Point cloud number approx. 16 millions
Final 3D objects: 0.5 m DTM equidistance,
virtual model and digital terrain model approx. 80000 faces.

Fig. 7.24 Hohenburg ruins, view at the main tower ruins

The history of the old Hohenburg castle comprises about 700 hundred years from its building in the 12th century and to its destruction due the burning in 1707. An inventory list from 1694 specifies the components of the buildings ensemble at that period: a seven meter wide quadratic tower (ruins, see Fig. 7.24), two large halls (one of them used as armory for four hundred people), accommodation for different social categories, 4 kitchens, 3 cellars on cliffs and a stable. At the end of 17th century the castle was developed and embellished to a palace, assumed to be similar with the present form of the south side of the Tratzberg palace [Ulrich, 2001]. In the years following the destruction of the old castle, a new palace was constructed in it's immediately vicinity.

Fig. 7.25 Laser scanner HDS 3000 mounted at one of the scanning positions to acquire data needed in DGM creation (the large vegetation coverage can be observed)

The main stages of the project are the creation of a digital terrain model, the ruins ground-plan and finally the 3D virtual reconstruction of the old castle. The project is realized in cooperation with the Bayerische Landesamt für Denkmalpflege which provide archaeological and cultural heritage information regarding the data acquisition and virtual reconstruction aspects.

The data acquisition was completed in two phases. Firstly, a geodetic network from three GPS points and 19 tachymeter points was used for referencing the measurements to the german grid. The network processing is made using SkiPro and Panda software and an average error varying from sub-millimetre (plateau area) to 3 mm is obtained. Parallel with the network surveying, a topographical survey of the plateau area was achieved in order to determine the ground-plan of the present ruins.

In the second phase a laser scanner HDS 3000 was deployed in 25 acquiring stations and a total of 12 million points are measured with an average raster of 2 cm. The point cloud registration and geo-referencing are realized exclusively with planar targets mounted on tripods over the marked survey points..

For the DTM and ruins survey-plan design the following stages are involved:

- unwanted data removal. Due to the large vegetation coverage (see e.g. Fig. 7.25) a significant part of the measured point clouds represents trees, bushes or other form of unnecessary data. A segmentation of the point clouds using the returned intensity was involved without satisfying results thus a manual removal was required. This stage required by far the most extensive work during the DTM creation, a total of approx. 40 hours were needed to remove all the unwanted details (see Chap. 4.2);

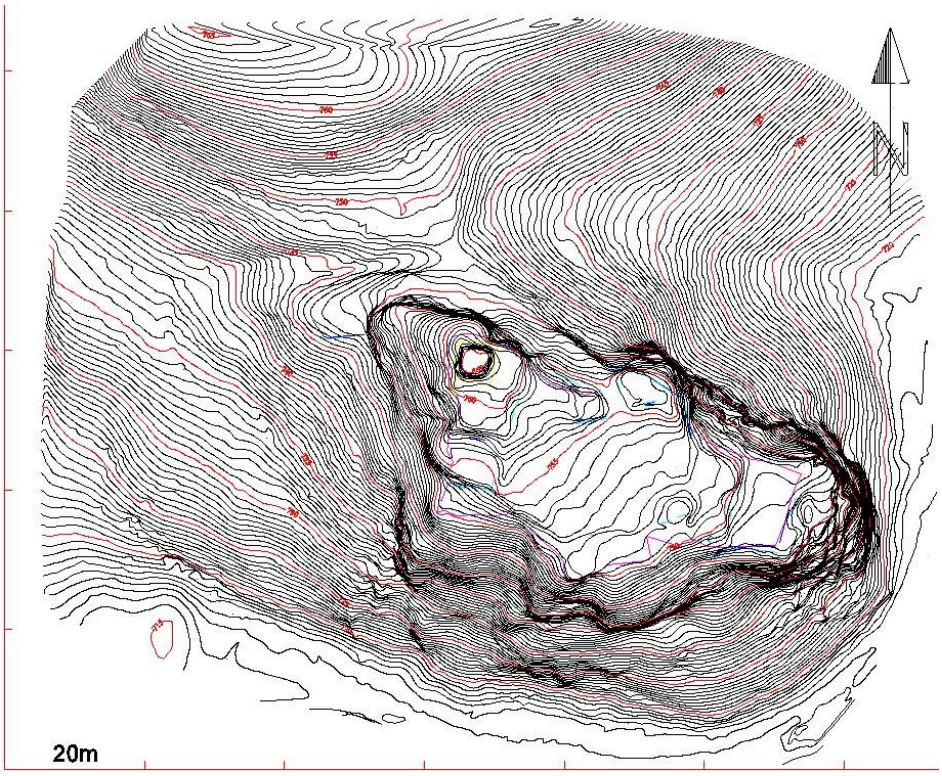

Fig. 7. 26 Contour lines obtained combining the software Cyclone and AutoCAD (red color - 5 m equidistance, black color – 0.5 m equidistance)

- contour lines creation. Due to the fact that not all the unwanted data could be removed in the previous stage and an equidistance of 0.5 m was planned to appear in the final DTM, a generalization of the point clouds is realized by creating contour lines at a fix intervals (0.2 m);
- contour lines processing. The contour lines created directly in Cyclone are exported in AutoCAD for further processing (removal of redundant vertices, correction of intersecting lines, spikes removal – see Chap. 4.8);
- DTM creation. The point cloud is resampled in Cyclone at a raster of 0.1 m and a TIN mesh was generated. This mesh is used for the 3D terrain representation purposes in the further virtual reconstruction;

- ruins survey-plan. The spatial data acquired with tachymeter is imported in AutoCAD and the positions of the ruins and surrounding environment are highlighted (see Fig. 7.27 for a perspective view);
- DTM modification. The ruins survey-plan is imported in Cyclone and the defining lines are used as break-lines to modify the TIN mesh.

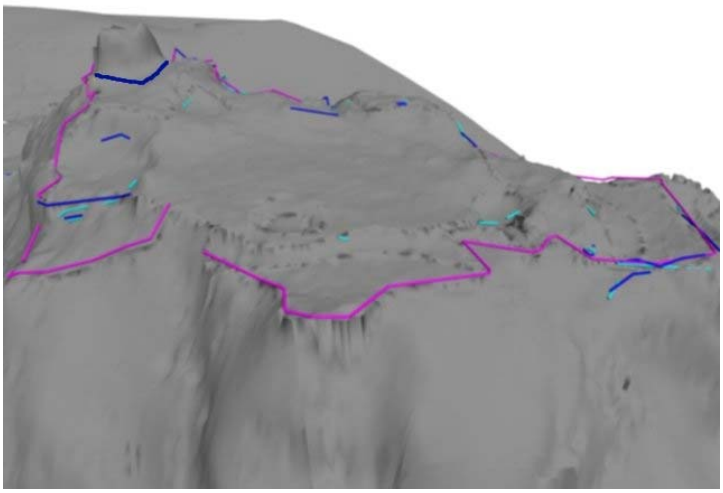

Fig. 7.27 DTM and break-lines. In order to be viewable the break-lines – magenta color - are displayed here with an offset in vertical direction. With blue color the topography of the remaining ruins is represented

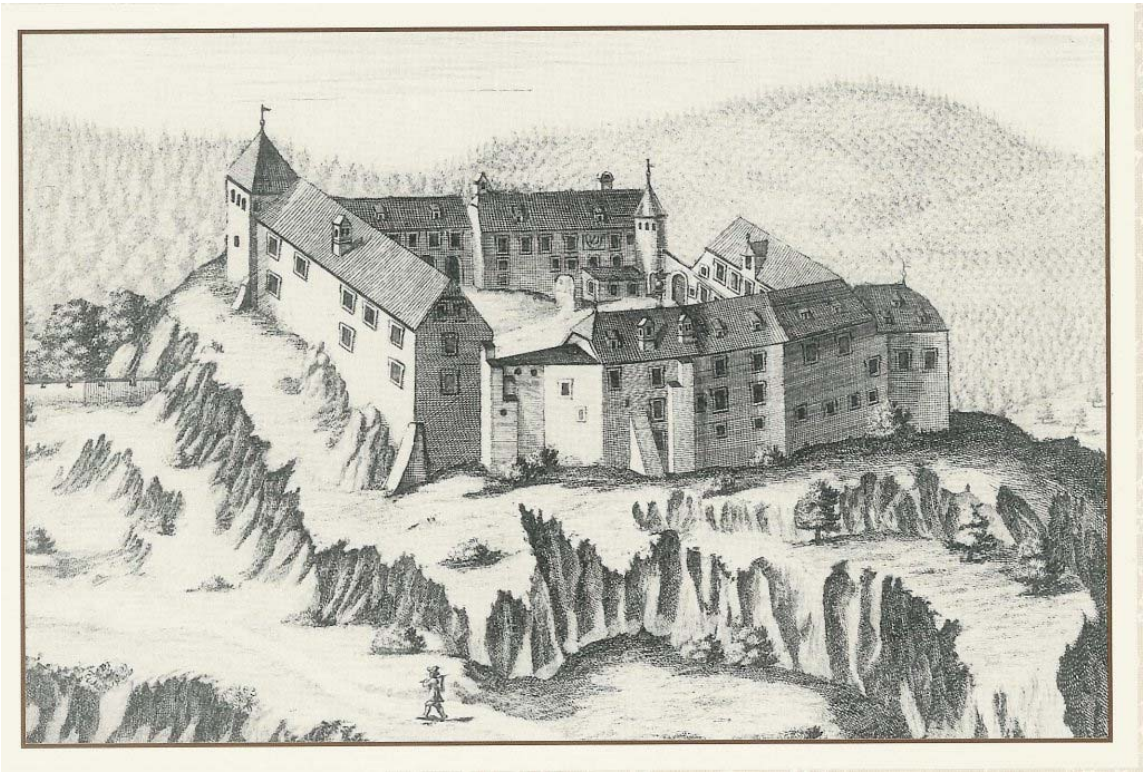

Fig. 7.28 Hohenburg seen from south, copperplate by M. Wenig [Ulrich 2001]

The second stage of the project is represented by the virtual reconstruction of the old castle. This process is accomplished starting with the following direct source data:

- 3D laser scanning and surveying data are the only sources that define the present ensemble geometry. A geo-electrical measurement was performed by a team from Bayerische Landesamt für Denkmalpflege (see Fig. 3.3) but the obtained result were not conclusive for the geometrical shape of the ensemble planned in the virtual reconstruction;
- the representation of the castle is restricted to few illustrations from the period 1699-1700 (copperplate engraving by Michael Wenig and a native landscape painting "Votivbild") [Ulrich, 2001].

The small amount of information is compensated by data collected from similar castles. The historical and the archaeological data are provided by Dr. Jochen Haberstroh and Dr. Gregor Schlicksbier from Bayerische Landesamt für Denkmalpflege. Thus information regarding the roofing type, windows, doors or wall geometry, construction materials, dimensions, etc. are available.

The reconstruction process is developed completely in 3ds Max 6 starting with ruins survey-plan and following the available illustrations. The virtual reconstruction so far is made purely as a technical representation without elements specific for a more photorealistic visualization (for further representations see the enclosed CD).

Fig. 7.29 Virtual reconstruction versus source data

Fig. 7.30 Virtual reconstruction versus source data

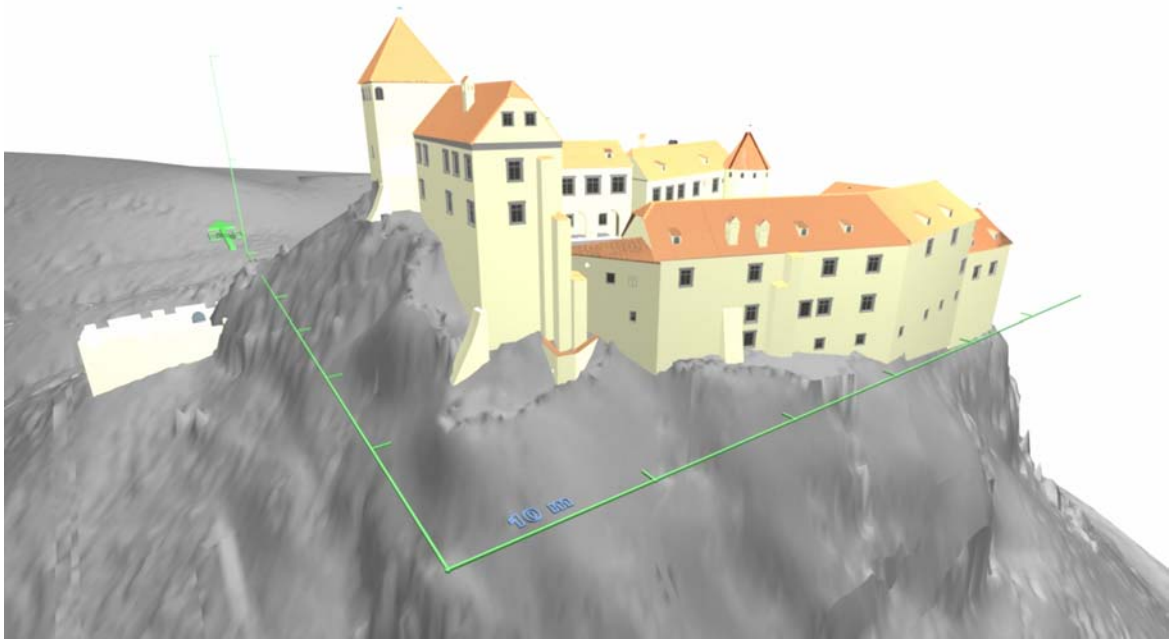

Fig. 7.31 Technical representation of the old Hohenburg castel – south view (DGM created from laser scanning data)

7.6 Aspects of a 3D Cultural Heritage Documentation System

The next step for a standardized 3D cultural heritage documentation is the creation of 3D cultural heritage documentation system comprising generic cultural heritage information (see Chap. 2) and 3D geometrical data. The transition from the present state to the 3D phase is irreversible and needed, for example, to enhance the data representation or to harmonize with the development of similar 3D information systems in various areas. Moreover, the generic users of cultural heritage systems (historians, archaeologists, architects, etc.) have the opportunity to interfere at this moment when such 3D information systems are under development.

A 3D cultural heritage documentation system is a cultural heritage information system enhanced with abilities to display and manipulate 3D geometrical data. The combination of 3D data with GIS is no longer a new topic, several GIS commercial applications have already implemented 3D capabilities: for instance ArcGIS 3D Analyst [www49] and Autodesk Map 3D [www50]. Currently, the real challenge is to provide to the user the capabilities to view and analyze large and complex 3D model in a form that represents the quality of the processed object.

Web based and local workstation applications are the main forms that could be used as a base for a cultural heritage system. The usage of one of them is highly depended of the role and scope of the information system. The web based application requires an internet connection with large data transfer rate and enables almost-real-time updates. The local workstation application is capable to manage large data in small amount of time but might present some problems (data or system update) in the absence of an internet connection or a previous knowledge.

Fig. 7.32 presents a generic concept for a 3D cultural heritage system in three main components. The user segment specifies mainly the level of access for the current users and contains information regarding the user profile (user inquiries, hardware and software specifications, area of interest, previous access characteristics, etc.).

The software segment identifies in three main categories the employed applications corresponding to the user inquiries and the access level. A user with limited access rights will be allowed only to visualize the inquired data, while a higher rang user will be able to manipulate, control, modify or complete the current available data. Another component of the software segment is identified by the application that creates and facilitates the communication between the user segment and the database.

The last segment is represented by the current database divided in spatial and non-spatial data. Subdivisions of the data base are organized in data type, structures and constrains. “Data type” component organizes the current data in proper data categories (2D or 3D spatial data, photographs, animation, written data, etc.) and “the data structures” are components used to define the relationship and connection between different types of data corresponding to the current “constrains”.

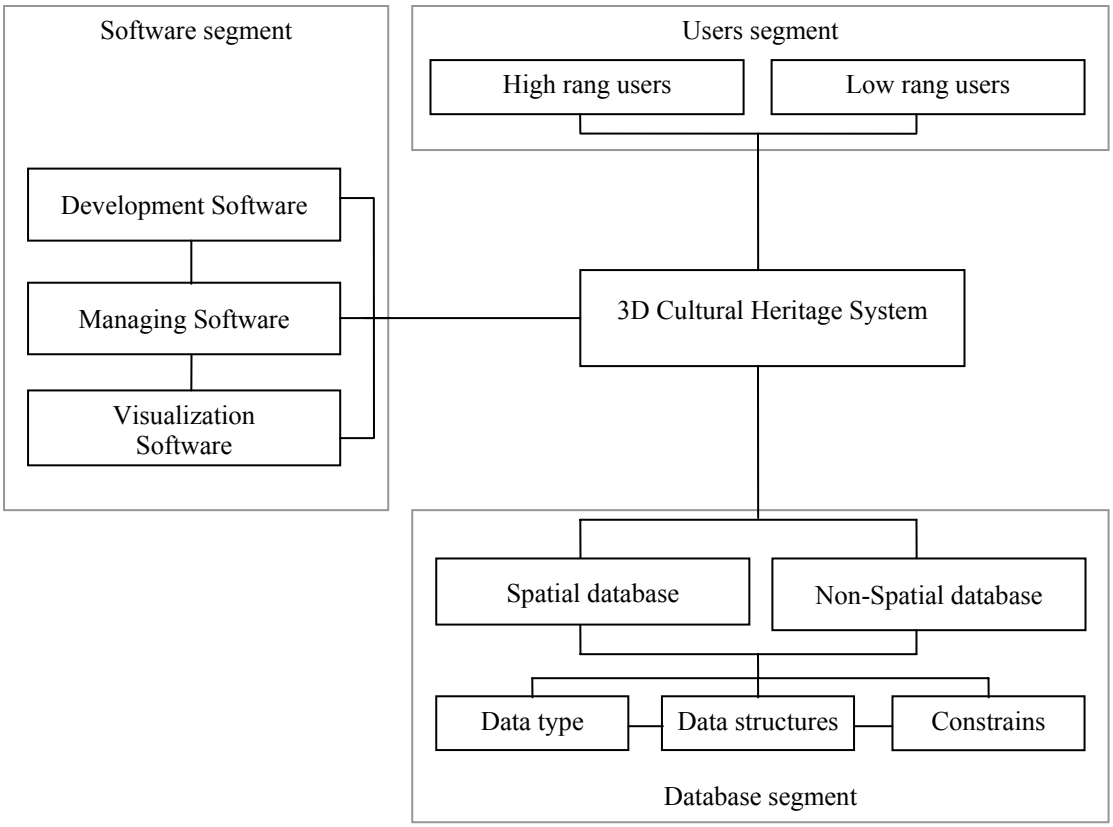

Fig. 7.32 Schematic view of a possible 3D cultural heritage documentation system[8]

Independent of the form of the 3D cultural informational system the following is needed for a good functionality:

- adaptive level of detail. Ability to select different levels of detail for the visualized environment and customize the level of detail for individual items. It is not necessary to load and display the entire level of detail of individual items when visualize the entire scene or when not facing an item. Also some users could have larger interest only for some objects from the environment;
- adaptive graphic engine for displaying 3D objects. The method used for displaying the 3D information has to be compatible and react similar with different graphic cards;
- update capabilities. The system has to be conceived in order to accept future modifications regarding the visualized data and visualization application;
- data compatibility and standardization. The represented data has to be compatible with similar systems and accessible from other applications without changing or modifying the copyright rights;
- user friendly interactivity. One of the most important abilities of an informational system is the capability to be learned and understand in its functionality in short amount of time.

[8] Connected elements are communicating in both directions.

In the annex VI and in the attached multimedia CD simple examples within a cultural heritage system can be found. The presented samples are organized in order to give a generic view on the concept of a 3D cultural heritage system and are limited to basic components:

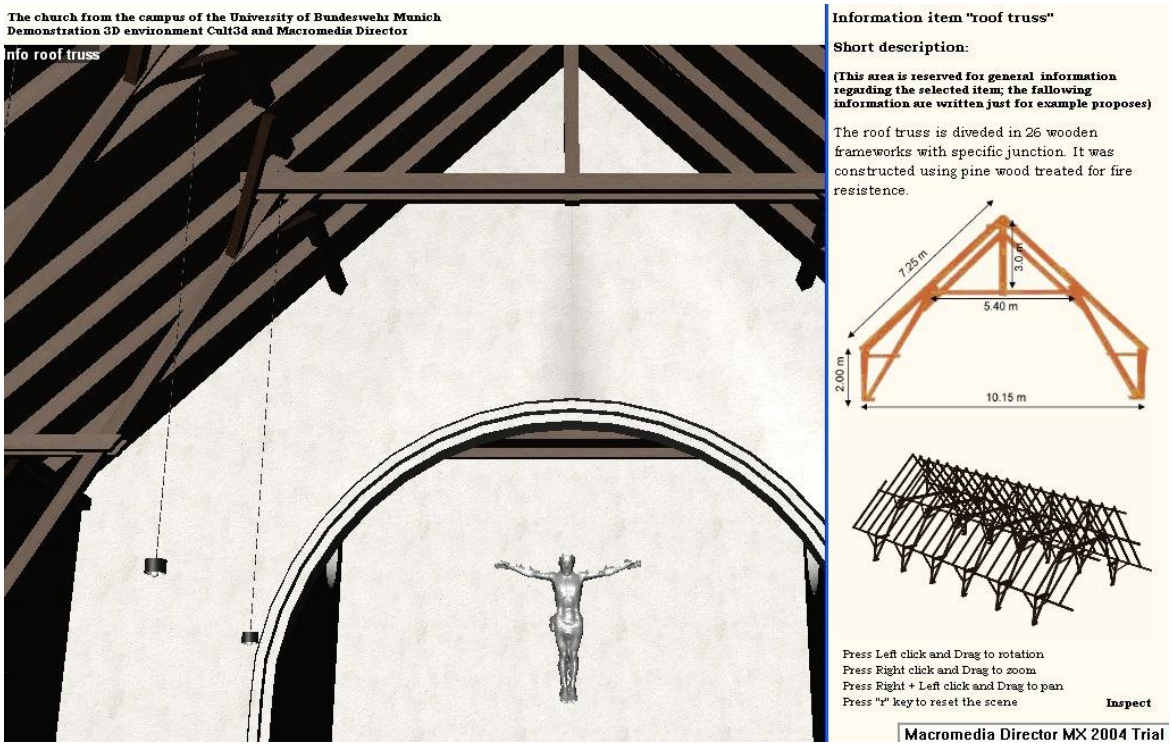

Fig. 7.33 3D environment – the church from the campus of University of Bundeswehr Munich

- annex VI contains the standard format [COE, 2001] for "Core data index to historical buildings and monuments of the architectural heritage" (see Chap. 2) accompanied by 3D geometrical information for the case studies previously presented. The examples are created using Adobe Acrobat 7.0 Professional and Deep Exploration (trial version 09.2005) for converting 3ds Max 6 files to Universal 3D file format;
- free walkthrough digital environment created using Cult3D and Director MX 2004 (trail version). The user can navigate in the entire scene representing the church from the campus of University of Bundeswehr Munich and can retrieve information regarding different items present in the scene. The walkthrough contains the entire geometry of the scene and is an example for a local workstation system (Fig. 7.33);
- constrained walkthrough digital environment created using Cult3D and Director MX 2004 (trial version). The user is able to analyze and navigate the scene representing the church St. Michael, Munich from three panoramic images and is enabled to retrieve information and detailed 3D geometrical data just for some important items. The parts investigation is allowed by using the ModelPress Reader and *.3df file formats. The user is allowed to perform measurements, cross-sections, cuts and to export the current view as Jpeg images. This digital environment stands for an example for web based applications.

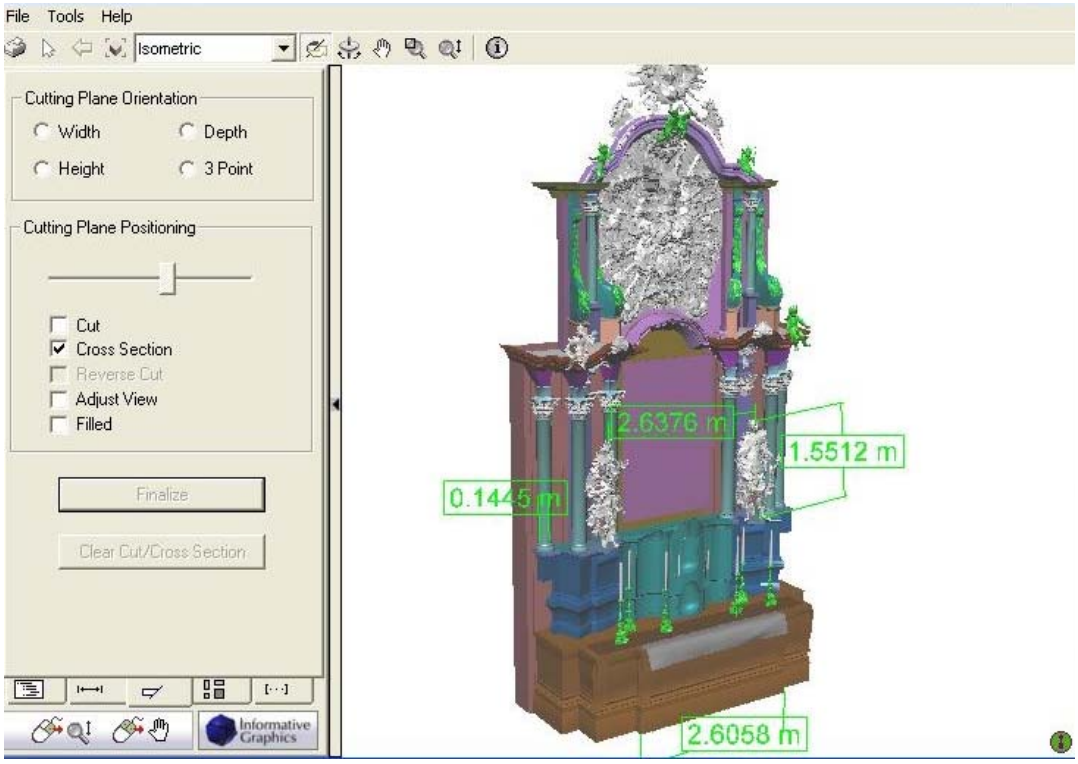

Fig. 7.34 Measurements performed with ModelPress Reader[9] –
St. Michael church main altar

For the inspection (measurements, cross sections, etc.) of the 3D models from the attached CD the free version software ModelPress Reader is required. The application allows the visualization of 3D models previously converted in *.3df file format using the ModelPress Publisher (free version). To access the models contained in the attached CD the viewer has to follow the instructions from the main application by clicking the "inspect" button (when available) or to manually identify the *.3df files.

[9] ModelPress Reader is a free version software of the Informative Graphics Corporation specialized in visualizes and inspect 3D models previously converted in *.3df file format.

Chapter 8

Conclusions

The classical measurement techniques used to acquire spatial data needed in documentations for areas like architecture, industry or cultural heritage are replaced, for the moment just at the beginning, by the newly emerged method of laser scanning. Nowadays, it seems that the technical community got through the initial enthusiasm of the first years from its development and the users are not exclusively interested in how fast and how many points this tool can acquired, rather more in how it can be optimally included in the current workflows. For now, the involvement level of the laser scanning technique in spatial data acquisition is given more by its disadvantages rather than by its abilities. The users are facing the option of including a tool and corresponding software rather expensive with the involvement of the established methods like photogrammetry or classical surveying. Due to this aspect, until now the laser scanning technique is used mainly in projects where the time factor is crucial. Moreover, the users are learning that it is more likely to try to combine the technique with previous tools than to replace entirely the current workflows.

Currently, starting with a more project-related market campaign of the hardware and software developing companies, the users are reorienting to the laser scanning tools that best serves their quality and economic needs. The economic benefits are coming mainly in areas like direct surveying costs, construction, asset management and safety dividend [SparView, 2005]. According to the same source the employment of 3D scanning tools generate savings in the order of 15-20% of the survey budget, or 5-10% on construction total project cost.

Starting with these pre-requisites and considering the laser scanning technology's growing potential, this thesis is concentrated mainly on spatial data acquisition with 3D scanning instruments and processes that generate 3D geometry. A data flow of the processes from the recording phase to the presentation stages is described in detail and analyzed. The work also considers the processes included in currently available commercial software and describes a possible workflow for specific projects. The thesis also refers to the operations performed in order to combine laser scanning data with surveying and photogrammetry data, or data specific to other types of measurements. A concept of 3D digital environment for cultural heritage documentation is proposed and exemplified with different case scenarios.

One of the advantages of the laser scanning technology is the ability to provide initial 3D representations (point clouds) for the documentation of the recorded item right after the acquiring processes. A better representation is realized by cleaning the recorded point clouds from all the unwanted or erroneous data. From this point further it might not be akways necessary to create a 3D solid model due to the presence and development of plug-ins that allow the import of the point clouds in the major CAD software or modeling application. This implies the fact that not all users need the entire capabilities of a specific 3D scanning software in their workflows and some of the purchase costs are not justified. This asks for a module-differentiation in the software licensing method that allows the

customer to acquire only the needed modules. Such a differentiation in modules is present in some of the available software (e.g. Cyclone 5.4) only on larger categories. However, a more sub-level orientation is needed. This would also help to a better management of the workflow where sub-level processes are distributed to separated users within the framework of the same company. In this way a company would not face higher costs when acquiring software and would be more encouraged to employ in it's workflow the needed tool. In the actual globalization conjuncture, it is rather unlikely that all the processes of an entire workflow to be realized involving the software products of the same developer, thus a universal data file format for 3D models is more than needed in order to remove the frustrating and time consuming methods used nowadays when changing the application platform.

It is expected that the current 3D scanning systems will evolve in instruments capable to acquire data with quality similar to the current classical measurement instrumentation. Thus, a more comprehend and generally accepted quality control system has to be developed, not only by identifying possible problems but also by correcting these errors. Other hardware categories are given by the machines that perform the algorithms needed to visualize and generate data specific to the scanning technology and 3D model creation. The development of the computer systems includes the enlargement of disk storage, disk access [ACM Queue, 2003], memory optimization and other components that are contributing to optimize the software usage.

Future developments in this research area might include aspects related to the expansion of the automatization level on the entire workflow, advance in the concept of virtual large sites (cultural, architectural, industrial, entire cities etc.), a new restoration concept that combines real data (captured with laser scanning instrumentation) and virtual data, augmented reality (e.g. museum with virtual exhibits), etc.

Another aspect is referring to the personal qualification regarding these new data acquisition, visualization and documentation techniques. Currently, personal training is realized mainly on company level or by the hardware and software providers. A larger immersion in these technologies at different study levels in universities or other form of studies it is expected and wanted.

The present circumstances encourage a social and economical globalization, which makes sustained campaign for cultural heritage promotion necessary. Mainly, due to the following reasons: firstly, to increase the cultural heritage's level of awareness between different nations and civilizations; secondly, to enhance the individual relationship to the cultural heritage. This could be realized also by overcoming the current phase of singular projects to large scale 3D digital cultural heritage documentation.

The 3D digital documentation of objects and sites having cultural heritage importance becomes more and more significant. Based on innovative measuring technique like terrestrial laser scanning – in addition with conventional procedures like tacheometry and GPS – and the possibilities of nowadays computer graphic software this can be performed in a way never known so far. These new possibilities are explored within this thesis in few case studies. In practice the next step must take full advantages of these new chances.

Acknowledgments

First, I would like to express my deep gratitude to my doctoral father Univ.-Prof. Dr.-Ing. O. Heunecke for his constant encouragement, guidance and help.

I am grateful to the committee members Univ.-Prof. Dr.-Ing. habil W. Niemeier and Univ.-Prof. Dr.-Ing. habil L. Gründig for reading my thesis and providing helpful criticism.

I also thank Dipl.-Ing Sönke Pink for assistance, many interesting and brain storming discussions and for his friendship.

I greatly appreciate the assistance of Christa Amato, who helped me on many occasions to deal with the inside information of English language.

Thanks also go to the members of the geodetic laboratory for their help and assistance in my work.

Special thanks go to the cooperation partners of the projects, especially to the Faculty of Geodesy, Bucharest and Bayerisches Landesamt für Denkmalpflege.

To my fellow group of friends, I express my appreciation for their friendship, understanding and continued support.

Finally, I would like to extend my warmest and deepest gratitude to Aurelija, for her love, support and patience.

Curriculum Vitae

Name	Eugen Dutescu
Date of birth	15.12.1978
Place of birth	Bucharest, Romania
Nationality	Romanian
1993-1997	High School „ Colegiul economic A.D. Xenopol" Bucharest, Romania (study of tourism)
1997-2002	Study of Geodesy at the Technical University of Civil Engineering of Bucharest
03-06.2002	Diploma Thesis at the Institut of Geodesy, University of Hannover with the title „Time Series Analysis of GPS data recorded with the GOCA System“
since Sept. 2002	Research associate at the Institute of Geodesy, Faculty of Civil Engineering and Surveying, University of the Bundeswehr Munich

Annex I

Basic 3D object creation

(partially available within 3ds Max 6, AutoCAD, Cyclone 5.4)

Lathe 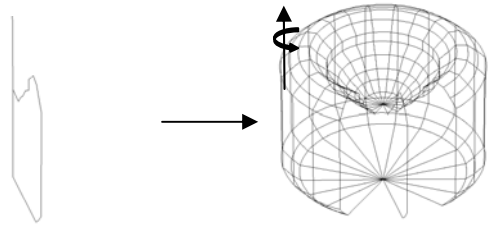	Lofting 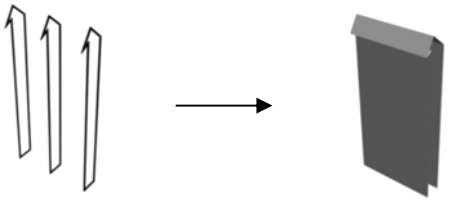
Lofting 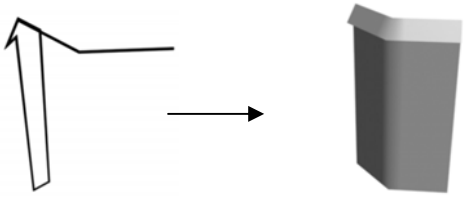	Extrude 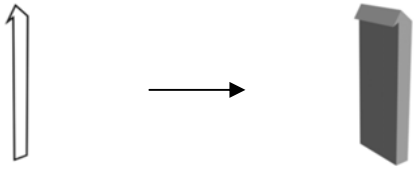
Boundary surface 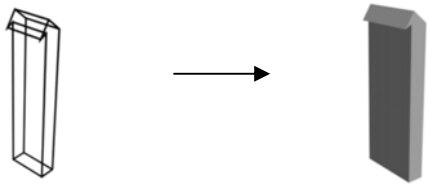	Ruled surface 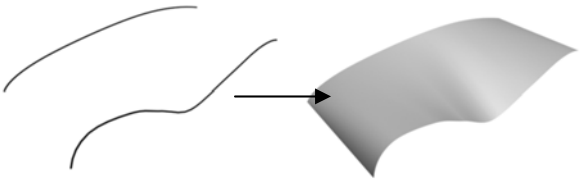
Cap surfaces 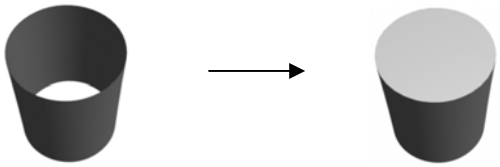	1-Rail sweep 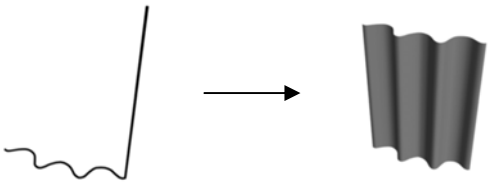
2-Rail sweep 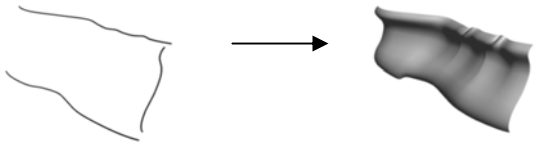	Blend 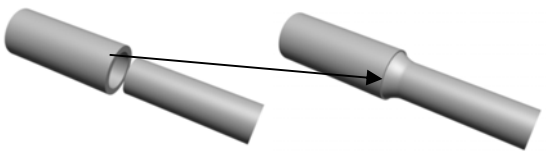
Extend 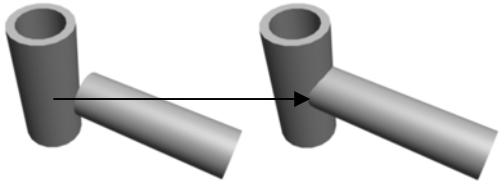	Trim 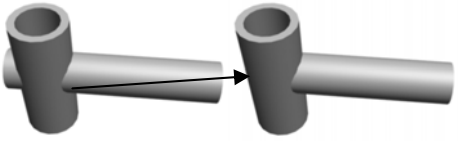

Annex II

Software

	Cyclone 5.4	Raindrop Geomagic Studio 6 [10]	RapidForm 2004[11]
Point cloud registration (4.1)			
- targets based registration (4.1.1)	■	■ only with spherical shape targets	□
- point cloud similarity (4.1.2)	■ not independent; requires an extra target registration	■	■
- feature registration (4.1.3)	■ not independent; requires an extra target registration	□	□
Point cloud treatment (semi-automatically) (4.2)			
- remove unwanted points (4.2.1)	□	□	□
- detect and remove outliers (4.2.2)	□	■	□
- detect and remove disconnected components (4.2.3)	□	■	□
- noise reduction (4.2.4)	□	■	■
- redundancy reduction (4.2.5)	□	□	■
- point cloud sampling and decimation (4.2.5)	■	■	■
- adding points (4.2.6)	□	■	□
- merging point clouds (4.1)	■	■	■
Fitting 3D basic objects (4.3)	■	□	□
- fitting 3D geometric primitives (4.4)	■	□	□
- fitting other objects pipes, steel sections (4.3)	■	□	□
Fitting basic shapes (4.5)			
- automatic line detection	□	■ (limited, not robust)	■ (limited, not robust)
- semi-automatic line generation	■	□	□
- digital tracing	■	□	■
- cross sections	■	■	■
Low-poly surface creation (4.6)	□	□	■ (limited)
Create triangular mesh (4.7)	■	■	■
Editing triangular mesh (semi-automatically) (4.8)			
- self-intersecting triangles	□	□	■
- crossing faces	□	□	■
- redundant faces	□	□	□
- non-manifold faces	□	□	■
- bad normal faces	□	■	■
- detect open edges	□	■	■
- remove spikes	□	■	■
- noise reduction	□	■	■
- smooth operator	□	■	■
- filling holes	■	■	■
- mesh zippering	□	□	□
- mesh stitching	□	□	□
- refine mesh	□	■	■
- decimate mesh	■	■	■

■ available □ not available

[10] Raindrop Geomagic Studio 6 trial version 22.10.2004- 22.11.2004
[11] RapidForm 2004 trial version 08.07.2003-08.08.2003

Annex III

Video Format Test

The following results were obtained using the following specifications:

- test object 1878107 face count in 3ds Max 6 (see Fig. 7.20);
- video length 101 frames with frame rate 30 fps (3,3 seconds animation);
- video resolution 320x240;
- computer specifications: Pentium 4, 2.4 GHz, 2GB RAM, Video Card 64 MB.

File format / codec	File capacity	Render Time (Scanline – 3ds Max 6)	Conversion from uncompressed format
avi Uncompressed	30416 KB	ca. 15 min	-
avi Microsoft Video 1	721 KB	ca. 15 min	1044 KB
avi Cinepak by Radius	743 KB	ca. 15 min	638 KB
avi DivX Codec 4.12	391 KB	ca. 15 min	102 KB
avi Indeo Video 5.10	290 KB	ca. 15 min	390 KB
avi MJPEG compressor	22841 KB	ca. 15 min	-
avi MS Mpeg4 3668 v3	335 KB	ca. 15 min	273 KB
avi VP31® compressor	199 KB	ca. 15 min	43 KB
avi Xvid Mpeg 4	391 KB	ca. 15 min	308 KB
avi DV video encoder	11933 KB	ca. 15 min	11698 KB
mov Mpeg4 Video	574 KB	ca. 15 min	-
mov 3ivx Delta 3.5	100 KB	ca. 17 min	-
mov DV-Pal	14204 KB	ca. 15 min	-
mov Video	538 KB	ca. 15 min	1743 KB
wmv 2.1 Mbit/s			537 KB
wmv 1.5 Mbit/s			522 KB
wmv 512 Kbit/s			231 KB
wmv 340 Kbit/s			168 KB
wmv 150 Kbit/s			76 KB
mpeg 2 DVD (Pal)			1341 KB
mpeg 2 SVCD (Pal)			847 KB
mpeg 1 VCD (Pal)			450 KB
real video 10			35 KB

Table III. 1 Video format test

Following the above results and the quality of the obtained videos from direct rendering (3ds Max 6) or from format conversion[12], the digital deliverables (animations) for the case scenarios presented in the enclosed CD of this thesis are mainly created as AVI/Xvid Mpeg4 files for distribution on CD/DVD and WMV or Real Video for LAN/Internet broadcasting.

For a more professional comparison between video codecs the report from CS MSU Graphics & Media Lab Video Group can be a starting point [Vatolin, 2005].

[12] For file conversion the following software is issued:
- freeware Virtualdub [www33] and RealProducer Basic 10 [www42];
- shareware (watermark) Digital Media Converter [www41].

Annex IV

Data flow performed within the case scenarios

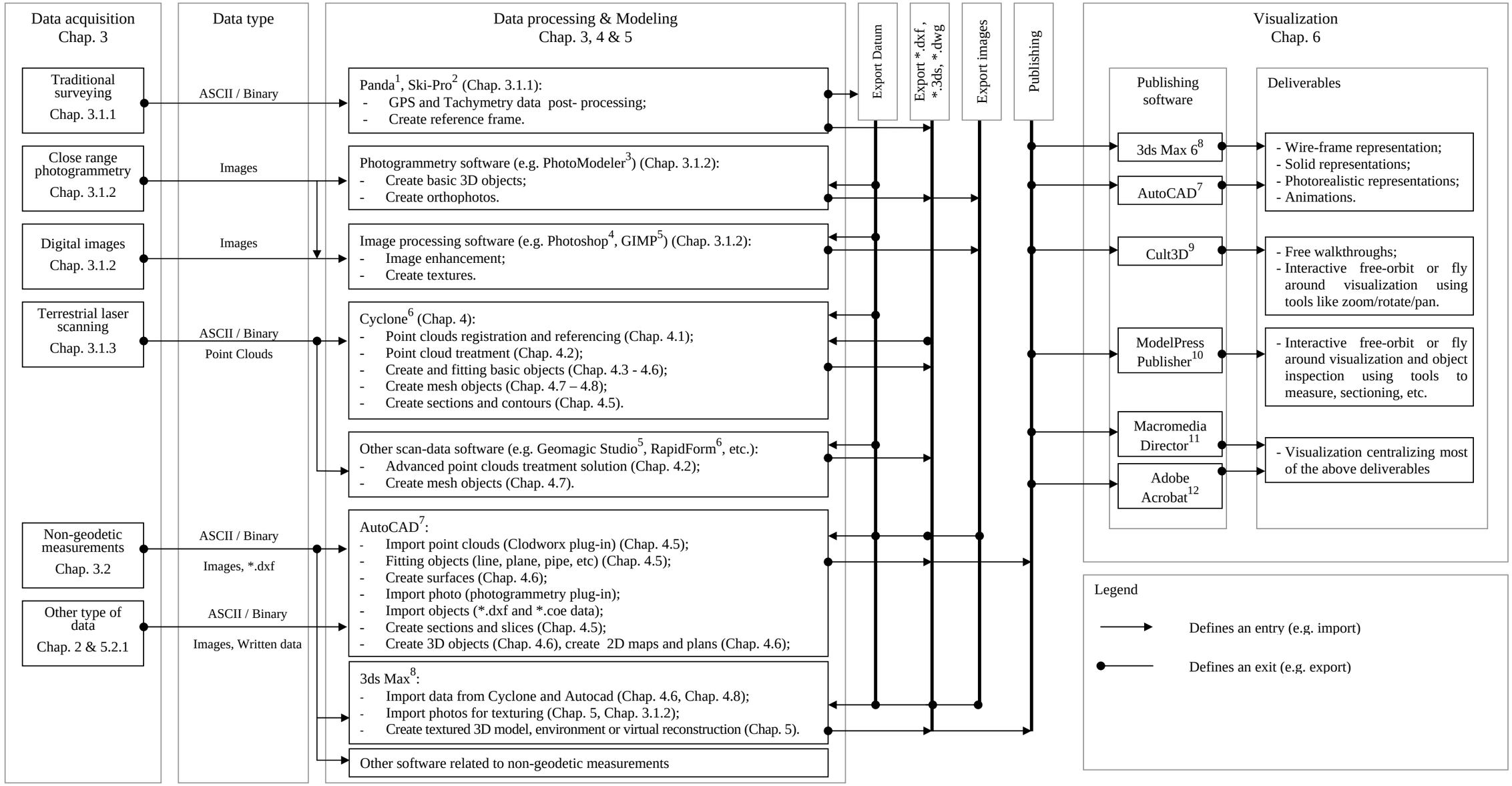

[1] Panda, GeoTec GmbH, http://www.geotec-gmbh.de/;
[2] Ski-Pro, Leica Geosystems, http://www.leica-geosystems.com;
[3] PhotoModeler, Eos Systems Inc, http://www.photomodeler.com;
[4] Photoshop, Adobe, http://www.adobe.de/products/photoshop/main.html;
[5] Gimp, GNU Image manipulation software, http://www.gimp.org/;
[6] Cyclone 5.4, Leica HDS software, http://hds.leica-geosystems.com;
[7] AutoCAD, Autodesk, http://www.autodesk.com;
[8] 3ds Max6, Autodesk, http://www.autodesk.com;
[9] Cult3D, Cycore, http://www.cult3d.com;
[10] ModelPress Publisher, Informative graphics, http://modelpress.com;
[11] Macromedia Director MX, Macromedia, http://www.macromedia.com;
[12] Adobe Acrobat, Adobe, http://www.adobe.com.

Annex V

Project Schönberg (Dealu Frumos), Romania – Virtual Reconstruction at different building stages (see Chap. 7.2)

- approx. 13th century	
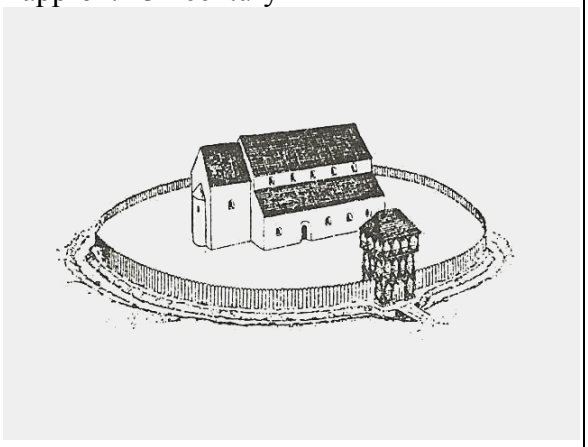	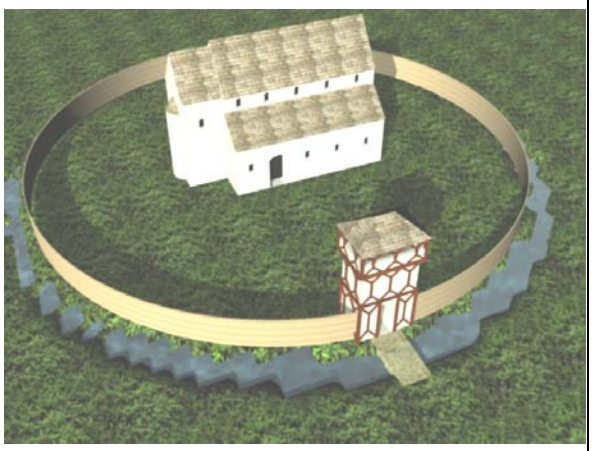
- approx. 16th century	
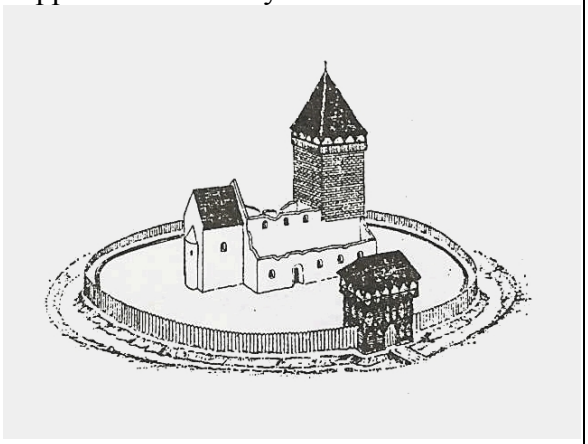	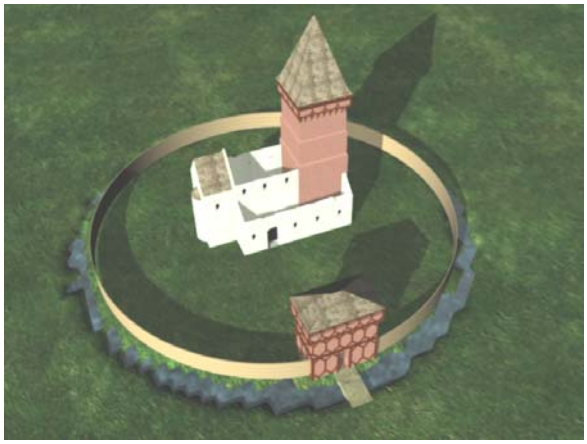
- approx. 16th century	
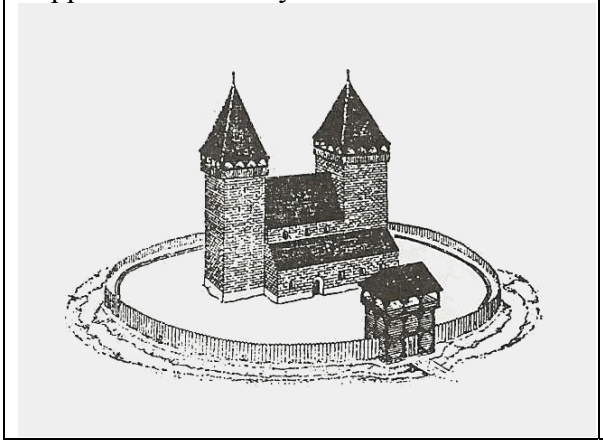	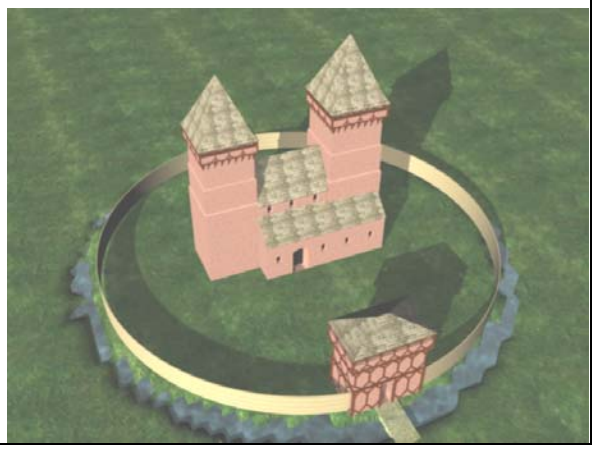

- first half of 16th century 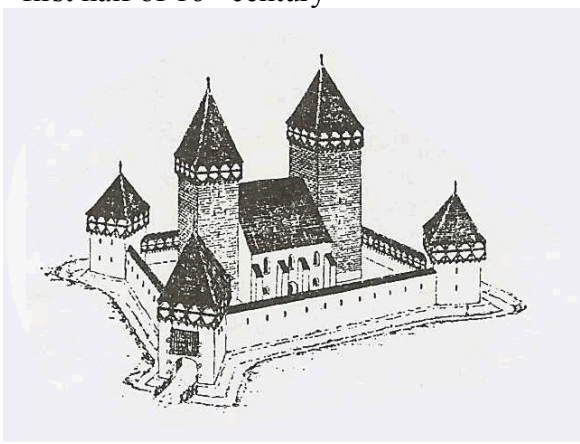	
- 16th century 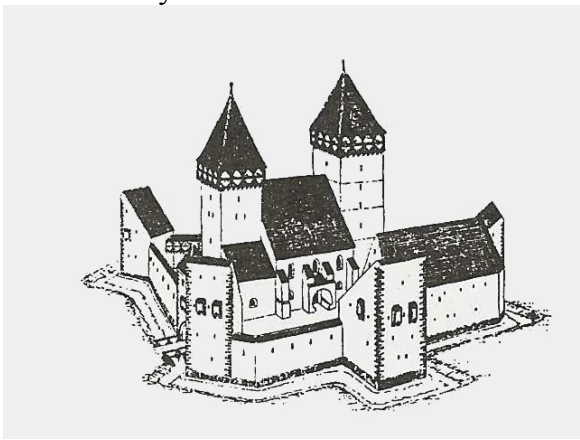	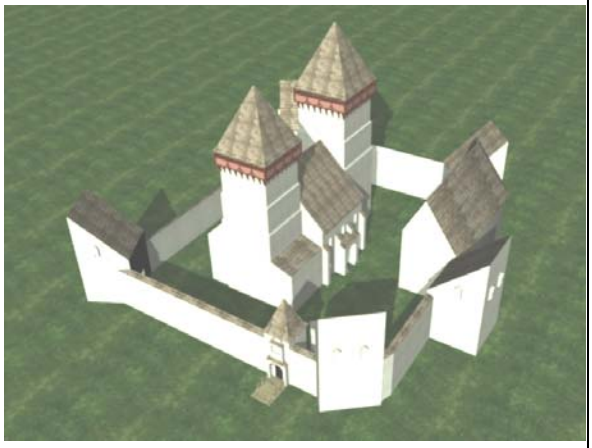
- approx. 1914 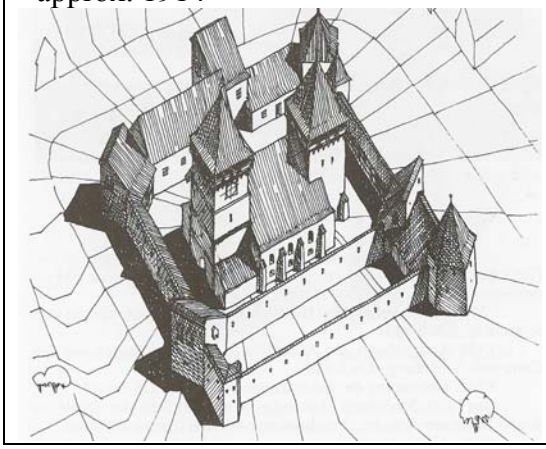	

The virtual reconstructions are realized based on the basic isometric illustrations from the publication "Die Kirchenburg in Schönberg" [Fabini, 1997]. The 3D representations realized with 3ds Max 6 are not performed for specific technical support. Further impressions can be obtained in the enclosed multimedia CD.

Annex VI

Core Data Index to Historical Buildings and Monuments of the Architectural Heritage (see Chap 2.1)

V.I Maximilian Straße

1.0. Names and references

1.1. Name of the building

Arcades Maximilian

1.2. Reference number

to be specified

1.3. Date of compilation

27.09.2005

1.4. Recording organization

1.5. Cross-reference to ensembles, etc.

not known

1.6. Cross-reference to fixture and movable items

not known

1.7. Cross-reference to documentation

not known

1.8. Cross-reference to environment

not known

2.0. Location

2.1. Administrative location

2.1.1. State

Germany

2.1.2. Geo-political unit

Bayern

2.1.3. Sub-division

Landeshauptstadt München

2.1.4. Sub-division

Altstadt

2.2. Address

2.2.1. Postal name

Maximilian Straße

2.2.2. Number

6

2.2.3. Street/road

Maximilian

2.2.4. Locality

München

2.2.5. Town/city

München

2.2.6. Postal code

D-80538

2.3. Cartographic reference
2.3.1. X co-ordinate

4468786

2.3.2. Y co-ordinate

5333508

2.3.3. Spatial referencing system

Gauß-Krüger (DHDN Potsdam/Bessel)

2.4. Cadastral reference/land unit

not known

3.0. Functional type

3.1. Type	3.1.1 Date	3.2 Category
1. Shops		*Commercial*

4.0. Dating

4.1. Period

4.2. Century

19th

4.3. Data range

4.3.1 From	4.3.2 To

4.4. Absolute date

approx. 1857

5.0. Persons & organizations

5.1. Name	5.2 Role	5.2.1 Date
not known		

6.0. Buildings materials/techniques

6.1. Walls

stone, brick

6.2. Roof

metal

7.0. Physical condition

7.1. General condition

good

8.0. Protection/legal status

8.1. Type	8.2 Present grade	8.3 Date granted

9.0. Notes
9.1. Historical summary
See Chap. 7.1
9.2. Descriptive summary

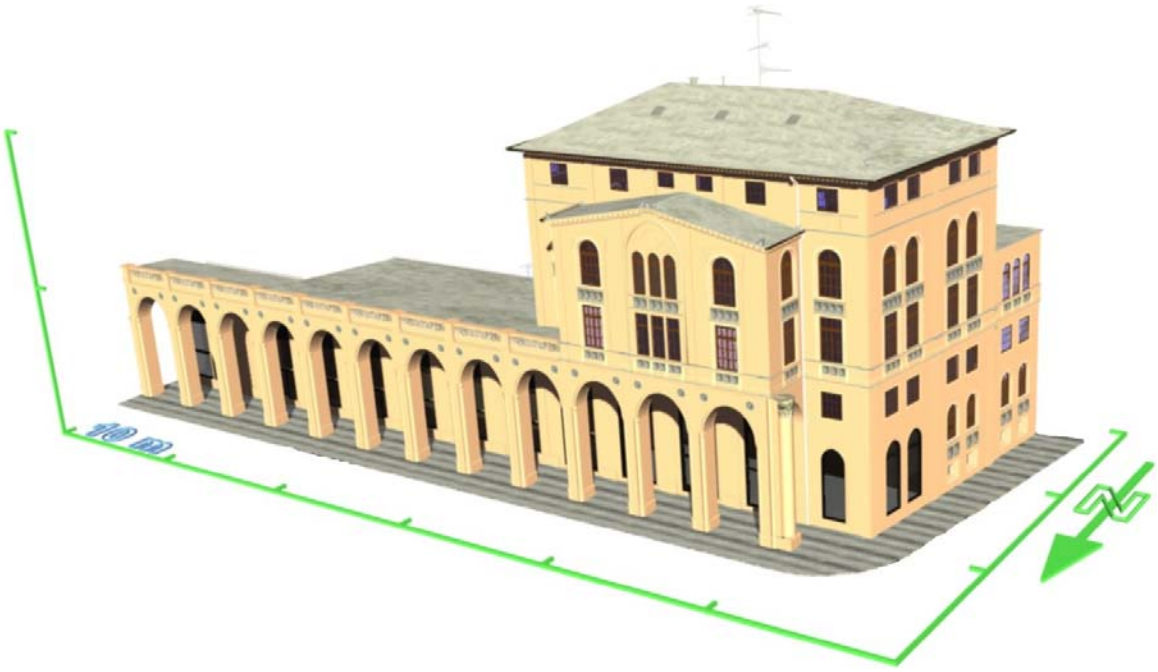

Fig. VI. 1 “Maximilian Straße” - Isometric view

Remark: in digital document double click on image to view the object in 3D space.

V.II Schönberg (Dealu Frumos)

1.0. Names and references

1.1. Name of the building

The Evangelic C.A Church Dealu Frumos

1.2. Reference number

to be specified

1.3. Date of compilation

30.09.2005

1.4. Recording organization

1.5. Cross-reference to ensembles, etc.

not known

1.6. Cross-reference to fixture and movable items

not known

1.7. Cross-reference to documentation

not known

1.8. Cross-reference to environment

not known

2.0. Location

2.1. Administrative location

2.1.1. State

Romania

2.1.2. Geo-political unit

Sibiu

2.1.3. Sub-division

Merghindeal

2.1.4. Sub-division

Dealu Frumos

2.2.. Address

2.2.1. Postal name

Dealu Frumos

2.2.2. Number

2.2.3. Street/road

2.2.4. Locality

Dealu Frumos

2.2.5. Town/city

Dealu Frumos

2.2.6. Postal code

RO-557141

2.3. Cartographic reference
2.3.1. X co-ordinate

476448

2.3.2. Y co-ordinate

498239

2.3.3. Spatial referencing system

Romanian Grid (Proiectia stereografica 1970)

2.4. Cadastral reference/land unit

not known

3.0. Functional type

3.1. Type	3.1.1 Date	3.2 Category
1. Study Centre	*since 2003*	*educational*
2. Church	*since 13th century*	*religious*

4.0. Dating

4.1. Period

4.2. Century

13th

4.3. Data range

4.3.1 From	4.3.2 To

4.4. Absolute date

5.0. Persons & organizations

5.1. Name	5.2 Role	5.2.1 Date
Evangelic C.A church		
"Ion Mincu" University of Architecture and Urbanism, Bucharest		*since 2003*

6.0. Buildings materials/techniques

6.1. Walls

stone, brick

6.2. Roof

ceramic tile

7.0. Physical condition

7.1. General condition

The constructions are suffering from physical degradation; a renovation proccess is under development

8.0. Protection/legal status

8.1. Type	8.2 Present grade	8.3 Date granted

9.0. Notes

9.1. Historical summary
See Chap. 7.2
9.2. Descriptive summary

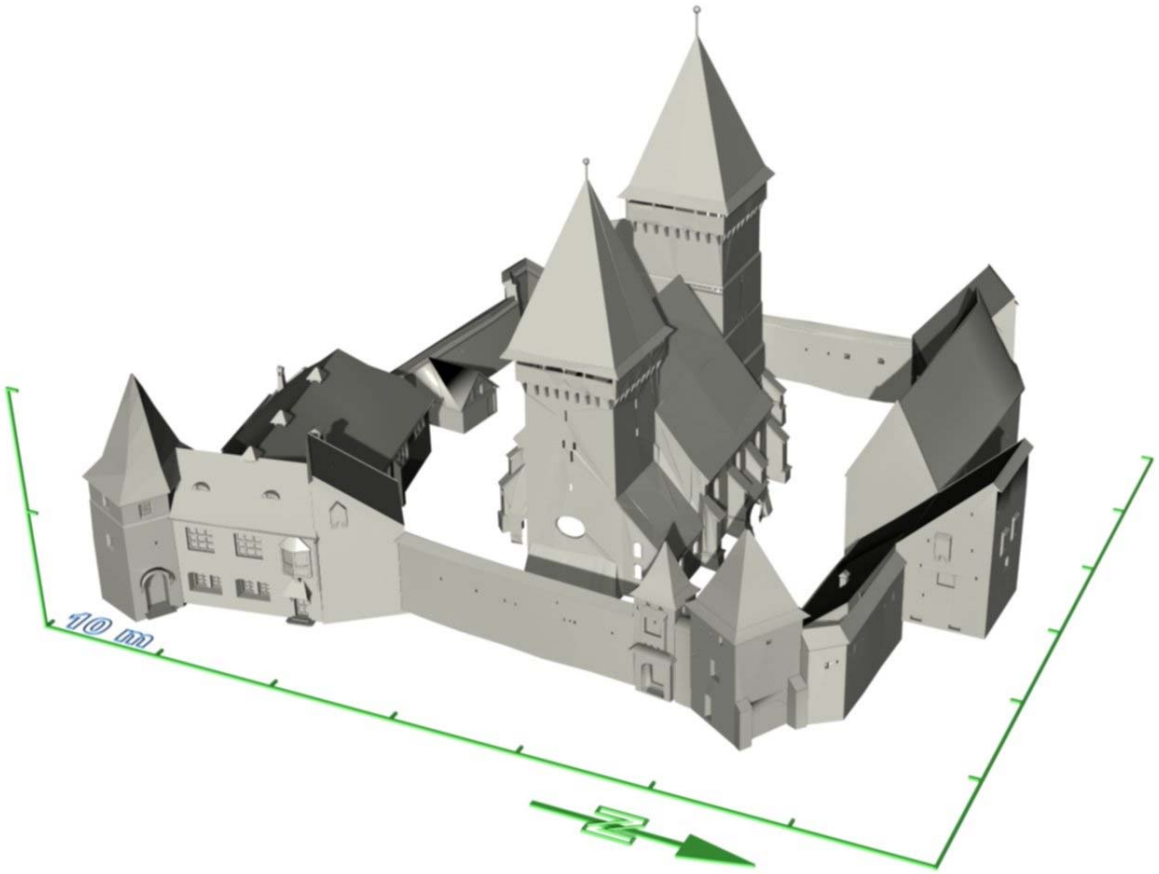

Fig. VI. 2 Fortified church Schönberg - Isometric view

Remark: in digital document double click on image to view the object in 3D space.

V.III Hohenburg

1.0. Names and references

1.1. Name of the building

The old Hohenburg castle

1.2. Reference number

to be specified

1.3. Date of compilation

05.10.2005

1.4. Recording organization

1.5. Cross-reference to ensembles, etc.

not known

1.6. Cross-reference to fixture and movable items

not known

1.7. Cross-reference to documentation

not known

1.8. Cross-reference to environment

not known

2.0. Location

2.1. Administrative location

2.1.1. State

Germany

2.1.2. Geo-political unit

Bayern

2.1.3. Sub-division

Bad Tolz

2.1.4. Sub-division

Lenggries

2.2.Address

2.2.1. Postal name

2.2.2. Number

2.2.3. Street/road

2.2.4. Locality

Lenggries

2.2.5. Town/city

Lenggries

2.2.6. Postal code

D-83661

2.3. Cartographic reference
2.3.1. X co-ordinate

4469200

2.3.2. Y co-ordinate

5281400

2.3.3. Spatial referencing system

Gauß-Krüger (DHDN Potsdam/Bessel)

2.4.Cadastral reference/land unit

not known

3.0. Functional type

3.1. Type	3.1.1 Date	3.2 Category
1. Ruins	since 1707	

4.0. Dating

4.1. Period

4.2. Century

12th

4.3. Data range

4.3.1 From	4.3.2 To

4.4. Absolute date

5.0. Persons & organizations

5.1. Name	5.2 Role	5.2.1 Date

6.0. Buildings materials/techniques

6.1. Walls

6.2. Roof

red roof tile

7.0. Physical condition

7.1. General condition

ruins partially covered by soil

8.0. Protection/legal status

8.1. Type	8.2 Present grade	8.3 Date granted

9.0. Notes

9.1. Historical summary

See Chap. 7.5

9.2. Descriptive summary

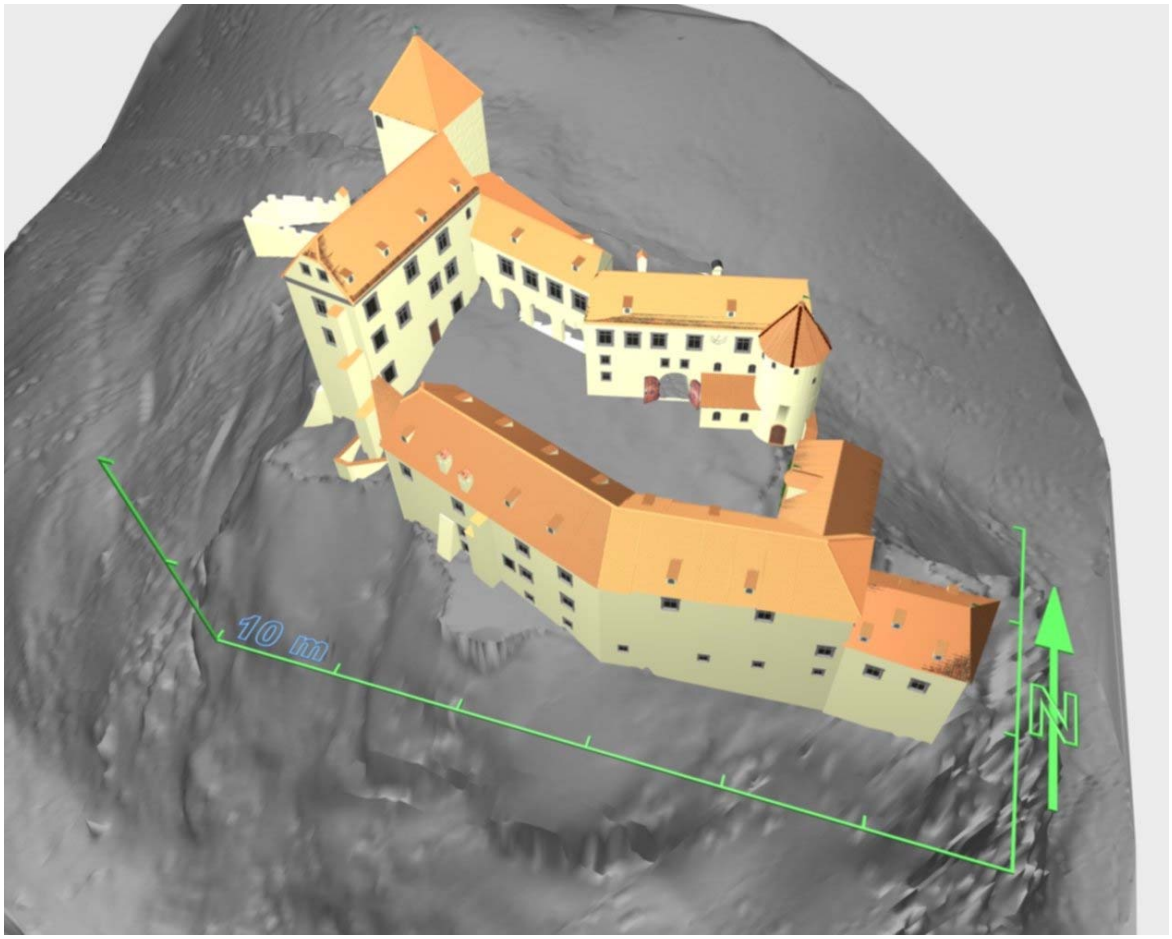

Fig. VI. 3 Virtual reconstruction of Hohenburg castle - isometric view

Annex VII

Collection of Common Shaders and Standard Mapping Techniques Used by Common CG Software (implemented in software like 3ds Max, Alias Maya, etc.)

Shader	*Description*	*Material suitability*
▪ Lambert (Lambert cosine Law)	The materials are reflecting the light evenly into all directions and independent of the observer position.	Matte surfaces without specular highlights (highlights are reflections of the light that illuminate the surface)
▪ Gouraud	Similar to Lambert however computes color interpolation between vertices thus the surfaces are rendered with even color and soft transition between faces.	Matte surfaces without specular highlights
▪ Anisotropic	The properties of the materials depend of orientation, the light is reflected various in different directions.	Hair, glass, brushed metal, fabrics like velvet or satin, etc.
▪ Phong	Used to render materials with hard specular highlights, the light reflection is computed as function of the size and direction of the normal vector.	Glassy or glossy surfaces
▪ Blinn	Similar to Phong used to render materials with soft specular highlights.	Metallic surfaces
▪ Oren-Nayar-Blinn	Derived from Blinn shader allows extra diffuse and roughness level computation.	Matte surfaces
▪ Strauss	Generally used to describe metal surfaces, the highlights are colored using the diffuse color.	Metallic surfaces
▪ Metal	Generally used to describe metal surfaces, the highlights are colored using the diffuse color.	Metallic surfaces
▪ Translucent	Similar to Blinn shader however allows the computing of the quantity of light passing through the object.	Glass, paper, frosted surfaces
▪ Multilayer	The material highlights are layered allowing also anisotropic computation. Combines two or more shaders.	Polished materials and special effects

Mapping method	*Description*
Diffuse level mapping	The diffuse level is controlled using a gray level image. White pixels are not changing the diffuse level whereas the black ones are turning it to 0.
Roughness level	White pixels increase level and black ones are turning it to 0.
Specular level mapping	Used to define the specular highlights of the material and their distribution. White pixels increase the specular level to maximum and the black one are turning off the specular component.
Reflection mapping	Creates the illusion of reflected objects
Refraction mapping	Similar to the reflection map. Creates the illusion that the diffuse image is seen through the surface.
Self-Illumination mapping	White pixels are fully self-illuminated whereas the self-illumination is turn off for black pixels.
Glossiness level mapping	Used to define the glossiness areas of the material and their distribution. Black pixels increase the glossiness level to maximum and the white one are turning off the glossiness component.
Opacity level mapping	Generates partial transparent materials. Black pixels are fully transparent whereas the lighter ones are opaque.
Filter color mapping	Can use also a colored imaged and define the color transmitted thought a transparent material.
Translucence mapping	Defines the translucence color.
Bump mapping	Creates the illusion of irregular or relief surfaces. White pixels define raised areas and black ones lowered areas.
Displacement mapping	Similar to bump mapping with difference that it actually modifies the geometry of the object.

Annex VIII

Case Scenarios – Enclosed Multimedia CD Content

Maximilian Straße (see Chap. 7.1):

- On site images	-on site collection of images;
- Point clouds	-collection of images represented the acquired point clouds exported from Cyclone;
- 3D Representations	-collection of images containing photorealistic or non-photorealistic rendition realized with 3ds Max 6;
- Video	-virtual walkthrough animation generated with 3ds Max 6;
- Interactive representation	-virtual model inspection using ModelPress Reader;
- Core data index to historical buildings and monuments of the architectural heritage	-Adobe Acrobat 3D document enhanced with 3D visualization capabilities.

Schönberg (see Chap. 7.2):

- On site images	-on site collection of images;
- Point clouds	-collection of images represented the acquired point clouds exported from Cyclone;
- 3D Representations	-collection of images containing photorealistic or non-photorealistic rendition realized with 3ds Max 6;
- Video	-virtual walkthrough animation generated with 3ds Max 6;
- Interactive representation	-virtual inspection of the roof truss model using Cult3D Viewer;
- Core data index to historical buildings and monuments of the architectural heritage	-Adobe Acrobat 3D document enhanced with 3D visualization capabilities.

St. Michael (see Chap. 7.3):

- On site images	-on site collection of images;
- Point clouds	-collection of images represented the acquired point clouds exported from Cyclone;
- 3D Representations	-collection of images containing photorealistic or non-photorealistic rendition realized with 3ds Max 6;
- Interactive representation	-constrained walkthrough using Cult3D Viewer and virtual inspection of the main altar model using ModelPress Reader.

Test objects (see Chap. 7.4):

- On site images	-on site collection of images;
- Point clouds	-collection of images represented the acquired point clouds exported from Cyclone;
- 3D Representations	-collection of images containing photorealistic or non-photorealistic rendition realized with 3ds Max 6;
- Video	-virtual walkthrough animation generated with 3ds Max 6;
- Interactive representation	-free walkthrough using Cult3D Viewer and virtual model inspection using Cult3D Viewer and ModelPress Reader.

Hohenburg (see Chap. 7.5)

- On site images	-on site collection of images;
- Point clouds	-collection of images represented the acquired point clouds exported from Cyclone;
- 3D Representations	-collection of images containing photorealistic or non-photorealistic rendition realized with 3ds Max 6;
- Video	-virtual walkthrough animation generated with 3ds Max 6.

References

ACM Queue — *A conversation with Jim Gray,* ACM Queue vol. 1, no. 4 - June 2003

Akca D. — *A new algorithm for 3D surface matching,* International Archives of the Photogrammetry, Remote Sensing and Spatial Information Sciences, vol. XXXV, part B7. 20th ISPRS Congress, Istanbul, Turkey, 12-23 July 2004, pp. 960-965

Altmann M. — *About Nonuniform rational B-Splines –NURBS,* http://www.cs.wpi.edu/~matt/courses/cs563/talks/nurbs.html, accessed 11.2004

Amanatides, J. — *Ray Tracing with Cones*. Computer Graphics, vol. 18(3), (July 1984), pp. 129-135

Arvo J. and Kirk D. — *Particle transport and image synthesis*, Computer Graphics, vol. 24, no. 4, August 1990 pp. 63 - 66 , Proceedings of the 17th annual conference on Computer graphics and interactive techniques

Bedny G., Karwowski W. — *Meaning and sense in activity theory and their role in the study of human performance,* Ergonomia IJE&HF, 2004, vol. 26, no. 2, pp. 121-140

Bergevin R., Soucy M., Gagnon H, and Laurendeau D. — *Towards a general multi-view registration technique*, IEEE Transaction on pattern analysis and machine intelligence, vol. 18, no.5 (May 1996) pp. 540-547

Besl P. J. and McKey N. D. — *A Method for registration of 3-D Shapes,* IEEE Transactions on pattern analysis and machine intelligence, vol. 14, no. 2, February 1992, pp. 239-256

Beyer. W. H. (Ed.). — *CRC Standard Mathematical Tables*, 28th ed. Boca Raton, FL: CRC Press, 1987

Biegelbauer G., Vineze M. — *Fast and robust bore detection in range image data for industrial automatization,* IEEE Proceedings of the 2nd international symposium on 3D data processing, visualization, and transmission (3DPVT 2004), Thessaloniki 6-9 September

Bourke P. — *Equation of a Sphere from 4 Points on the Surface*, June 2002, http://astronomy.swin.edu.au/~pbourke/geometry/spherefrom4/, accessed 10.2004

Equation of a plane, March 1989 http://astronomy.swin.edu.au/~pbourke/geometry/planeeq/, accessed 10.2004

Bülow Th. and Daniilidis K. — *Surface Representations using Spherical Harmonics and Gabor Wavelets on the Sphere*. Technical Report MS-CIS-01-37, Dept. of Computer and Information Science, University of Pennsylvania, 2001

Chaperon T., Goulette F. — *Extracting cylinders in full 3D data using a random sampling method and the Gaussian image,* VMV 2001, Stuttgart 21-23 November

Chen C. — *Top 10 Unsolved Information Visualization Problems,* Computer Graphics and Applications, IEEE vol. 25, Issue 4, July-August 2005 pp. 12 - 16

Chen Y. and Medioni G. — *Object modeling from multiple range images,* Image and Vision Computing 10, 3 April 1992, pp. 145-155

Cheok S., Leight S., Rukhin A. — *Calibration experiments of a laser scanner,* National Institute of Standards and Technology, Building and Fire Research Laboratory, NISTIR 6922, September 2002

Chetverikov D., Svirko D., Stepanov D. and Krsek P.	*The trimmed iterative closest point algorithm,* Proceedings of 16th International Conference on Pattern Recognition 2002, vol. 3, pp. 545-548
COE	*Guidance on inventory and documentation of the cultural heritage,* Council Of Europe 2001
Cook R. L., Porter Th., Carpenter L.	*Distributed Ray Tracing*, Computer Graphics vol. 18, no. 3, July 1984 pp. 137-145, Proceedings of the 11th annual conference on Computer graphics and interactive techniques
Curless B.	*From Range Scans to 3D Models*, ACM SIGGRAPH Computer Graphics, Vol. 33, Issue 4, Nov 2000, pp.38-41.
Cutler B., Dorsey J., McMillan L., Müller M., Jagnow R.	*A procedural approach to authoring solid models,* International Conference on Computer Graphics and Interactive Techniques, Proceedings of the 29th annual conference on Computer graphics and interactive techniques San Antonio, Texas 2002, pp. 302-311
Demaus R.	*Non-Destructive Investigations*, The Building Conservation Directory 1996, http://www.buildingconservation.com/articles/nondestr/nondestr.htm
Deriche. R.	*Recursively Implementing the Gaussian and its Derivatives*. Proceedings of 2nd International Conference on Image Processing, Singapore, pp. 263-267, September 1992
DigiCULT	*Core Technologies for the cultural and scientific heritage sector, DigiCULT Technology Watch Report 3,* January 2005
H. Dietrich,	Personal notes, November 2005
Eberly D.	*Least squares fitting data, 2001*, www.magic-software.com
Fabini	*Die Kirchenburg in Schönberg*, Baudenkmäler in Siebenbürgen Heft 27, Monumenta Verlag Sibiu-Hermannstadt, Architekturbüro Fabini GmbH Hermannstadt, 1997
Faugeras O. D., Ponce J.	*Prism Trees: A Hierarchical Representation for 3-D Objects,* Proceedings of the 8th International Joint Conference on Artificial Intelligence. Karlsruhe, August 1983, pp. 982-988
Fischler M. A. and Bolles R. C.	*Random sample consensus: a paradigm for model fitting with applications to image analysis and automated cartography*, Communication of the ACM vol. 24, no. 6 (June 1981), pp. 381-395
Fleck D. E., Berch D. B., Shear P. K, Strakowski S. M.	*Directed forgetting in explicit and implicit memory: The role of encoding and retrieval mechanisms,* The Phsyhological Record, Spring 2001
Fröhlich C. and Mettemleiter M.	*Terrestrial laser Scanning – New Perspectivein 3D Scanning,* Proceedings of the ISPRS working group VIII/2, Freiburg, Germany, 03-03 October 2004
Förstner W.	*Robust Estimation Procedures in Computer Vision, in Third Course in Digital Photogrammetry*, 1998, Bonn, Germany. Institute for Photogrammetry at Bonn University and Landesvermessungsamt Nordrhein-Westfalen.
	A Framework for Low Level Feature Extraction, pages 383-394. LNCS 802. Springer, 1994
Fusiello A., Castellani U. , Ronchetti L. , Murino V.	*Model Acquisition by Registration of Multiple Acoustic Range Views*, Computer Vision –ECCV 2002, Proceedings of the 7th European Conference on Computer Vision-Part II , pp.805-822

Gökalp E. and Boz Y.	*Outlier detection in GPS networks with fuzzy logic and conventional methods*, FIG Working Week 2005 and GSDI-8, Cairo, Egipt 16-2 April, 2005
Golub G. H. and Charles F. Van Loan	*Matrix Computation, Second edition*, 1989 The Johns Hopkins University Press
Harris C. and Stephens M.	*A combined corner and edge detector*, Fourth Alvey Vision Conference, pp. 147-151, 1988
Heckberl P. S. and Hanrahan P.	*Beam tracing polygonal objects*, Computer Graphics (SIGGRAPH '84 Proceedings, vol. 18(3), July 1984, pp. 119-127
Hibbard B.	*Top Ten Visualization Problems*, VISFILES, vol.33, no.2, May 1999 ACM SIGGRAPH http://www.siggraph.org/publications/newsletter/v33n2/columns/hibbard.html, accessed 09.2005
Jensen H. W. and Christensen N. J.	*Photon maps in bidirectional Monte Carlo ray tracing* Computers and Graphics, 19(2), pp. 215-224, March-April 1995. CODEN COGRD2. ISSN 0097-8493
Johnson C.	*Top Scientific Visualization Research Problems***,** Computer Graphics and Applications, IEEE vol. 24, Issue 4, July-August 2004, pp. 13 - 17
Joy Kenneth I.	*Utilizing parametric hyperpatch methods for modeling and display of free-form solids*, ACM Symposium on Solid Modeling and Applications, Proceedings of the first ACM symposium on Solid modeling foundations and CAD/CAM applications Austin, Texas, United States 1991, pp. 245 - 254
Karbacher S., Campagna S.	*Principles of 3D Image Analysis and Synthesis*, B.Girod, G. Greiner und H. Niemann (Ed), Kluwere Academic Publishers, Boston – Dordrecht – London 2000, pp. 141-143
Kim Sang-Hoon, Jung-Kak Seo, Hyun-Ki Hong, Min-Hyung Choi,	*Iterative Registration of Multiple 3D Data Sets Using Covariance Matri,* Proceedings of International Conference on Virtual Systems and MultiMedia VSMM 2002
Klingert M.	*Methoden der Digitalen Bildverarbeitung in der Infrarotbauwerksthermografie* in Forum Bauinformatik (Hrsg.: F. Schley, L. Weber), pp. 287-294, BTU Cottbus, 2005
Kobbelt L., Campagna S., Seidel H.-P.	*A General Framework for Mesh Decimation***,** Graphics Interface '98 Proceedings, 1998, pp. 43 - 50
Kraus, K	*Photogrammetry Volume 2. Advanced Methods and Applications,* Dümmler Verlag, Bonn, Germany, fourth edition 1997
Kruse R., Gebhardt,J. and Klawonn F.	*Foundations of Fuzzy Systems,* Wiley, Clichester, 1994
Lehmann E. H., P. Vontobel, E. Deschler-Erb, Soares M.	*Non-invasive studies of objects from cultural heritage,* Nuclear Instruments and Methods in Physics Research A 542 (2005) pp. 68–75, available online at www.sciencedirect.com, accessed 09.2005
Low K.-L., Tan T.-S.	*Model simplification using vertex-clustering,* Symposium on interactive 3D graphics, Providence, Rhode Island, USA 1997, pp. 75-81

Lukacs G., Marshall A. D., Martin R. R.	*Faithful Least-Squares Fitting of Spheres, Cylinders, Cones and Tori for Reliable Segmentation,* Lecture Notes In Computer Science, vol. 1406, Proceedings of the 5th European Conference on Computer Vision, vol. 1, 1998, pp. 671 - 686
Manner Kim J.	*ME 232: Geometric Modeling for Engineering Applications* http://homepages.cae.wisc.edu/~me232/lecture_notes/solid2.pdf, accessed 12.2004
Marschner S. R., Davis J., Garr M., and Levoy M.	*Filling Holes in Complex Surfaces Using Volumetric Diffusion*, In Proceedings of First International Symposium on 3D Data Processing, Visualization and Transmission. Padua, Italy, June 2002
Marshall J. and Bethel J.	*Basic concepts of L1 norm minimization for surveying applications*, Journal of surveing engineering, November 1996, pp. 168-179
Masuda T. and Yokoya N.	*A robust method for registration and segmentation of multiple range images,* Computer Vision and Image Understanding, vol. 61, no. 3 (May 1995), pp. 295-307
McDonald Tr. C. Jr	*Preservation Brief 35: Understanding Old Buildings: The Process of Architectural Investigation*, National Park Service, 1994, http://www.cr.nps.gov/hps/tps/briefs/presbhom.htm
McGlone C. with Mikhail Ed. and Bethel J.	*Manual of Photogrammetry, 5th Edition*,American Society for Photogrammetry and Remote Sensing, 2004, ISBN 1-57083-071-1
Medkeff J.	*Using Image Calibration to Reduce Noise in Digital Images*, photo.net 2004, http://www.photo.net/learn/dark_noise/, accessed 02.2005
O'Rourke J., and Badler N.	*Decomposition of three-dimensional objects into spheres*, IEEE Transactions on pattern analysis and machine intelligence, PAMI-1, 3 (July 1979), pp. 295-305.
Owen S. G.	*HyperVis – Teaching Scientific Visualisation Using Hypermedia,* SIGGRAPH 1999, http://www.siggraph.org/education/materials/HyperVis/hypervis.htm, accessed 09.2005
Piegl L.	*On NURBS: A Survey,* IEEE Computer graphics and applications, vol. 11, no. 1, Jan 1991, pp. 55-71
PlaneTracer, Plane2Model	www.csoft.com
Preparata F.P. and Shamos M.I..	*Computational Geometry: an Introduction*. Springer - Verlag, 1985
Pulli K., Duchamp T., Hoppe H., McDonald J., Shapiro L., Stuetzle W.	*Robust Meshes from Multiple Range Maps* 3dim , p. 205, 1997.
Roth G.	*Registering two overlapping range images,* Proceedings of the second international conference on recent advances in 3D digital imaging and modeling (3DIM'99), Ottawa, October 4-8, pp. 191-200
Salomon D.	*Data Compression: The complete Reference,* AppendH: Human Visual system, 2000, http://www.ecs.csun.edu/~dsalomon/DC2advertis/AppendH.pdf, accessed 09.2005
San Jose R., Brun A. and Westin C.-F.	*Robust generalized total least squares iterative closest point registration,* Seventh International Conference on Medical Image Computing and Computer-Assisted Intervention (MICCAI'04), September, 2004

Schowengerdt R. A.	*ECE/OPTI533 Digital Image Processing class notes* 2003, http://www.ece.arizona.edu/~dial/ece533/notes12.pdf, accessed 02.2005
Sederberg T.	http://cagd.cs.byu.edu/~557/text/ch5.pdf, accessed 12.2005
Shaji T. , Somayaji S. and Mathews M. S.	*Ultrasonic Pulse Velocity Technique for Inspection and Evaluation of Timber,*J. Mat. in Civ. Engrg., vol. 12, Issue 2, pp. 180-185 (May 2000)
Shakarji Craig M.	*Least-squares fitting algorithms of the NIST algorithm testing system,* Journal of research of the national institute of standards and technology, vol. 103, no. 6, November-December 1998
Shapiro L. G., Mulgaonkar P. G., Moriarty J. D., Haralick R. M.	*A generalized blob model for three-dimensional object representation,* IEEE Proceedings of the workshop on picture data description and management, Asilomar, California, August 27-28 1980, pp. 109-116
Shneiderman B.	*Crossing the Information Visualization Chasm,* 1999, http://www.cs.umd.edu/hcil/pubs/presentations/info-viz-chasmslides/index.htm, accessed 09.2005
SparView	*Business and technology trends in capturing and managing existing-conditions data for engineering / construction /operations*, July 12, 2005 vol. 3, no. 23
Strothotte T.	*Computational Visualization: Graphics, Abstraction and Interactivity,* Springer 1998
Strothotte Th., Masuch M., Isenberg T.	*Visualizing Knowledge about Virtual Reconstructions of Ancient Architecture,* In Proceedings of CGI'99 (Canmore, June 8–11). Computer Graphics Society, IEEE Computer Society Press, 1999
Sun Y., Page D. L, Paik. J. K., Koschan A., Abidi M. A.	*Triangle Mesh-Based Surface Modeling Using Adaptive Smoothing and Implicit Surface Texture Integration* 3dpvt , p. 588, 2002.
Tanimoto S. L., Jackins C. L.	*Geometric modeling with oct-trees,* IEEE Proceedings of the workshop on picture data description and management, Asilomar, California, August 27-28 1980, pp.117-123
Teubner	*Taschenbuch der Matematik*, 1996
Thomas R., Bold .	*Documenting the Cultural Heritage,*The J. Paul Getty Trust, 1998
Turk G., Levoy M.	*Zippered Polygon Meshes from Range Images,* International Conference on Computer Graphics and Interactive Techniques Proceedings of the 21st annual conference on Computer graphics and interactive techniques 1994, pp. 311 - 318
Ulrich J.	*Die Burg über dem Dorf, 700 Jahre Hohenburg,* 2001
UNESCO	*Convention Concerning the Protection of the World Cultural and Natural Heritage*, UNESCO General Conference at its 17th session, 16.11.1972
Vatolin D., Kulikov D. and Parshin A.	*Mpeg-4 Video codecs comparision,* CS MSU Graphics & Media Lab Moscow , 2005, http://www.compression.ru/video/codec_comparison/pdf/MSU_MPEG4_Comparison_eng.pdf, accessed 09.2005
Veach E. and Guibas L. J.	*Metropolis light transport.* SIGGRAPH 97 (August 1997), pp. 65-76. Proceedings of the 24th annual conference on Computer graphics and interactive techniques

Wang J., Oliviera M. M.	*A hole filling strategy for reconstruction of smooth surfaces in range images,* Computer Graphics and Image Processing, 2003. SIBGRAPI 2003. XVI Brazilian Symposium on 12-15 October 2003, pp. 11 - 18
Wang Miao and Tseng Yi-Hsing	*LIDAR data segmentation and classification based on octree structure,* 20th ISPRS congress, 12-13 July Istanbul 2004
Watson G.A.	*Least squares fitting of parametric surfaces to measured data,* Department of Mathematics, University of Dundee, Scotland, 2000
Weferling U., Heine K. and Wulf U.	*Messen, modellieren, darstellen von Handaufmass bis High-Tech Aufnahmeverfahren in der historischen Bauforschung*, 2001
Wieser A., Brunner F.K.	*Short static GPS sessions: robust estimation results*, Preprint GPS Solution 2001
www1	http://www.baygeo.com/html/resistivity.html, accessed 02.2005
www10	http://mathworld.wolfram.com/DelaunayTriangulation.html, accessed 09.2005
www11	http://www.mathworks.com/access/helpdesk/help/techdoc/ref/delaunayn.shtml, accessed 09.2005
www12	*http://www-i8.informatik.rwth-aachen.de/teaching/cg2/downloads/MeshZippering.pdf,* accessed 12.2004
www13	*http://www.cs.cornell.edu/boom/2003sp/ProjectArch/3DEffectsAnim/lodfig1.pdf,* accessed 12.2004
www14	*Nurbs Curves: A Guide for The Uninitiated,* http://devworld.apple.com/dev/techsupport/develop/issue25/schneider.html, accessed 09.2005
www15	www.britannica.com, accessed 05.09.2005
www16	www.webster-dictionary.org, accessed 05.09.2005
www17	http://gillonj.tripod.com/culturalheritagechartersandstandards/, accessed 06.09.2005
www18	http://cm.coe.int/ta/rec/1995/95r3.htm, accessed 09.2004
www19	www.tiris.gv.at, accessed 09.2005
www2	*Documentation of the Merlion for relocation (using digital close range photogrammetry),* http://www.photomodeler.com/pdf/Merlion%20Relocation.pdf, accessed 12.09.2005
www20	mycolex.collector.ch, accessed 07.09.2005
www21	http://dea.brunel.ac.uk/project/murale/home.html, accessed 07.09.2005
www22	http://www.online-archaeology.com, accessed 07.09.2005
www23	archeoguide.intranet.gr, accessed 07.09.2005
www24	http://www.cast.uark.edu/~kkvamme/geop/army_city.htm#Fuse, accessed 02.2005
www25	*http://whatis.techtarget.com/definition/0,,sid9_gci213311,00.html,* accessed 09.2005
www26	http://www.irfanview.com/, Irfanview, accessed 03.2005
www27	http://www.stintercorp.com/ic.php, ImageConverter accessed 03.2005

www28	http://www.gimp.org/, The GIMP, GNU Image Manipulation Program, accessed 12.2005
www29	http://www.adobe.de/products/photoshop/main.html, Adobe Photoshop cs2
www3	www.infratec.de, accessed 03.2005
www30	http://www.corel.com, CorelDraw family software, accessed 12.2005
www31	http://www.free-codecs.com/, audio-video codecs, accessed 12.2005
www32	http://audacity.sourceforge.net/, Audacity, accessed 12.2005
www33	http://www.virtualdub.org/, Virtualdub, accessed 12.2005
www34	http://www.cult3d.com, accessed 12.2005
www35	http://www.lattice3d.com/, accessed 12.2005
www36	http://www.myvr-software.com, accessed 12.2005
www37	http://www.walkinside.com, accessed 12.2005
www38	http://web.axelero.hu/karpo/, 3D Object converter, accessed 12.2005
www39	http://www.righthemisphere.com/products/dexp/index.htm, Deep Exploration, accessed 09.2005
www4	www.flirthermography.com, ThermaCAM Image Builder™, accessed 03.2005
www40	http://www.ngrain.com/home.html, accessed 11.2005
www41	http://www.deskshare.com/, Digital Media Converter, accessed 11.2005
www42	http://www.realnetworks.com/, Real Producer Basic 10, accessed 11.2005
www43	Amtlicher Stadtplan der Landeshauptstadt München, http://www.geoinfo-muenchen.de/cityguide/muenchen/800x600.html, accessed 09.2005
www44	Bauwerk Maximilianeum, Die Planungs-, und Baugeschichte http://www.bayern.landtag.de/bauwerk_maximilianeum.html, accessed 09.2005
www45	www.muenchen.de, http://www.muenchen.de/Rathaus/lhm_alt/mtour/deutsch/stadtinformationen/plaetze/46102/maximilianstrasse.html, accessed 09.2005
www46	http://www.bayerische.staatsoper.de/c.php/info/nationaltheater/69_de.rsys?l=de&dom=dom1, accessed 09.2005
www47	www.hog-schoenberg.de, accessed 09.2005
www48	http://www.iaim.ro/cercetare/dealufrumos, accessed 09.2005
www49	http://www.esri.com/software/arcgis/extensions/3danalyst/index.html, accessed 10.2005
www5	*A simple guide to investigative tools and methods*, http://www.gbg.co.uk/techniques/techniques.shtml, accessed 09.2005
www50	http://usa.autodesk.com/adsk/servlet/index?siteID=123112&id=3081357, accessed 10.2005
www51	http://electron.ugent.be/ugct/index.htm, accessed 09.2005

www52	http://www.rapiscansystems.com/, accessed 09.2005
www53	http://www.aperio.co.uk/techniques/tech_magnetic.html, accessed 02.2005
www54	http:/www.ltimagery.com, accessed 10.2005
www55	http://hds.leica-geosystems.com, accessed 12.2005
www56	http://www.riegl.com, accessed 12.2005
www57	http://mathworld.wolfram.com/Plane.html, accessed 10.2004
www58	Edinburg Online Graphics Dictionary http://homepages.inf.ed.ac.uk/rbf/GRDICT/grdict.htm, accessed 11.2004
www59	PlanTracer www.csoft.com, accessed 03.2005
www6	http://www.ipf.tuwien.ac.at/fr/buildings/diss/node57.html, accessed 12.2004
www60	Htpp://www.stereolithography.com
www7	http://www.infratec.de/thermographie/index_de.html, accessed 02.2005
www8	L. Paul Chew, Cornell University, http://www.cs.cornell.edu/Info/People/chew/Delaunay.html, accessed 09.2005
www9	http://www.qhull.org/, accessed 09.2005
Zhang Zhengyou	*Iterative point matching for registration of free- form curves,* Rapports de Recherche no. 1658, Programme 4 Robotique, Image et Vision, INRIA Sophia Antipolis, 1992
Zomorodian A. and Edelsbrunner H.	*Fast Software for Box Intersections*, International jurnal of computational geometry and applications 2002, 16th ACM symposium on computational geometry Hong Kong 2000